Controlling transmission of infectious diseases in spatially structured populations by culling, vaccination and non-pharmaceutical interventions

by

Notice Ringa

A Thesis

Presented to

The Faculty of Graduate Studies

of

The University of Guelph

In partial fulfilment of requirements

for the degree of

Doctor of Philosophy
in
Mathematics and Statistics - Applied Mathematics

Guelph, Ontario, Canada

ABSTRACT

Controlling transmission of infectious diseases in spatially structured populations by culling, vaccination and non-pharmaceutical interventions

Notice Ringa
University of Guelph, 2014

Advisors:
Dr. C.T. Bauch

This thesis demonstrated the value of pair approximation models in (i) describing spatial transmission and strategic control of foot and mouth disease (FMD) by vaccination and culling in view of the situations in endemic or near-endemic countries and (ii) exploring impacts of adoption of non-pharmaceutical interventions (NPIs) resulting from interactions between spatially connected individuals, on the spread of a general infection. Factors relevant to the dynamics of FMD in endemic or near-endemic and often low-income countries that we considered are frequent disease re-introduction, long-term waning of natural immunity, vaccine waning and constrained culling and vaccination. To minimize the impact of disease re-importation, vaccine waning and natural immunity waning on the dynamics of FMD by a limited supply of vaccines or vaccination resources, it is ideal to combine rapid deployment of ring vaccination in farms neighboring infected premises, with spread-out deployment of prophylactic vaccination during disease-free phases, such that supplies last as long as possible. The advantage of rapid culling in farms neighboring confirmed

FMD source infections (direct contact or DC culling) over culling in infected premises (IP culling) only is that the former removes a population of farms that would otherwise provide ground for infection and further transmission of the disease. However, the optimal strategy for controlling FMD by culling is prompt diagnosis and rapid deployment of IP culling and DC culling. Secondly, this thesis explored the interaction between spatial transmission of an infection and the spread of adoption of NPIs, which is stimulated by being neighbors of infected individuals (exposure learning) or individuals who practice NPIs (social learning). A newly introduced infection is likely to die out without developing into an epidemic if the neighborhood of the source infection is made up of individuals who can avoid infection and further disease transmission through the practice of strict NPIs at all times. If adoption of NPIs begins to take place during an outbreak, then exposure learning followed by prompt adoption of strict NPIs and avoidance of infection from the infectious neighbors, is more effective than social learning. However, social learning can outperform exposure learning if the former begins well in advance of the infection outbreak. Contrary to commonly observed phenomena, increasing the initial source infections, who are surrounded by individuals who exercise strict NPIs, can decrease the infection peak. We conclude that (i) in order to attain global eradication of FMD, more spatially oriented mathematical models tailored to countries that are still endemic or near-endemic should be developed and (ii) more spatially oriented models that explore effects of NPIs on the regulation of infectious diseases should be developed.

Acknowledgments

I would like to express my deepest thanks to my supervisor Dr. C.T. Bauch for his unflagging support, guidance, patience and motivations throughout my PhD journey. I have enjoyed the opportunity to watch and learn from his immense knowledge and experience. I could not have imagined having a better advisor and mentor for my PhD study.

I would also like to thank all members of my PhD advisory committee for offering encouraging and constructive feedback on the earlier version of my thesis.

I am also grateful for having been a member of the Bauch lab at the University of Guelph. I thank my colleagues for their friendly and team-work spirit as well as their helpful suggestions and comments about my work during lab group meetings and occasional conversations in the lab or along the corridors of the McNaughton building.

I thank the Botswana International University of Science and Technology (BIUST) and the government of Botswana for their generous support in funding my PhD program.

Last but not least, I would like to express my sincerest thanks to my family: my mother, my siblings and my wife for their support, encouragement, inspiration and patience during my pursuit of the PhD in Mathematics.

Table of Contents

List of Tables

List of Figures

Chapter 1

Introduction

1.1 Preliminaries

This thesis predominantly focuses on the use of the spatially oriented pair approximation models to describe and explore long-term dynamics and control of foot and mouth disease (FMD) in endemic or near-endemic countries. Because of the global economic importance of FMD and inadequacy of the literature dealing with spatially oriented mathematical models of FMD that capture factors that affect the disease in endemic or near-endemic and often low-income countries, this thesis identifies, incorporates and models factors surrounding the dynamics of the disease in endemic or near-endemic settings. Such factors include occurrence of repeated outbreaks in the long-term, loss of natural and vaccine immunity, frequent disease re-importations and gravely constrained control measures. Also, this thesis develops a pair approximation model for the spatial spread of a general infectious disease, and explores impacts of adoption of non-pharmaceutical interventions (NPIs) by members of the host population, on the dynamics of an infection outbreak.

In this chapter we discuss basic concepts of mathematical modeling in epidemiology as background to the type of models derived and discussed in the rest of

the thesis.

1.2 Epidemiology and Mathematics

Epidemiology is the study of frequency, distribution and determinants of infectious diseases (among human or animal populations, including micro-organisms) as well as their prevention [110, 71, 49]. An epidemiological study of an infectious disease involves its basic description through understanding the causes and mechanisms leading to spread of the disease into the host population. The host population is a group of humans, animals, etc., affected by an infection outbreak. Stages of epidemiological investigations include (i) surveillance and descriptive phases: description of populations at risk and the distribution of the disease, (ii) analytical phase: study of causes and determinants of disease outbreaks, (iii) intervention and decision-making phases: selection and implementation of control measures and (iv) monitoring phase: ensuring whether control measures are applied properly and/ or have the desired effect [110, 22].

The use of mathematical techniques to describe and analyze dynamics of infectious diseases has led to the development of a research area that combines both mathematics and epidemiology: mathematical epidemiology. Mathematical epidemiology studies are carried out by collecting available epidemiological information about infections, and describing it in terms of mathematical models, followed by analysis and interpretation of the models. In general, a mathematical model is defined as a description of real-world phenomena using mathematical concepts and language,

usually represented by a single or a system of mathematical equations [102]. The overall aim of mathematical modeling of infectious diseases is to develop a deeper understanding of transmission dynamics of diseases, and devise potentially effective disease control strategies. [46].

Mathematical models are also often used to test ideas and make predictions about real-world infections. For instance, mathematical models have been used, with varying success, to forecast the future of incidence of infectious diseases such as Pertussis, flu and HIV [46]. Despite their importance, it is challenging and often very difficult to construct and analyze accurate mathematical models. Limitations of mathematical modeling include difficulty to incorporate and explore the complex nature of infectious diseases, resulting in failure to address all important factors and instead focusing only on factors that are perceived important. However, because it is cost effective to test several control scenarios using mathematical models (versus time and cost of large-scale experiments of actual real systems), mathematical modeling has been widely adopted as a guide to understanding the mechanism of spread and strategic disease control measures.

1.3 Background to mathematical modeling approach used in this thesis

There exist various types of mathematical models in epidemiology. The difference between types of mathematical models lies in the way they capture characteristics of infectious diseases and the available techniques for solving such models.

Here we discuss in general the construction, analysis and uses of mathematical models, which forms the background to the modeling approach we develop in this thesis.

1.3.1 Compartmental models

Early mathematical models in epidemiology are based on the idea of dividing the host population (usually humans or animals) into smaller units (called compartments) such that individuals that have the same disease status belong to the same compartment. For example, if upon contact with the disease a previously susceptible individual (individual who has no immunity to the disease) acquires the disease and becomes infectious (individual who is currently infected and can transmit the disease), and later recovers (individual who has gained immunity) from the disease, then the corresponding mathematical model will divide the population into *susceptible, infectious* and *recovered* compartments. Because contact between individuals in the susceptible compartment and those in the infectious class may lead to disease transmission, resulting in movement of individuals from the previously susceptible (S) compartment to the infectious (I) compartment, followed by recovery (movement from infectious to recovered (R) class), such a model is referred to as the SIR compartmental model [55, 77, 53]. Figure 1.1 is a pictorial representation of transitions between disease states in a SIR model.

Note that if S, I and R represent the numbers of susceptible, infectious and recovered individuals, respectively, then at any point in time the total population size is $N = S + I + R$. The values S, I and R are also referred to as state *variables* of the model. In compartmental models the nature and time rates of transfer of individual

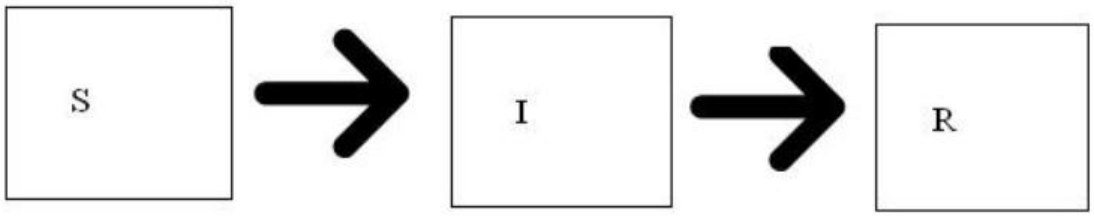

Figure 1.1: The basic SIR model.

members of the host population from one compartment to another are defined such that when N is sufficiently large, then S, I and R can be treated as continuous variables and the resulting mathematical model is comprised of a system of ordinary differential equations,

$$\begin{aligned} \frac{dS}{dt} &= -\tau(I)S \\ \frac{dI}{dt} &= \tau(I)S - \sigma I \\ \frac{dR}{dt} &= \sigma I, \end{aligned} \tag{1.1}$$

where the initial conditions are

$$S(0) = S_0 \ , \ I(0) = I_0 \ , \ R(0) = R_0 \ , \ S_0 + I_0 + R_0 = N.$$

$\tau(I)$ is the force of infection (the rate at which susceptible individuals become infected) and σ is the recovery rate (i.e. mean infectious period is $\frac{1}{\sigma}$). The transition rates from one compartment to another, $\tau(I)$ and σ, are also referred to as model *parameters*. Simply put, the term $-\tau(I)S$ in the first row of Equations (1.1) describes transmission of the disease from an infectious I individual to a susceptible S member of the host population, and the process decreases (captured by the *negative* sign) the number

of susceptible individuals. The the same process increases the number of infectious individuals in the population (hence, $+\tau(I)S$ in the second second row of Equations (1.1)). Similarly, an infectious individual recovers from the infection after $\frac{1}{\sigma}$ time units (e.g. days), leaving the I compartment (represented by $-\sigma I$ in the second row) to join the R compartment (represented by $+\sigma I$ in the third row).

In basic compartmental models the force of infection, $\tau(I)$ is usually described in terms of the transmission rate, contact rate between susceptible and infectious individuals, and the proportion of infectious individuals as follows,

$\tau(I)$ = (transmission rate, λ) $\times$ (effective contact rate, c) $\times$ (proportion of contacts infected, $\frac{I}{N}$) $= \lambda c\frac{I}{N} = b\frac{I}{N}$, where $b = \lambda c$.

Therefore, the transmission term in Equations (1.1) can be written as $\tau(I)S = bSI/N = \beta SI$, where $\beta = b/N$. Thus, the rate at which new infections occur is proportional to both the density of infectious individuals and the density of susceptible individuals in the host population. This assumption is referred to as *homogeneous-mixing* or *mass-action* mixing [56, 70, 6, 37] because it is silent about the relevance of the geographical locations of members of the host population to the disease spread, but infers that any susceptible individual is equally likely to acquire the infection from any infectious individual within the population.

We also remark that mathematically, the description of the recovery rate used in Equations (1.1) implies that the duration of infectiousness is *exponentially* distributed with average $\frac{1}{\sigma}$. The assumption of exponentially-distributed waiting times is a typical feature of compartmental models in general.

Further extensions of the basic SIR model have been developed. These ex-

tensions include employing more realistic assumptions and exploring effective disease control measures. In Section (1.3.2) we discuss some of the early improvements of the basic SIR model.

Solution of the SIR model

As indicated above incorporating more realistic scenarios into mathematical models enables better understanding and more accurate analysis of infectious diseases and their control. However, this increases the complexity of such models, making it difficult to solve or analyze them. In the event that it is difficult to solve a mathematical model analytically, one can resort to the use of computer programs to test the model validity and obtain meaningful numerical approximations to the true solutions. Below we reveal difficulties incurred when attempting to solve the basic SIR model analytically and discuss alternative ways of analyzing this model.

Solving the basic SIR model means finding the numbers of susceptible, infectious or recovered individuals at time t from the onset of the outbreak (i.e we solve for $S(t)$, $I(t)$ and $R(t)$), for a prescribed set of model parameters τ and σ and *initial conditions*, $S(0)$, $I(0)$ and $R(0)$ (i.e. numbers of susceptible, infectious and recovered individuals at the beginning of an epidemic outbreak). Where possible, model parameters are often chosen to fit observed data about specific infectious diseases. For instance, if t represents time in days, and if upon infection, the newly infected individual stays infectious for x days before they recover, then the recovery rate is $\sigma = \frac{1}{x}\ day^{-1}$.

The condition $N = S + I + R$ (i.e. $R = N - S - I$) means that we can

reduce Equations (1.1) to a system of two ordinary differential equations,

$$\begin{aligned} \frac{dS}{dt} &= -\beta SI \\ \frac{dI}{dt} &= \beta SI - \sigma I. \end{aligned} \tag{1.2}$$

Taking the ratio of the rows of Equations (1.2) shows that

$$\frac{dI}{dS} = -1 + (\frac{\sigma}{\beta})\frac{1}{S}.$$

Integrating both sides of this equation with respect to S gives

$$I(S) = -S + \frac{\sigma}{\beta}\ln S + k,$$

where k is a constant of integration. Substituting the initial conditions $I(0)$ and $S(0)$ into this equation shows that

$$k = I(0) + S(0) - \frac{\sigma}{\beta}\ln S(0).$$

Therefore

$$I(S) = I(0) + S(0) - S + \frac{\sigma}{\beta}\ln\Big(S/S(0)\Big). \tag{1.3}$$

This is an exact solution of the number of infectious individuals, but it is a function of the number of susceptible individuals, and not a function of time t. Unfortunately solving for $I(t)$ is an expensive task despite the simplicity of the basic SIR model.

Rather than finding explicit forms of the solutions $S(t)$, $I(t)$ and $R(t)$ of Equations (1.1), most studies resort to the use of computer programs to obtain numerical approximations of the solutions. Programming languages often used to solve

differential equations are *Mathematica, Maple* and *MATLAB*. This process generally involves writing a computer code, which specifies the model equations (motion equations for the state variables), the initial conditions and model parameters. Once the code has been written appropriately, the program can be run to output desired outcomes. We used *MATLAB* to obtain solutions $S(t)$, $I(t)$ and $R(t)$ of the basic SIR model, Equations (1.1), as line graphs, where the initial conditions and model parameters are given in the caption provided (see Figure 1.2). As expected, variation

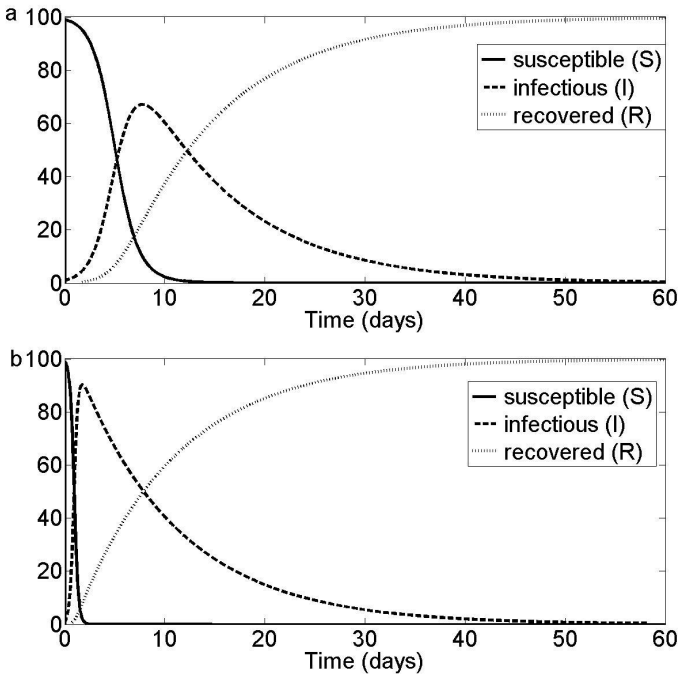

Figure 1.2: Solutions of the basic SIR model (1.1), where transmission rates are $\beta = 0.01\ day^{-1}$ (a) and $\beta = 0.05\ day^{-1}$ (b). Population size is $N = 100$, recovery rate is $\sigma = 0.1\ day^{-1}$ and initial conditions are $S(0) = 99$, $I(0) = 1$ and $R(0) = 0$.

of the population size, model parameters and the initial conditions changes the shapes of solution curves (compare Figure 1.2a to Figure 1.2b).

Other epidemiological features captured by compartmental models

Not only do mathematical models enable evaluation of time series for model state variables, but they also allow for exploration of other important features of the dynamics of infectious diseases. Below we discuss some properties of infectious diseases that can be captured by the basic SIR model, and remark that similar methods can be used to study other types of compartmental models.

The basic reproduction number

Recall that the force of infection for the basic SIR model, Equations (1.1) is $\tau(I) = bI/N = \beta I$ and the duration of infectiousness is $\frac{1}{\sigma}$. If at the initial stage of an outbreak almost all members of the host population are susceptible, i.e. $S \approx N$, then the newly introduced infectious individual is expected to transmit the disease to $\frac{\beta N}{\sigma}$ individuals throughout the infectious period. The quantity $\frac{\beta N}{\sigma}$ is a very important feature in many epidemiological models. It is referred to as the *basic reproduction number* [31, 56, 107] and is denoted by R_0. That is,

$$R_0 = \frac{\beta N}{\sigma}. \tag{1.4}$$

The convention that an epidemic outbreak will take off if $R_0>1$ and the disease will die out if $R_0<1$, has been widely adopted. Clearly the second row of Equations (1.1) shows that I will not increase unless $R_0>1$ (i.e. $\frac{dI}{dt}>0$ only when $R_0>1$). Thus, in order to avoid occurrence of an epidemic outbreak it is important to put in place, control measures that will reduce R_0 to values below 1. Simple inspection of Equation (1.4) reveals that the basic reproduction number increases with the transmission parameter β (and the number of infectious individuals at the beginning of an outbreak) and

decreases with the recovery rate σ. R_0 also increases with the population size.

There exist several techniques of calculating the basic reproduction number from model equations (see Section 1.4.5), but for models such as Equations (1.1) and models developed in Chapters 2, 3 and 4 of this thesis, the basic reproduction number is calculated as follows. We note that the disease will spread if the number of infectious individuals increases, i.e. $\frac{dI}{dt}>0$. From Equations (1.1), this implies the condition for infection growth is $\beta SI - \sigma I>0 \Rightarrow \frac{\beta SI}{\sigma I} \Rightarrow \frac{\beta S}{\sigma}>1$. But initially $S \approx N$, so the disease will increase if $\frac{\beta N}{\sigma}>1$. Hence the expression of the basic reproduction number is $R_0 = \frac{\beta N}{\sigma}$. We discuss limitations and possible improvements of this formulation of R_0 is Section 1.4.5.

An infection with a high basic reproduction number produces large epidemic outbreaks, and is difficult to control. The basic reproduction number for N3N2 (one of the strains of the flu virus) is approximately 2.5 [82]. The basic reproduction numbers for smallpox, measles and malaria are known to be 3 to 5, 16 to 18 and over 100, respectively [66].

Dynamics in the long term

The following theorem shows that the basic reproduction of the basic SIR model, Equations (1.1), or any epidemiological model, determines whether an infectious disease will *quickly die out* or *cause an epidemic*.

Theorem 1 *(a) If $R_0 \leq 1$, then the number of infectious individuals $I(t)$ decreases monotonically to zero as as $t \to \infty$.*

(b) If $R_0>1$, then $I(t)$ increases to a maximum value $I_{peak}(t)$, and then decreases to

zero as $t \to \infty$.

The scenario described in the second part of this theorem (i.e. increase of the number of infectious individuals) is referred to as an *epidemic*. Therefore the bell-shaped infection curves in Figure 1.2 indicate that the basic reproduction number of such a disease is greater that 1.

1.3.2 Extensions of the basic SIR model

Modeling demographic changes

The dynamics of infection outbreaks that span longer periods of time or in populations with shorter lifespans (e.g. microorganisms), are often affected by changes in the population size and composition of the host population. For instance, birth of new individuals is expected to increase the proportion of susceptible individuals. Similarly, natural death of susceptible or infectious individuals also affects the dynamics and feasibility to control the infection outbreak. Below we show how the basic SIR model can be improved to incorporate births and deaths.

We assume that there is birth of susceptible individuals into the population at a rate α, and natural death of members of the host population regardless of their disease statuses at a rate γ. Then the resulting modified SIR model is

$$\begin{aligned} \frac{dS}{dt} &= -\gamma S + \alpha - \beta SI \\ \frac{dI}{dt} &= -\gamma I + \beta SI - \sigma I \\ \frac{dR}{dt} &= -\gamma R + \sigma I. \end{aligned} \tag{1.5}$$

Similar to the discussion about the basic SIR model above, when model parameters

are chosen appropriately, the model can be solved and analyzed. The expression of the basic reproduction number for this model is

$$R_0 = \frac{\beta N}{\sigma + \gamma}.$$

The distinguishing feature between this expression and Equation (1.4) is that here R_0 contains an additional parameter γ (death rate) in the denominator, which carries information that reduction of the infectious population through natural death, reduces the basic reproduction number and the overall magnitude of the disease.

Modeling disease control

Depending on whether the host population are humans or animals, conventional methods of controlling infectious diseases include isolation, quarantine, vaccination, and culling. Therefore in order to understand (and help alleviate) real epidemics, there is need for mathematical models to incorporate and explore impacts of more factors affecting the infection (rather than only two events: transmission and recovery in the basic SIR model, Equations (1.1)). Here we show how vaccination can be incorporated into basic compartmental models.

Suppose vaccination of a proportion ψ of all newborns is introduced and that vaccine provides life-long immunity (i.e. vaccinated individuals remain immune to such a disease for life). Then we can modify Equations (1.5) so that some newborns gain immunity from vaccine and move to the recovered compartment (where the R compartment now constitutes individuals who have gained immunity through recovery from the disease and those who have been vaccinated), while other newborns remain

susceptible. The resulting model is

$$\begin{aligned}\frac{dS}{dt} &= -\gamma S + \alpha(1-\psi) - \beta SI \\ \frac{dI}{dt} &= -\gamma I + \beta SI - \sigma I \\ \frac{dR}{dt} &= -\gamma R + \sigma I + \alpha\psi.\end{aligned} \tag{1.6}$$

Modeling incubation period

The basic SIR model discussed above is applicable in diseases where upon contact with the disease agent (e.g. virus, bacteria), a susceptible individual is infected and immediately becomes infectious for some period of time, before they recover. However some infections such as foot and mouth disease are known to have the incubation period (where after contacting the disease, animals do not immediately show clinical signs, but remain non-infectious and transition into the infectious phase after a certain period of time- the incubation period). In this case the basic SIR model needs to be modified by including an additional compartment: the *exposed*, E compartment, which represents individuals/ animals that have had contact with the disease but are not yet infectious. The resulting model is referred to as the SEIR model. If the latency period (period of time spent in the E compartment) is $\frac{1}{\nu}$ then the corresponding SEIR model (with births, deaths and vaccination) is

$$\begin{aligned}\frac{dS}{dt} &= -\gamma S + \alpha(1-\psi) - \beta SI \\ \frac{dE}{dt} &= -\gamma E + \beta SI - \nu E \\ \frac{dI}{dt} &= -\gamma S + \nu E - \sigma I \\ \frac{dR}{dt} &= -\gamma R + \sigma I + \alpha\psi,\end{aligned} \tag{1.7}$$

where the initial conditions are

$$S(0) = S_0 \ , \ E(0) = E_0 \ , \ I(0) = I_0 \ , \ R(0) = R_0 \ , \ S_0 + E_0 + I_0 + R_0 = N.$$

Some compartmental models consider more than four compartments, but the characteristics of the disease and the purpose of the model determine the choice of compartments to include in a model. For instance, upon contact with the human immunodeficiency virus (HIV) a previously susceptible S individual acquires the virus and remains infectious I for the rest of their life, therefore, the appropriate compartmental model formulation is a SI model; the SIS model is applicable to diseases in which already infected individuals may be re-infected (e.g. chlamydia, gonorrhea) [63]. Other acronyms for compartmental models are SEIRS, SEI, SEIS, MSEIR, etc, where the M compartment contains individuals with passive immunity (applicable to childhood infections where, for example, a previously infected mother passes immunity to a newborn infant across the placenta)[56].

1.4 Some limitations of compartmental models in epidemiology

Despite the development and successful application of basic compartmental models to some infections, this modeling approach involves making a number of simplifying assumptions that often influence the dynamics of most diseases. Below we discuss some notable shortcomings of modeling using the basic compartmental models, and comment on alternative mathematical modeling frameworks in the literature.

1.4.1 Homogeneity vs. Heterogeneity

Basic compartmental models are formulated by averaging over individuals belonging to the same compartment such that susceptible individuals possess the same attributes with respect to the disease, the infectious compartment constitutes characteristically equal individuals, etc. That is, compartmental models assume homogeneity of individuals occupying the same compartments. However, in reality individuals who have the same disease states are themselves heterogeneous entities and their differences affect the dynamics of most infectious diseases. For instance, the spread of airborne infectious such as flu is likely to be more prominent among school-going kids, than between kids and adults because of a higher level of interactions among kids, e.g. in schools and playgrounds. Besides age, other human heterogeneities that affect the dynamics of infectious diseases are gender, personal habits and the location of members of the population in relation to risk of acquiring or transmitting the disease. Thus, basic compartmental models ignore such heterogeneities, and instead assume that, for instance, individuals in the susceptible compartment have the same level of susceptibility.

Early extensions of the basic compartmental models have incorporated the heterogeneities mentioned above by subdividing each of the S, I and R compartments to reflect greater structure within the host population. For example, the susceptible pool can be divided into S_a (the number of susceptible adults) and S_k (the number of susceptible kids) and the infectious pool can be divided into I_a (the number of infectious adults) and I_k (the number of infectious kids). Next, different transmission

parameters β_a, β_k and β_{ak}, can be prescribed to describe the rates at which the disease is transmitted among adults, among kids and between adults and kids, respectively. The resulting modification of Equations (1.1) is

$$\begin{aligned}
\frac{dS_a}{dt} &= -\beta_a S_a I_a - \beta_{ak} S_a I_k \\
\frac{dS_k}{dt} &= -\beta_k S_k I_k - \beta_{ak} S_k I_a \\
\frac{dI_a}{dt} &= \beta_a S_a I_a + \beta_{ak} S_a I_k - \sigma I_a \\
\frac{dI_k}{dt} &= \beta_k S_k I_k + \beta_{ak} S_k I_a - \sigma I_k \\
\frac{dR_a}{dt} &= \sigma I_a \\
\frac{dR_k}{dt} &= \sigma I_k,
\end{aligned} \tag{1.8}$$

where the initial conditions are

$S_a(0) = S_a0$, $S_k(0) = S_k0$, $I_a(0) = I_a0$, $I_k(0) = I_k0$, $R_a(0) = R_a0$, $R_k(0) = R_k0$ and $S_a0 + S_k0 + I_a0 + I_k0 + R_a0 + R_a0 = N$.

However, the problem with subdividing the host population to introduce heterogeneities as described above is that homogeneity still characterizes individuals occupying each of those subgroups. That is, the compartments containing kids or adults are assumed to be homogeneous themselves. Therefore, even though it will increase the number of equations and overall complexity of the model, more heterogeneities need to be considered in order to model real epidemics. For instance, for infections such as flu, it is epidemiologically realistic to divide the kids compartment further into school-going kids and those who do not go to school. Because of the uniqueness of individual members of the host population, it appears the most ideal approach is to consider a completely heterogeneous system, where the population is

subdivided to the level of an individual (i.e. one unique individual per compartment). This is known as *individual or agent-based modeling*.

In epidemiology, an individual-based model is a modeling framework in which each individual member of the population is considered to possess a set of unique attributes (such as gender, age, personal habits, contact rate, compliance to public health recommendation), which affect the disease dynamics [11, 109]. That is, actions of each individual and local interactions between members of the host population are determinants of the global consequence of an infectious disease. Computer programs such as $NETLOGO$ are usually used to develop and run simulations of individual-based models. The coding procedure involves distributing agents on a two-dimensional space, assigning each agent a set of rules and running simulations to observe the global behavior of the system. Individual-based models have also been widely used in social sciences to study systems such as patterns of consumer behavior towards adoption of new products or political ideologies.

1.4.2 Mass-action mixing vs. Spatial structure

The basic compartmental models are also referred to as *mean-field equations* (or mean-field approximations) because their widely used transmission term βSI implies that members of the host population mix homogeneously so that an infectious individual is equally likely to transmit the infection to any susceptible individual within the population (regardless of their location in relation to the infection source). This modeling approach fails to capture the *spatial* spread of infectious diseases.

Spatiality is defined as the effect that space has on interactions between

individuals [100, 85]. In the context of airborne infectious diseases such as influenza, SARS and foot and mouth disease, *space* refers to geographical proximity, such that the risk of infection decreases with the geographical distance between susceptible and infectious individuals. For example, foot and mouth disease is more likely to be transmitted between neighboring farms than between those that are far apart; flu is more likely to spread within a school, than between schools in the same town, etc. For sexually transmitted diseases such as HIV, spatiality is defined in terms of other mechanisms of interactions, e.g. sexual partnership networks. That is, HIV is more likely to spread from infected individuals to susceptible individuals within their sexual partnership network, than across networks. Rabies among the fox population of western Europe is understood to spread through local (rather than random) interactions among territorial animals [88].

It is apparent that while spatially oriented models tend to slow the rate at which the disease is disseminated within the population because of the assumption of localized transmissions, models that do not include the spatial structure of the host population, such as the mass-action mixing basic compartmental models, overestimate the spread of infectious diseases. In general a mathematical model that takes spatial transmission into consideration is expected to be more accurate than its non-spatial counterpart.

Most of this thesis focuses on the use of pair approximation models to explore (i) the impacts of spatial proximity of farms within the host population, on the dynamics and effective control of foot and mouth disease in endemic or near-endemic settings, and (ii) the impacts of space on the regulation of infectious diseases by

social interactions between members of the host population. Thus, spatiality forms the basis of the modeling approach adopted in this thesis. We discuss the importance of spatiality using a few models from the literature in Section 1.5, and describe and illustrate the derivation and general use of pair approximation models in Section 1.6.

1.4.3 Deterministic vs. Stochastic modeling

The basic SIR model discussed above is an example of a class of models referred to as *deterministic models*. These are models whose outputs are fully determined by the model parameters and the initial conditions [47, 127]. Thus in deterministic models, prescribing a unique set of parameters and initial conditions, leads to unique model outputs, regardless of the number of simulations carried out. For instance, the graphs in Figure 1.2 will take exactly the shapes when the model is re-run under the same parameter regime and initial conditions.

Deterministic models describe phenomena that occur on the basis of some certain physical law. However the natural world constitutes uncertain and sometimes random events and activities. For example, in Figure 1.2a the basic SIR model predicts that the infection I will decay and go extinct in about 50 days. However, in reality it is possible that at this point change in the behavior of members of the host population or change in environmental factors such as climatic conditions, may increase the transmission rate and prevent the outbreak from dieing out. Compared to deterministic models, models that incorporate inherent randomness of events by for example, prescribing varying model parameters to account for factors such as climate change and variability within and between individuals throughout the epidemic

outbreak, are generally more realistic. These are referred to as *stochastic models*.

Stochastic models model phenomena with random components such that the same set of model parameters and initial conditions will lead to different outputs when simulations are carried out more than once [47]. Two forms of stochasticity are often considered. Demographic stochasticity (also knows as demographic noise or internal fluctuations) describes the randomness that results from the discrete nature of individual members of the host population. Environmental stochasticity (or external fluctuations) accounts for sources of randomness such as change in climatic conditions.

Despite their importance, stochastic models are generally more complicated and lack analytical tractability. Thus, compared to basic compartmental models, it is more difficult to carry out analytic derivation and interpretation of the basic reproduction number from a stochastic model. As will be indicated in Section 1.6 and Chapters 2, 3 and 4, the spatially oriented models discussed in this thesis are derived for large population sizes, where we assume that the demographic noise around the averaged quantities tend to zero. We point out, however, that essentially every deterministic model is an approximation of some stochastic model. Thus, when model parameters are chosen carefully, a deterministic model is able to capture and study dynamics of real epidemics.

1.4.4 Exponential waiting times vs. Waiting times in real epidemics

The construction of mean-field equations models (or ordinary differential equations models in general) is based on the assumption that the periods of transition from one compartment to another are exponentially distributed. To see this, let T

be an exponential distribution. Then its probability density function takes the form $f(t) = 0$ if $t<0$ or $f(t) = re^{-rt}$ if $t \geq 0$ and $r > 0$. If a compartment had q individuals that each drew randomly from this distribution to determine when they will leave, then the resulting number of people in the compartment over time would be precisely the exponential decaying curve. In this case the average time spent in a compartment is calculated as $time = \int_0^\infty e^{-rt}dt = \frac{1}{r}$. Therefore, the basic SIR model (1.1) is based on the assumption that the average time spent in the *infectious* compartment is $\frac{1}{\sigma}$ time units.

However, the assumption of exponential waiting times for model variables is somewhat biologically unrealistic. For example, time to recovery is often better described by the normal distribution [111]. Other real distributions can also be adopted to describe waiting times, but this will lead to other, potentially more complex modeling frameworks than the simpler, but to some extent informative, ordinary differential equations models. In [7] the authors explored a general vaccine waning (loss of vaccine-induced immunity) function (i.e. non-exponentially-distributed period of protection by vaccine) to describe the disease dynamics as a system of integro-differential equations (equations involving both derivatives and integrals of model state variables). Solving integro-differential equations is generally more expensive than dealing with ordinary differential equations.

1.4.5 Inadequate estimation of the basic reproduction number

Because the basic reproduction number provides information about the potential extent of spread of an infection and feasibility for its control, calculations or

estimations of this quantity need to be as accurate as possible. The fact that basic compartmental models assume homogeneous-mixing of members of the host population, means that the corresponding calculated expressions of the basic reproduction number do not take into consideration the spatial spread of infectious diseases. Thus, while local interactions between spatially connected members of the host population are crucial in the spread of an infection, calculating R_0 under an assumption that an infectious individual can transmit the disease to any susceptible individual in the population, regardless of their spatial distance from the infection source, overestimates the true value of the basic reproduction number. Secondly, in real epidemics, stochastic events such as sudden change in climate or re-introduction of an invasive infection agent can lead to a rapid spread of the disease even when the calculated R_0 falls below unity. Similarly, stochasticity can lead to a halt in the spread of an infection even when the calculated expression of the basic reproduction number is greater than 1. Therefore, it is important to construct reasonably realistic model equations, which incorporate as much as possible, all aspects of infectious diseases, and derive more informative expressions of the basic reproduction number.

General limitations of the application of basic reproduction number

The use of different calculation methods to derive the basic reproduction number results in the construction of different expressions of R_0 for the same disease. However, such expressions have the common property that they all have a threshold at 1 [76]. Besides the technique used in this thesis, other methods for calculating the basic reproduction number include the survival function, the next generation matrix method, eigenvalues of the Jacobian matrix and the existence of the endemic

equilibrium. While some of these methods produce similar expressions of the basic reproduction number, others do not agree with each other [76]. Thus, it is important for a method of the derivation of R_0 to provide thorough information about the underlying model assumptions and evidence that its threshold is epidemiologically meaningful. However, we remark that comparison of various methods for calculating the basic reproduction number is beyond the scope of this thesis.

1.5 Spatially oriented mathematical models of infectious diseases

As mentioned above, this thesis develops and investigates spatial transmission and control of infectious diseases. Therefore, before we present the modeling approach adopted in this thesis, we discuss ways in which some types of mathematical models incorporate spatiality.

1.5.1 Metapopulation models

A metapopulation is a group of same-species populations that are separated into subpopulations by space. Metapopulations exist in virtually all life forms. Examples metapopulations include human subgroups residing in different parts of cities, countries and continents, animals and plants occupying different habitats. For animals and humans, biologically important interactions (e.g. disease transmission) between subpopulations often take place through movement of individuals from one subpopulation to another, while seed dispersion through wind, insects or animals

and/ or humans facilitates interaction between subpopulations of plants. Figure 1.3 is a pictorial illustration of a metapopulation. The arrows connecting subpopulations

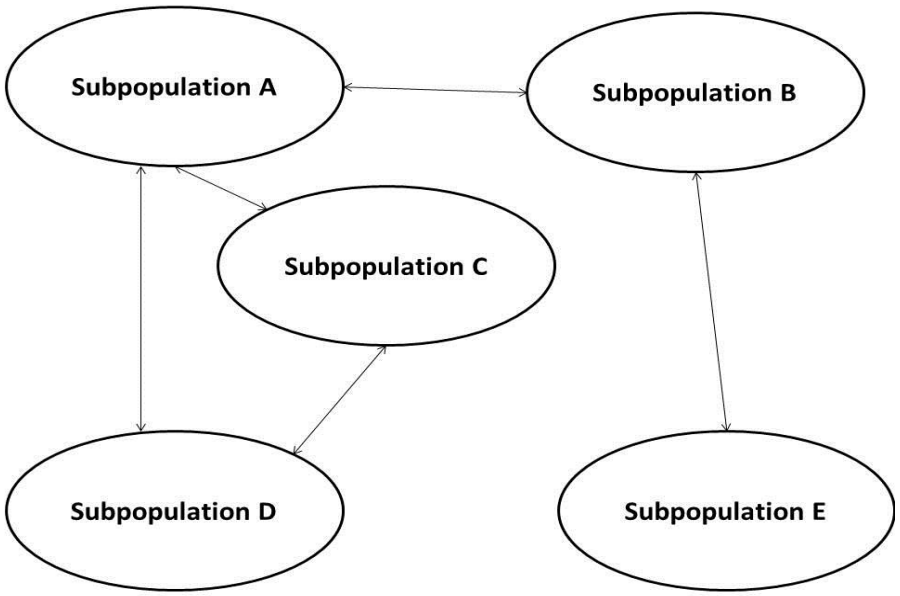

Figure 1.3: Flow diagram for metapopulations.

in the diagram indicate possibilities for interaction between the subpopulations.

One of the simplest ways for modeling metapopulations is to derive mean-field equations for the spread of the disease within each subpopulation and define coupling terms, which measure the rates at which hosts migrate from one subpopulation to another.

1.5.2 Reaction-diffusion equations

Reaction-diffusion equations models are presented as partial differential equations (PDEs) of the form,

$$\frac{\partial u}{\partial t} = F(u) + D \bigtriangledown^2 u, \tag{1.9}$$

where in epidemiology, $u = u(t, x)$ represents the density/ concentration of state u (e.g. susceptible) individuals occupying a position $x \in \Omega \subset \mathbb{R}^n$ at time t where Ω is an open set; $F(u)$ represents transmission of the infection to a susceptible individual occupying a given point x at time t; D is the diffusion term and it corresponds to dispersion of members of the host population; $\bigtriangledown$ is the Laplace operator [58, 133, 36].

Equation (1.9) can be extended to incorporate more than one class of disease states so that u and $F(u)$ are considered to be vectors, while D is a column vector consisting of diffusion coefficients. For instance, the diffusion-reaction equations governing the dynamics of the SEIR-type model requires that state variables be defined in terms of both time t, and space x: $S = S(t, x)$, $E = E(t, x)$, $I = I(t, x)$ and $R = R(t, x)$. Therefore, System (1.7) transforms to the following spatially oriented system,

$$\begin{aligned}
\frac{\partial S}{\partial t} &= -\gamma S + \alpha(1 - \psi) - \tau SI + D_1 \frac{\partial^2 S}{\partial x^2} \\
\frac{\partial E}{\partial t} &= -\gamma E + \tau SI - \nu E + D_2 \frac{\partial^2 E}{\partial x^2} \\
\frac{\partial I}{\partial t} &= -\gamma S + \nu E - \sigma I + D_3 \frac{\partial^2 I}{\partial x^2} \\
\frac{\partial R}{\partial t} &= -\gamma R + \sigma I + \alpha\psi + D_4 \frac{\partial^2 R}{\partial x^2}.
\end{aligned} \tag{1.10}$$

where τ (> 0) is the transmission rate, ν (> 0) the rate of transition from the exposed to the infectious state, σ (> 0) the recovery rate, α (> 0) the birth rate, γ (> 0) the

death rate and D_i (> 0) $(i = 1, 2, 3, 4)$ the diffusion coefficients. The initial conditions are

$$N_0 = \frac{1}{|\Omega|} \int_\Omega [S(0,x) + E(0,x) + I(0,x) + R(0,x)] d\Omega,$$

while the boundary conditions are

$$\varphi : (t,x) \in \Omega \times \mathbb{R}^+ \to \varphi(t,x) \in \mathbb{R}^+ \ , \forall \varphi \in \{S, E, I, R\}.$$

Reaction-diffusion equations have also been used to study spatially oriented systems in natural sciences [60, 115], social sciences [61], and ecology [89].

1.5.3 Network models

A network is a collection of points and connections between them. In mathematical terms, a network is also referred to as a graph, and it is described as a structure consisting of a set of *vertices* and *edges* connecting the vertices. That is, a graph G is defined as $G = (V, E)$ where V is a set of vertices and E is a set of edges connecting vertices, i.e. $E \subseteq V \times V$ [97, 28].

Networks are generally used to describe the spatial distribution of a variety of systems such as technological systems (e.g. the Internet, power grid, telephone networks, transportation networks), social networks (e.g. social groups, affiliation networks) and biological systems (e.g. neural networks, food webs), where each node represents a discrete entity of the system. In technological systems such as telephone networks, information is transmissible between points i and j, only if the two are connected (i.e. when i and j share an edge); in social sciences, transfer of an idea

from individual i to individual j occurs when the two are connected on a social network, etc. In epidemiology vertices (or nodes) represent individuals or groups of individual members of the host population while edges represent forms of interaction, so that transmission of the disease can take place between individuals i and j, only if they are connected and one is infectious while the other is susceptible.

Where necessary, it may be beneficial to construct and explore networks in which nodes are connected through direction-oriented edges to indicate the direction of flow of information. Such graphs are referred to as *directed graphs* [97]. For example, in telephone networks, if nodes i and j are connected, and if information is transmissible from i to j, and can also be transmitted from j to i, then the corresponding notation is $i \leftrightarrow j$. However, in epidemiology the infection is transmitted from an infectious individual to their susceptible contacts. Therefore $i \rightarrow j$ implies that individuals i and j are connected and i is infectious while j is susceptible. Figure 1.4 provides pictorial representations of directed and *undirected graphs*.

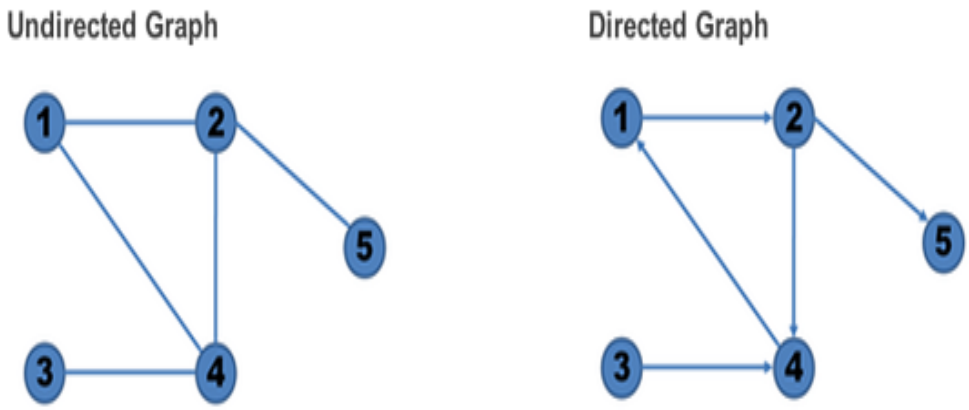

Figure 1.4: Undirected and directed graphs [1].

The number of edges leaving or departing from a node is referred to as its *degree*. That is, the degrees of nodes labeled $1, 4$ and 5 in Figure 1.4 are 2, 3 and 1, respectively. Consider the directed graph in Figure 1.4. Then in epidemiological terms, a susceptible individual at location 1 can acquire the disease directly only from an infectious individual at location 4; individuals at location 5 do not have contacts to whom they could transmit the disease.

In some applications, graphs are improved by assigning weights to each edge such that edges with more weight can transmit larger amounts of information (or transmit it at higher rates), while those that weigh less transmit smaller amounts of data (or transmit it at lower speeds). Such networks are referred to as *weighted graphs*. For example, in epidemiology this concept can be used to address the idea that an infected individual is more likely to transmit an infection to friends with whom they interact regularly than to friends with whom they rarely associate. In this case transmission rates on edges connecting closely related individuals will be larger than on those connecting individuals who are friends but interact less frequently.

In epidemiology the connections between individuals may be on the basis of geographical distance or other forms of relationships such as sexual partnership relations. Connected individuals on the network are sometimes also referred to as neighbors. Therefore in epidemiology, network models capture spatiality by considering the transmission of the disease through connected, but discrete susceptible and infectious individuals. The node degree and weights of edges (e.g. force of infection carried through the edge) connecting nodes on a network, affect the pattern of spread of infectious diseases.

It is often difficult to establish actual networks within which real infections propagate, but spatially oriented mathematical models have been used to study the dynamics of infectious diseases on several network types, which are usually based on the following classification: *regular, random , small-world* networks [4, 13, 72, 63, 56]. The distinguishing feature between these types of networks is mainly the level of randomness p in the neighborhood size of each individual. $p = 0$ represents regular networks (same number of neighbors per individual), $0 < p < 1$ represents small world networks (a few individuals with more contacts than others) while $p = 1$ represents random networks (random neighborhood size). The evolution of infectious diseases differ with the network structures within which the host population resides. Figure 1.5 shows these three typical network structures.

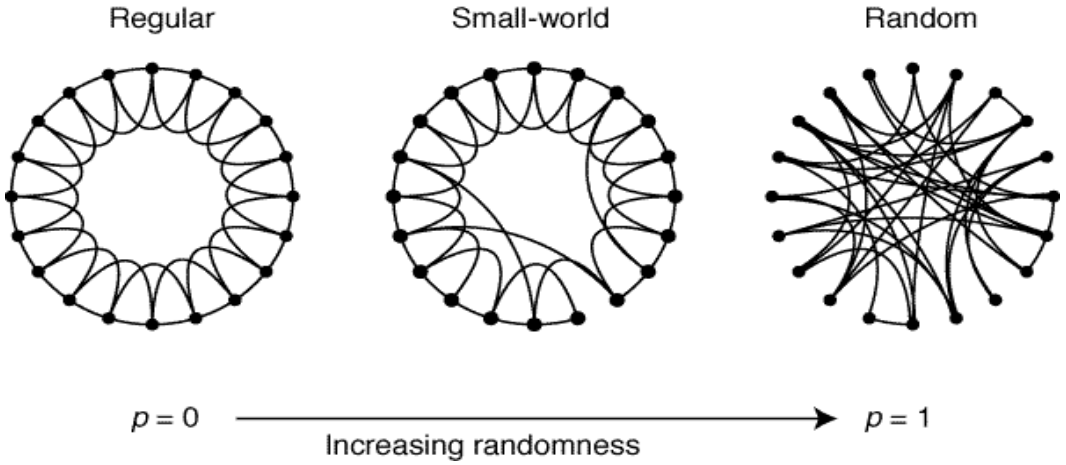

Figure 1.5: Network structures [130].

The development of powerful computer software has enabled generation and exploration of other more complicated, but supposedly suitable, network structures,

which mimic as much as possible, the spatial the spread of diseases. For example, dynamic and evolving networks (i.e. non-*static* networks), where individuals' neighborhood size varies with time, have been developed and used to study impacts of change of sexual partnerships overtime, on the dynamics of sexually transmitted infections such as HIV [12]. In the context of social sciences nodes can be created or change their degree based on factors such as variability in popularity of other nodes in the network.

Once a suitable network structure on which the disease disseminates has been chosen, an appropriate mathematical model can be designed and applied to study spatial dynamics of an infection. We remark that the mathematical modeling approach adopted in the next three chapters of this thesis, is based on the concept of spatial spread of infections on a number of network types, using ordinary differential equations. Below are other common descriptions of infectious diseases modeling on network structures.

Cellular automata

Cellular automaton is a special network framework characterized by a collection of *cells* on a *grid* that evolve over time (i.e. change in color, shape or labeling, etc.) due to a number of set rules and states of neighboring cells [132, 64]. A cell may constitute one or more individuals. Computer software is often used to program and run simulations of cellular automata models to observe the emerging behavior of a system. One of the widely recognized applications of cellular automata models is in John Conway's *game of life* that was devised in 1970 [73]. In this game the cellular automata grid consists of a collection of cells that, based on some mathematical rules,

can live, die or multiply, so that depending on the prescribed initial conditions of the system, the cells form various patterns throughout the course of the game. Typical rules that determine transition from one time step to another include: *any live cell with fewer than two live neighbours dies, as if caused by under-population; any live cell with two or three live neighbours lives on to the next generation; any live cell with more than three live neighbours dies, as if by overcrowding; any dead cell with exactly three live neighbours becomes a live cell, as if by reproduction* [132]. Figure 1.6 is a two-dimensional representation of a pattern of cells formed in a cellular automata model.

Figure 1.6: Game of life [129].

In the context of infectious diseases, each cell on the cellular automata grid corresponds to one or more individuals and spatial spread is captured by transmis-

sion of the disease between neighboring cells. For instance, if each cell contains one individual and if three adjacent cells labeled s, i and r (where s and r are not directly connected, but are both neighbors of i) represent susceptible, infectious and recovered individuals, respectively, at time t, then in the next time step, $t+1$, a previously s cell may transform to i due to disease transmission. This newly infected cell may remain infectious for a number of time steps, and ultimately turn to r. For a disease that does not provide life-long immunity, the recovered cell may neighbor an infectious cell resulting in re-infection. Various patterns of disease spread result from varying prescriptions of the initial conditions of the model.

The grid in Figure 1.6 serves as illustration of this concept, but grids of other cellular automata models include a one-dimensional line and two-dimensional triangular and rectangular grids. Although it seems simple to prescribe rules and observe emerging behavior from a cellular automata system, analysis of these models is complicated.

Pair formation models

In epidemiology, pair formation models are often used to capture spatiality by considering repeated contacts within relationships that occur in non-geographical networks such as sexual partnerships. Figure 1.7 illustrates the processes involved in the formation and disintegration of sexual partnerships, and their impacts on the dynamics of a *susceptible-infectious-susceptible* (SIS) pair formation model. This model captures the idea that individuals may stay single or enter into sexual relations with individuals of the same or different disease status. The rates of transition from one compartment to another can be defined to formulate an ODE system with five

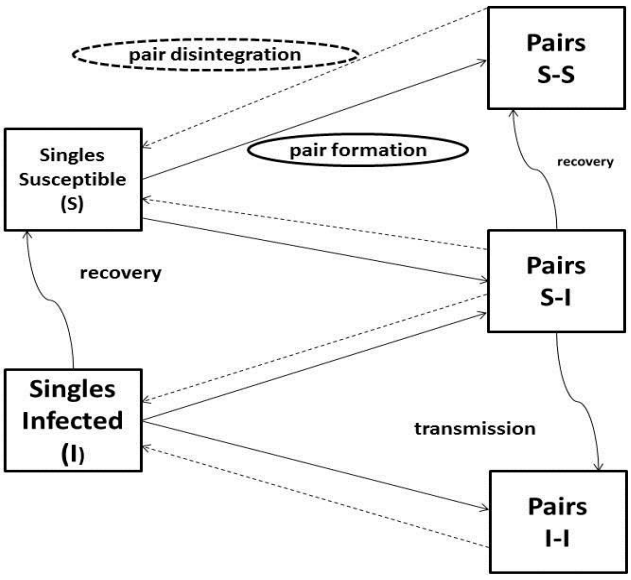

Figure 1.7: Flow chart for SIS pair formation model.

state variables (S, I, S-S, S-I and I-I), which can then be studied to evaluate, among others, effects of long term or short term pair formations and disintegration on the disease dynamics.

Pair formation models are a special case of pair approximation models, which we describe below, and apply in the rest of this thesis.

1.6 Pair approximation models

As indicated above, realistic epidemiological models are those that capture as much as possible, the actual aspects of infectious diseases such as characteristic heterogeneities of members of the host population, spatially oriented disease transmission and control, and stochastic effects. The quest to model infectious diseases

accurately has led to the invention of explicitly spatial population models that incorporate absolute discreteness of individual members of the host population, as well as effects of stochasticity and probability. However, even though explicitly spatial, individual-based models are good for developing intuition and formulation of conjunctures, most of them suffer from a number of deficiencies such as lack of mathematical understanding of the models (making it difficult to make conclusions about reasonableness of model outputs), inadequacy of biological realism, lack of analytical tractability (resulting in exploration of simulations alone) [104, 15].

This thesis develops and explores pair approximation models (a subclass of *moment closure approximations*), which not only address the spatial spread of infectious diseases, discreteness of members of the host population and stochasticity, but are also *more tractable* and their derivation makes use of biologically reasonable assumptions. Below, we discuss moment closure approximations in general and describe and illustrate the derivation of pair approximation models.

1.6.1 Moment closure approximations

Moment closure approximations (MCAs) are mathematical models that capture spatiality by considering a network of individuals or sites whose states change at rates determined by the states of their neighbors [64]. This description of propagation or dissemination of information across a network, is similar to the processes involved in cellular automata models, but as will be discussed in Section (1.6.3), MCAs also capture the variety of statistical structures governing the neighborhoods of each node in the network. Depending on the dynamical system of interest, MCAs

models capture spatiality by modeling spread of information/signal among pairs of connected nodes $(X - Y)$, connected triples $(X - Y - Z)$, quadruples, etc., on a network [57, 95, 66]. The dynamics of the system are then described by a set of differential equations, which track down time evolution of the numbers of pairs, triples, quadruples, etc.

In epidemiology, moment closure approximations can be described as models that capture spatiality by employing connected pairs, triples, etc., of individuals as state variables, and allowing disease transmission to take place only between connected susceptible and infectious individuals in the network. That is, in moment closure approximations, the overall pattern of spread of the disease is determined by local transmissions within each individual's neighborhood. Some solutions of a SIR-type moment closure approximation model are the number of edges joining susceptible and infectious individuals at time t, $[SI](t)$ and the number of *infected-susceptible-recovered* triples at time t, $[ISR](t)$.

In Section (1.6.3), we show that the construction of moment closure approximations involves derivation of *stochastic differential equations*, which describe time evolution of connected individuals on the network. These differential equations are also referred to as *equations of motion*. The following order of basic steps involved in the derivation of equations of motion for moment closure approximations, with regards to infectious diseases, is obtained from [64, 104, 18, 42, 17, 15, 95].

The first step is to derive the equations of motion for the number of connected pairs of individuals on a network. The equations of motion for pairs contain terms involving triples. Constructing the equations of motion for triples will have

terms involving quadruples. Continuation of this procedure will produce terms involving even higher correlations, leading to a possibly infinite hierarchy of equations of motion. Very large systems of equations are difficult to manage. Therefore suitable truncation techniques are usually adopted. Truncation of the hierarchy of equations of motion at a desired level, is carried out through a process known as *moment closure*. Moment closure techniques are based on statistical distributions of neighboring individuals, and they often rely on estimation of high-order correlations by lower-order correlations. When closure is done at the level of pairs (so that triples are approximated using pairs and singletons) then the process is called a *pair approximation*; when closure is made at the level of triples, then a triple approximation is adopted, etc. We demonstrate the derivation of pair approximation models in Section 1.6.3, and show how various forms of moment closures, at the level of pairs, are used to approximate triples with lower-order correlations.

1.6.2 Applications of moment closure approximations

Moment closure approximations have been applied in various research areas including physics (where the equations of motion describe statistical structure of complex fields) and chemical kinetics (to estimate the mean concentrations and the variances and covariances of the concentration fluctuations of species involved in stochastic chemical reactions, in spatially oriented media) [50, 74, 119]. Because dynamical systems in areas such as ecology and epidemiology are largely characterized by interactions between two sites/ individuals (e.g. an infectious disease is transmissible only between two individuals), the applicable moment closure approximations for

these systems are pair approximations (also referred to as second order moments). In epidemiology pair approximations have been used to describe spatial spread and control of human infections such as HIV [18] and measles [104, 66], and animal diseases such as foot and mouth disease [42, 95, 107].

1.6.3 Derivation of pair approximation models

Pair approximation models are the simplest correlation equations extending the homogeneous-mixing, mean-field equations [104, 15]. The equations of motion for pair approximation models describe time evolution of the number of singletons, $[X]$ and pairs of connected individuals, $[XY]$ on the network. Equations of motion for singletons contain terms involving pairs while equations of motion for pairs have terms involving the number of triples, $[XYZ]$. Several closure techniques for approximating triples into lower-order correlations (pairs and singletons) have been developed. They include the ordinary pair approximation (OPA), the triangular pair approximation (TPA) and the invasory pair approximation (IVPA), [64, 104, 18, 95, 107]. These closure techniques differ from one another in the way they make assumptions about the statistical distribution of neighbors around each individual, which affects the spread of the disease. For instance, the *binomial* ordinary pair approximation,

$$[XYZ] \approx \frac{(n-1)}{n}\frac{[XY][YZ]}{[Y]}, \tag{1.11}$$

where n is the average number of contacts per individual, assumes *conditional independence* of the infection statuses of neighbors of a given individual. For example, if a triple $X-Y-Z$ represents a *infectious-susceptible-susceptible* triple, i.e. $I-S-S$

triple, then the infection is transmissible directly from individual X to individual Y, but not to individual Z. Thus, there are *no triangles*. However, the triangular pair approximation,

$$[XYZ] \approx \frac{(n-1)}{n}\frac{[XY][YZ]}{[Y]}\left((1-\phi)+\phi\frac{N}{n}\frac{[XZ]}{[X][Z]}\right), \tag{1.12}$$

allows for the existence of a proportion ϕ of triangles in the network. These techniques are the most widely used pair approximation closures. The choice of a closure technique is generally dictated by the transmission dynamics of the disease or the scope of a mathematical model.

Below we use a procedure developed in [104, 18] to partially demonstrate the derivation of a pair approximation model that corresponds to the basic SIR model, Equations (1.1). We do this by constructing the equation of motion for the number of susceptible-infectious pairs, $[SI]$. After the derivation, we present the resulting full SIR pair approximation model. The following notations and conventions will be adopted in the derivation of pair approximations model equations:

$n_x(i)$ - number of state i neighbours of a node x;

$n_{xy}(i)$ - number of state i neighbours of a node x that has node y as a neighbour. That is, x and y are neighbours, therefore if y is in state i, then $n_{xy}(i)$ is at least 1;

ζ_x - disease state of node x;

ζ_{xy} - disease state of an edge involving x and y;

$[i]$ - number of state i nodes;

$[ij]$ - number of edges connecting a state i individual to a state j individual where $i \neq j$;

$[ii]$ - twice the number of edges connecting a state i individual to another state i individual. This convention is a consequence of the distinction between the edge from x to y and the edge from y to x;

$[ijk]$ - the number of triples connecting a state j individual to individuals of states i and k where $i \neq k$;

$[iji]$ - twice the number of triples connecting a state j individual to two state i individuals;

$n(i|j)$ - population-averaged value of $n_x(i)$ when $\zeta_x = j$. That is,

$$n(i|j) = \frac{1}{[j]} \sum_{\zeta_x = j} n_x(i).$$

Therefore,

$$n(i|j) \ = \frac{[ij]}{[j]} \text{ and } n(i|i) \ = \frac{[ii]}{[i]}; \tag{1.13}$$

$n(i|jk)$ - population-averaged value of $n_{xy}(i)$ when $\zeta_{xy} = jk$. That is,

$$n(i|jk) = \frac{1}{[jk]} \sum_{\zeta_{xy} = jk} n_{xy}(i).$$

Therefore,

$$n(i|jk) \ = \frac{[ijk]}{[jk]}, \text{ where } i \neq k \text{ and } n(i|ji) \ = 1 + \frac{[iji]}{[ij]}; \tag{1.14}$$

$\rho_x(i|j)$ - stochastic fluctuations of quantities $n_x(i)$ from the corresponding population-averaged values $n(i|j)$. That is, $\rho_x(i|j) = n_x(i) - n(i|j)$ and it satisfies

$$\sum_{\zeta_x = j} \rho_x(i|j) = 0;$$

$\rho_{xy}(i|jk)$ - stochastic fluctuations of quantities $n_{xy}(i)$ from the corresponding population-averaged values $n(i|jk)$. That is, $\rho_{xy}(i|jk) = n_{xy}(i) - n(i|jk)$ and it satisfies

$$\sum_{\zeta_{xy}=jk} \rho_x(i|jk) = 0.$$

To find higher order moments $n(i|jk)$ we must know how $n_{xy}(i)$ are distributed across the network. If individuals i and k are conditionally independent and each individual in the population has the same number of contacts n, then it can be argued on heuristic grounds that triples can be approximated into lower-order moments by the binomial ordinary pair approximation

$$n(i|jk) = \frac{n-1}{n} n(i|j) \ , \ i \neq k \tag{1.15}$$

and

$$n(i|ji) = 1 + \frac{n-1}{n} n(i|j). \tag{1.16}$$

The expressions are different for a random network that allows for conditional independence of neighbors of an individual. Here the Poisson ordinary pair approximation is appropriate

$$n(i|jk) = n(i|j) \ , \ i \neq k \tag{1.17}$$

and

$$n(i|ji) = 1 + n(i|j). \tag{1.18}$$

We proceed with the derivation of the equation of motion for susceptible-infectious pairs of individuals as follows. Let $g(t)$ be a real-valued function of time

t representing any state variable of a model. The equation of motion for $g(t)$ is determined by summing over all events in the network that affect $g(t)$. Thus, the dynamics of $g(t)$ are governed by

$$\frac{dg(t)}{dt} = \sum_{\epsilon \in events} r(\epsilon)\Delta g(\epsilon), \tag{1.19}$$

where $r(\epsilon)$ is the rate at which event ϵ takes place and $\Delta g(\epsilon)$ is the change this event causes in $g(t)$. Equation (1.19) is referred to as the *master equation*. Note that we are deriving a SIR pair approximation model that has no control measures, therefore, the only events we consider are *infection* across links connecting susceptible and infectious individuals at a rate τ and *recovery* of infectious individuals at a rate σ, moving them to the R compartment. The changes that these events make on $S-I$ pairs are either *creation* or *destruction*, resulting in an increment or reduction $[SI]$. A complete list of events and their effects on the time evolution of the number of susceptible-infectious pairs is:

(a) Infection at a rate τ of the susceptible individual by their infectious neighbour in a $S-I$ pair. This process destroys a $S-I$ pair and creates a $I-I$ pair. Also, infection at a rate τ of the susceptible individual *from the left* in a triple $I-S-I$, destroys a $S-I$ pair to create a $I-I$ pair.

(b) Infection at a rate τ of a susceptible individual in a $S-S$ pair, by a neighboring infectious neighbor creates a $S-I$ pair.

(c) Recovery at a rate σ of the infectious individual in a $S-I$ pair transforms $S-I$ to $S-R$. Thus, this process *destroys* a $S-I$ pair.

We contextualize the network-based notations outlined above to the SIR model, cal-

culate the contribution of each event to the sum in the master equation for $[SI]$ and write

$$\frac{d[SI]}{dt} = \sum_{\zeta_{xy}=SI} \tau(n_{xy}(I))(-1) + \sum_{\zeta_{xy}=SS} \tau(n_{xy}(I))(+1) + \sum_{\zeta_x=S} \sigma(n_x(I))(-1). \quad (1.20)$$

The first term of Equation (1.20) corresponds to event (a) above, the second term to event (b), and the third term to event (c). The *positive* + and *negative* − signs in this formulation indicate *creation* or *destruction* of the $S - I$ pair, respectively.

Next, we replace quantities $n_x(I)$ and $n_{xy}(I)$ by their population-averaged values plus the stochastic fluctuations of those quantities from the means at the nodes x and pairs xy. For example, if the state of a node y is I, then $n_{xy}(I)$ is replaced by $n(I|SI) + \rho_{xy}(I|SI)$. Therefore, the equation of motion for $[SI]$ transforms to

$$\begin{aligned} \frac{d[SI]}{dt} &= -\sum_{\zeta_{xy}=SI} \tau(n(I|SI) + \rho_{xy}(I|SI)) + \sum_{\zeta_{xy}=SS} \tau(n(I|SS) + \rho_{xy}(I|SS)) \\ &\quad - \sum_{\zeta_x=S} \sigma(n(I|S) + \rho_x(I|S)). \end{aligned} \quad (1.21)$$

In this way, the equation of motion for $[SI]$ is a stochastic ordinary differential equation.

We simplify Equation (1.21) by taking out terms such as $n(I|SI)$ and the model parameters out of the sums and further noting that terms such as $\sum_{\zeta_x=S} \rho_x(I|S)$, which represent fluctuations are zero by definition. Evaluating the sums yields

$$\frac{d[SI]}{dt} = -\tau n(I|SI)[SI] + \tau n(I|SS)[SS] - \sigma n(I|S)[S].$$

Applying the identities in Equations (1.13) and (1.14) and the binomial ordinary pair approximation, Equations (1.15) and (1.16) simplifies the equation of motion for $[SI]$

to

$$\frac{d[SI]}{dt} = -\tau[SI] - \tau[ISI] + \tau[ISS] - \sigma[SI] \tag{1.22}$$

where

$$[SSI] \approx \frac{(n-1)}{n}\frac{[SS][SI]}{[S]} \text{ and } [ISI] \approx \frac{(n-1)}{n}\frac{[SI]^2}{[S]}.$$

The full SIR pair approximation model (before applying a closure technique) is given as

$$\begin{aligned}
\frac{d[S]}{dt} &= -\tau[SI] \\
\frac{d[I]}{dt} &= \tau[SI] - \sigma[I] \\
\frac{d[R]}{dt} &= \sigma[I] \\
\frac{d[SS]}{dt} &= -2\tau[SSI] \\
\frac{d[SI]}{dt} &= \tau([SSI] - [ISI] - [SI]) - \sigma[SI] \\
\frac{d[SR]}{dt} &= -\tau[ISR] + \sigma[SI] \\
\frac{d[II]}{dt} &= 2\tau([ISI] + [SI]) - 2\sigma[II] \\
\frac{d[IR]}{dt} &= \tau[ISR] + \sigma([II] - [IR]) \\
\frac{d[RR]}{dt} &= 2\sigma[IR].
\end{aligned} \tag{1.23}$$

The factor 2 in the equations of motion for same-status pairs $[XX]$ comes from the counting convention of edges explained above, such that, for example, $[II]$ denotes twice the number of infected-infected pairs. If the disease spreads on a regular network where the neighborhood size is n and the total population size is N, then at any time

t, the condition

$$n \times N = [SS] + 2[SI] + 2[SR] + [II] + 2[IR] + [RR]$$

holds.

Simulation results of pair approximation models

The system of Equations (1.23) as well as a chosen closure technique can can be simulated using a computer program (e.g. *MATLAB*) to obtain, among others, graphs showing time series of the numbers of susceptible, infectious, recovered individuals, susceptible-susceptible, susceptible-infectious, etc., pairs of individuals. Figure 1.8 compares time series for infectious individuals from the pair approximation model described by Equations (1.23), for scenarios where the neighborhood sizes are $n = 2$ (closed line graph) and $n = 4$ (square grid on a torus). Figure 1.8 illustrates that pair approximation models capture local transmission dynamics, where the disease is transmissible only between connected individuals, so that the larger the number of contacts per individual, the large would be the disease magnitude. In contrast, because mean-field equations models are derived under an assumption that members of the host population mix homogeneously (so that essentially the number of neighbors per individual is $n = N$, where N is the total population size), they overestimate the actual basic reproduction numbers of infectious diseases.

Modeling disease control in pair approximation models

Strategic deployment of disease control measures, such as prompt vaccination or culling in at-risk premises (determined by their spatial distance from the infection source point), have been found to be more cost effective than nonstrategic

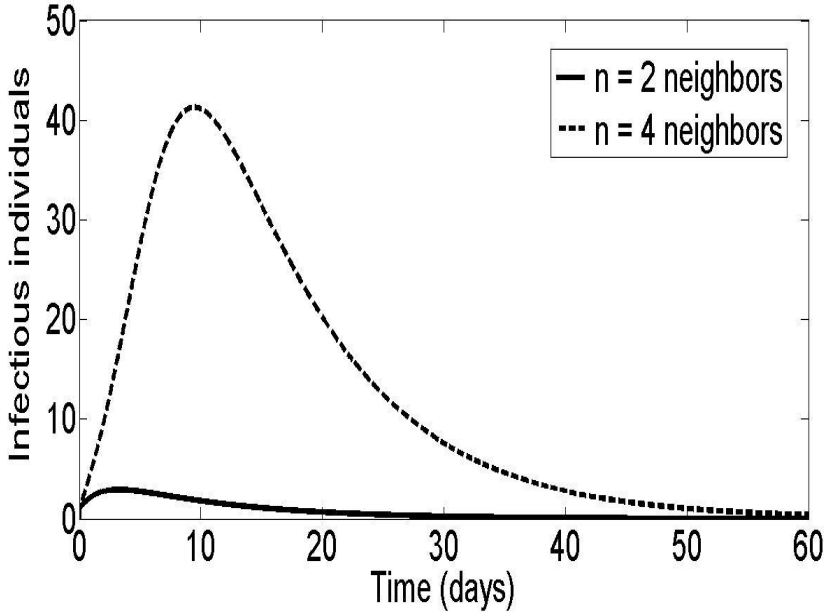

Figure 1.8: Time series of infectious individuals for the SIR pair approximation model, Equations (1.23), varying the neighborhood size, n. $\tau = 0.9\ day^{-1}$ and $\sigma = 0.1\ day^{-1}$. The population size is $N = 100$ and initial conditions are 1 infectious and 99 susceptible individuals.

administration of control measures. Pair approximation models allow for spatially targeted deployment of control strategies such as vaccination of individuals nearest to the infection source, culling of animals neighboring infected premises, etc. Vaccination of susceptible individuals who are highly at risk due to their close connection to infectious contacts, can be incorporated into the derivation process of $\frac{d[SI]}{dt}$ as one of the events that affect $[SI]$. For instance, let the rate of vaccination of susceptible individuals neighboring an infectious individual be ψ. Then Equation (1.22) is modified by adding vaccination terms $-\psi[ISI]$ and $-\psi[SI]$, so that

$$\frac{d[SI]}{dt} = \tau([SSI] - [ISI] - [SI]) - \sigma[SI] - \psi([ISI] + [SI]). \tag{1.24}$$

If vaccine confers life-long immunity, then vaccinated individuals may avoid infection and *move* from the S to the R compartment (which will now have to be defined accordingly), and remain in this compartment permanently. Alternatively, a separate compartment for vaccinated individuals V can be included, but this will increase the size of the system. However, if previously vaccinated individuals lose immunity from the vaccine in the long run, then another event (referred to as vaccine waning) comes into play, and this will reflect in the equations of motion of a model. We do not present the full model with vaccination here, but refer the reader to extensions of this concept in the subsequent chapters of this thesis.

Correlation function

A crucial aspect of pair approximation models lies in their capability to include correlations between neighboring individuals in the network. The correlation function, C_{XY} between neighboring individuals with disease statuses X and Y is given by:

$$C_{XY} = \frac{N}{n}\frac{[XY]}{[X][Y]}, \tag{1.25}$$

where n is the number of neighbours per individual (or average number of neighbors per individuals for networks where nodes have variable neighborhood sizes) and N is the total population size. The condition $C_{XY}<1$ corresponds to avoidance ($C_{XY} = 0$ to complete avoidance); $C_{XY} = 1$ random mixing and $C_{XY}>1$ aggregation of contacts with disease statuses X and Y [64, 95]. As illustrated in [64], correlation functions can be used to reduce the order of Equations (1.23), in order to deal with a smaller, easier-to-handle system referred to as *correlation equations*. However, in this thesis,

we make use of correlations between neighboring individuals as well as biologically reasonable assumptions about the disease, to derive spatially oriented expressions of the basic reproduction number for pair approximation models.

The basic reproduction number for pair approximation models

Here we demonstrate the derivation of the basic reproduction number for Equations (1.23), and comment on its qualitative value in comparison to the basic reproduction number computed under homogeneous-mixing, mean-field equations. An epidemic is expected to occur if the number of infectious individuals in the population increases. Thus the condition under which an outbreak will take off is

$$\frac{d[I]}{dt}>0 \Rightarrow \tau[SI]-\sigma[I]>0 \Rightarrow \frac{\tau[SI]}{\sigma[I]}>1.$$

Therefore, by definition, the expression of basic reproduction number is given by

$$R_0=\frac{\tau[SI]}{\sigma[I]}.$$

We simplify this expression by expressing the number of susceptible-infectious pairs of individuals, in terms of the correlation function between susceptible and infectious individuals, $C_{SI}=\frac{N}{n}\frac{[SI]}{[S][I]}$. This step transforms the above equation to

$$R_0=\frac{\tau}{\sigma[I]}\frac{n}{N}[S][I]C_{SI}=\frac{\tau}{\sigma}\frac{n}{N}[S]C_{SI}.$$

Recall that the basic reproduction number is described by the state of the disease at the initial stage of an outbreak, when almost the entire population is susceptible, i.e. when $[S]\approx N$. Therefore the basic reproduction number can be written as

$$R_0=\frac{\tau n}{\sigma}C_{SI}. \tag{1.26}$$

The correlation C_{SI} is not a constant, but its time evolution is controlled by the evolving proportions and spatial distributions of infectious and susceptible individuals, as the infection spreads. In fact, at the initial stage of an infection, when only one individual in the entire population is infected, so that $[S] \approx N$, then

$$C_{SI} = \frac{[SI]}{n[I]} \approx 1.$$

As the infection spreads (i.e. increase in the number of infectious individuals), C_{SI} decreases, and the *clustering* of infectious individuals creates a situation where there are few or no susceptible individuals neighboring the infection cluster. This gives rise to a decrease in the rate of spread of the disease, and the the outbreak may die out. Thus, C_{SI} reaches a minimum value C_{SI}^{min}. The infection may only start spreading again beyond this point if additional susceptible individuals neighbor the infection cluster. Therefore, the nature of events at the minimum value C_{SI}^{min}, determines whether or not an invasion will succeed. Thus, the actual expression of the basic reproduction number is a function of C_{SI}^{min},

$$R_0 = \frac{\tau n}{\sigma} C_{SI}^{min}. \tag{1.27}$$

The quantity C_{SI}^{min} is obtained by solving

$$\frac{d}{dt} C_{SI} = 0.$$

The equation of motion for the correlation between susceptible and infectious individuals is given by

$$\frac{d}{dt} C_{SI} = \frac{N}{n} \left(\frac{1}{[S][I]} \frac{d}{dt}[SI] + \frac{[SI]}{[S][I]} \left(-\frac{1}{[I]} \frac{d}{dt}[I] - \frac{1}{[S]} \frac{d}{dt}[S] \right) \right).$$

Next, we substitute the equations of motion for $S-I$ pairs, infectious and susceptible individuals from Equations (1.23), into the equation of motion for C_{SI} above. Further, when we apply the binomial OPA to approximate triples into pairs and singletons, then the resulting equation of motion for the correlation between susceptible and infectious individuals simplifies to

$$\frac{d}{dt}C_{SI} = \tau(n-1)\frac{[S]}{N}C_{SS}C_{SI} - \tau(n-1)\frac{[I]}{N}C_{SI}^2 - \tau C_{SI} - \tau n\frac{[S]}{N}C_{SI}^2 + \tau n\frac{[I]}{N}C_{SI}^2.$$

We make biologically reasonable assumptions about the disease to simplify this equation follows. At the beginning of an outbreak there are very few infectious individuals and the entire population constitutes almost only susceptible individuals. That is, when the total population size N is very large then at the initial stage of an outbreak $[I] << N$ and $[S] \approx N$. Implementation of these assumptions yields

$$\frac{d}{dt}C_{SI} = \tau(n-1)C_{SS}C_{SI} - \tau C_{SI} - \tau n C_{SI}^2.$$

Furthermore, we use the idea that if all individuals in the network have the same number of contacts then $[SS] \approx n[S]$, to write $C_{SS} = \frac{N}{n}\frac{[SS]}{[S][S]}$ as

$$C_{SS} = \frac{N}{n}\frac{n[S]}{[S][S]} = \frac{Nn}{n[S]} \approx 1,$$

. since at initial inoculation $[S] \approx N$. Therefore

$$\frac{d}{dt}C_{SI} = \tau(n-1)C_{SI} - \tau C_{SI} - \tau n C_{SI}^2,$$

and

$$C_{SI}^{min} = \frac{n-2}{n}$$

so that an explicit approximation of the expression of the basic reproduction number for the model described by Equations (1.23) is given by

$$R_0 = \frac{\tau(n-2)}{\sigma}. \tag{1.28}$$

Unlike the corresponding mean-field equations model, Equations (1.1), whose basic reproduction number is given by Equation (1.4), the basic reproduction number under pair approximation models is controlled by the spatial structure of the network (described by the neighborhood size n of each individual). In fact, when the neighborhood size is large, then the basic reproduction number will be large (see Equation 1.28). Since mean-field equations ignore effects of local correlations between members of the host population, but assume that an infectious individual is equally likely to transmit the disease to any susceptible member of the host population, regardless of the spatial location of the latter, the basic reproduction number derived from homogeneous-mixing models overestimates the true value of R_0 for most infectious diseases.

As mentioned before, in Chapters 2 and 3 of this thesis we develop pair approximation models and discuss the dynamics and control of foot and mouth disease (FMD) in endemic and near-endemic countries. The overall objective of these research manuscripts (Chapters 2 and 3) was to mimic as much as possible, the dynamics of FMD in Botswana, and explore feasible control strategies applicable to this near-endemic country. Below we present a survey of notable mathematical models of FMD in the literature, as well as the situation of the disease in Botswana. Also as stated above, Chapter 4 of this thesis discusses the use of pair approximation models to study

the control of infectious diseases by NPIs. Therefore, we also provide a discussion of some remarkable mathematical models that study the regulation of infectious diseases by non-pharmaceutical interventions.

1.7 Foot and mouth disease models

The following epidemiological information about FMD is found in almost any article discussing the disease including in [95, 124, 107]. FMD is caused by a highly contagious virus belonging to the Picornaviridae family. The FMD virus exists in 7 different strains and has up to 60 subtypes. It affects cloven-hoofed animals such as cattle, goats, sheep and some wild animals such as deer and buffalo. The virus is spread from one animal to another through, among others, direct contact with saliva, urine, seminal fluids and through expired air and excreted fecal matter. Upon contact with the virus susceptible animals become exposed, but are not yet symptomatic until a few days later (about 4 days in cattle, depending on the virus strain). When infectious, animals also display symptoms such as ruptured feet leading to limping, blistered mouth, stunted growth and overall poor quality of animal products such as milk and meat. Animals rarely die from FMD, rather infected animals recover to a health-compromised state, rendering them less profitable. Because during an outbreak health states of animals transition through the susceptible, exposed, infectious and recovered phases, the dynamics of FMD are best described by the SEIR-type modeling framework.

The availability of data on the 2001 epidemic outbreak of FMD in the United

Kingdom (UK) resulted in the development of several mathematical models describing the mechanism of the disease spread and exploration of impacts of control measures such as isolation and culling, which were adopted in the UK, as well as other plausible control strategies (e.g. vaccination) that could have controlled the disease more effectively or those that can potentially be used to prevent or control future outbreaks. Since 2001 efforts have been made to use country-specific databases to model patterns of spread and feasible control strategies against FMD in other countries (mostly in Europe and Asia). Because outbreaks in the UK and other developed countries are generally less frequent, traditional models of FMD have described dynamics and control of a single outbreak, and rarely consider long-term effects such as vaccine waning, natural immunity waning and re-importation of new disease agents. Below are brief descriptions of some widely referenced models of FMD in the literature.

1.7.1 The foot and mouth epidemic in Great Britain: pattern of spread and impact of interventions. N.M. Ferguson et al, 2001

This paper used data from the 2001 UK FMD epidemic outbreak entailing the pattern of spread and extent of control of the disease, to design a pair approximation model that was then used to explore impacts of potentially more effective control strategies, which could have been adopted in the UK. These control methods are ring culling (slaughtering of animals in farms deemed to be at a high risk of infection due to their geographical proximity to infectious farms) and ring vaccination (vaccination of animals in farms deemed to be at high risk of infection due to their geographical proximity to infectious farms). The state variables of this model are the numbers

of susceptible farms $[S]$, exposed farms $[E]$, infectious farms $[I]$, recovered farms $[R]$ and pairs of farms $[XY]$, where X and Y represent disease statuses- susceptible, exposed, infectious or recovered. In this article the equation of motion for the number of susceptible-infectious pairs of farms $[SI]$ is given by

$$\frac{d[SI]}{dt} = \nu[SE] - (\tau + \mu + \omega)([ISI] + [SI]) - \rho\beta[SI][I]/N,$$

where N is the total number of farms. The spatially oriented transmission rate across a contact, $\tau = (1-\rho)\beta/n$ is a function of the transmission coefficient of the virus, β, the proportion of contacts that are long range, ρ, and the average number of neighbors per farm, n. The rate at which exposed farms become infectious and the rate at which infectious farms recover are ν and σ, respectively. The parameters μ and ω are rates of ring culling and ring vaccination, respectively. This paper uses the triangular pair approximation, Equation (1.12), to approximate triples into lower order correlations.

Simulation results of this paper show that both ring culling and ring vaccination control foot and mouth disease more rapidly (than isolation, movement restriction, biosecurity and mass culling as well as surveillance, which where implemented during the 2001 epidemic outbreak in the UK) because they target infection *hot-spots* and reduce the *fuel* essential to maintaining the epidemic. However ring culling brings the disease under control more effectively than vaccination of susceptible animals during an outbreak, possibly due to the fact that vaccination delays to confer immunity after administration while implementation of culling immediately gets rid of animals, avoiding disease transmission instantly.

Dynamics of the 2001 UK foot and mouth epidemic: stochastic dispersal in a heterogeneous landscape. Keeling et al, 2001

This research paper explores the dynamics and control of the 2001 UK FMD outbreak using an individual farm-based stochastic model, where each farm is classified as either susceptible, incubating (i.e. infected, but not yet infectious), infectious and slaughtered (or removed by culling). Transmission of FMD between farms is determined by the number and type of livestock (so that e.g. the susceptibility and infectiousness of cattle are different from those of sheep), and the distance between susceptible and infectious farms (described by the spatial infection kernel- a carefully chosen function of distance that decreases with the distance between susceptible and infectious farms). In addition to consideration of various animal species, other heterogeneities adopted by this modeling framework include distinction between localized spread of the disease and possibility of long-range transmissions. The basic stochastic mathematical model is described as follows. The probability that a susceptible farm i becomes infected in a given day is

$$Probability = 1 - \exp\left[-S \times N_i \sum_{j \in infectious} T \times N_j K(d_{ij})\right],$$

where N_i is a vector of the number of animals of each type in farm i, and S and T are the corresponding vectors of susceptibility and transmission. $K(d_{ij})$ is the infection kernel (i.e. a decreasing function of the the distance, $d(i,j)$ between farms i and j).

The main results of this paper include the following. Culling of farms neighboring infected premises controls the disease more effectively by reducing the number of cases as well as the total number of culled farms, compared to culling of infected

premises only. This implies that it is ideal to implement both infected premises culling and well as culling in the neighborhood of infected premises. Even though vaccination was not used to control FMD in the UK in 2001, the simulation results of the model adopted in this paper show that while vaccination would have reduced the epidemic impact, culling of farms neighboring infected premises is a better strategy than ring vaccination combined with culling of infected premises. This is because vaccines do not immediately confer immunity upon administration, but they protect animals after a number of days, depending on the virus strain and animal species affected.

1.7.2 Modelling vaccination strategies against foot-and-mouth disease. Keeling et al 2003

Using the the dynamics and control of the 2001 UK FMD epidemic outbreak (i.e. single outbreak of FMD) as a motivating scenario, this article proposes potentially more effective means that could be used to prevent or control future epidemic outbreaks- implementation of both reactive vaccination (defined as vaccinating farms deemed to be at a great risk of infection during epidemic outbreaks) and prophylactic vaccination (defined as pre-outbreak vaccination, i.e. vaccination of farms in advance of an outbreak to prevent introduction of the disease into a population of farms). The modeling formulation adopted here is an extension of the article discussed in Section 1.7.1 above, since it uses a spatial individual farm-based model in which farms are assumed to be heterogeneous in terms of the composition of animal species, but the control strategies are either national prophylactic vaccination campaign or a combination of reactive vaccination and culling strategies (culling of infected premises and

culling of farms deemed to be at risk of infection) during an epidemic outbreak. Here the rate R at which a susceptible farm i is infected is given by

$$R_i = \sum_{L \in livestock} S_L N_L^i \times \sum_{j \in infectious} \sum_{L \in livestock} T_L N_L^j \times K(d_{ij}),$$

where N_L^i is the number of livestock of type L within a farm i; S_L is the susceptibility of livestock L; T_L is the transmission rate of livestock L; K is the transmission kernel, which is a decreasing function of the distance d_{ij} between farms i and j.

According to this article, prophylactic vaccination of a significant proportion of farms (about 30% based on the dynamics of the 2001 UK FMD outbreak), reduces the basic reproduction number of foot and and mouth disease below unity, therefore, will prevent occurrence of a major epidemic outbreak. Prophylactic vaccination of highly susceptible animal species, such as cattle, is particularly more effective. Prompt identification of infectious farms, followed by rapid deployment of reactive vaccination on farms neighboring infected premises, is also an effective control strategy. However, as also discussed in Section 1.7.1, one of the shortcomings of vaccinating during an outbreak is that vaccines delay to confer immunity (relative to the rate of spread of the disease).

1.7.3 Optimal reactive vaccination strategies for a foot-and-mouth outbreak in the UK. Tildesley et al 2006

This paper paper focuses on optimal deployment of reactive vaccination (vaccination of farms deemed to be at high risk of infection due to their connection to

infected premises), in addition to culling in infected premises (IP culling) and in farms neighboring infected premises (contagious premises culling or CP culling and direct contacts or DC culling), to control a single outbreak of foot and mouth disease in situations where vaccine coverage is constrained by logistical resources such as vaccine capacity or manpower. Logistical constraints affecting vaccine coverage basically determine the number of farms that can be vaccinated per day. This article assumes a *vaccination-to-live* strategy such that vaccinated farms are not culled. Similar to the models of FMD discussed above, the overall aim is to offer potentially more effective control mechanisms, which could help prevent or better contain future outbreaks of FMD in the UK. Therefore model parameters are chosen by fitting the model to the 2001 UK FMD outbreak epidemiological profile (particularly by matching the cumulative number of cases and culls in specific regions of the UK), and exploring possible control measures that could be implemented in the event that the UK is hit by another outbreak. The individual farm-based model adopted here also considers a heterogeneous distribution of animal species within farms such that the probability that a susceptible farm i is infected on a given day D is given by

$$P_{i,D} = 1 - exp\Bigg(- S^{(i)} \sum_{j \in infectious(D)} T^{(j)} K(d_{ij}) \Bigg)$$

$$S^{(i)} = s_{cow} n_{cow}^{(i)} + s_{sheep} n_{sheep}^{(i)}$$

$$T^{(j)} = t_{cow} n_{cow}^{(j)} + t_{sheep} n_{sheep}^{(j)},$$

where $S^{(i)}$ and $T^{(j)}$ represent the susceptibility and transmissibility of a susceptible farm i and an infectious farm j, respectively; s_A and t_A refer to the susceptibility and transmissibility of animal species A and $n_A^{(i)}$ is the number of species A on a farm i.

The general conclusion of this paper is that while optimal control is largely dependent on logistical constraints and model parameters, rapid deployment of reactive vaccination to farms closest to any previously reported cases, can significantly reduce the epidemic size.

1.8 The situation of foot and mouth disease in Botswana

The most abundant FMD-affected domestic animals in Botswana are cattle. Even though they keep other FMD-susceptible animals such as goats, sheep and pigs in villages and farms, most Batswana (people from Botswana) own large herds of cattle for family consumption and as source of income. In Botswana and most other African countries, owning large herds of cattle is seen as a symbol of wealth and is associated with overall high social status. Culturally, trade in cattle is carried out in social practices such as payment of bride price by the groom's family during traditional marriages in Botswana. Therefore almost all Batswana are involved in pastoral farming, but on different scales.

The importance of cattle in Botswana is not only seen at the level of individual families or farmers, but the beef industry is one of the main contributors to the country's economy (other main sectors of the Botswana economy are mining and tourism). The Botswana meat commission, an organization that facilitates local and international trade in cattle and their products, buys cattle from local farmers, processes them and sells beef and other cattle products to markets within Botswana and to neighboring countries as well as the the European union (EU). In fact the EU

is the largest market of Botswana beef.

Because of the reasons above, and since strict international regulations on beef trade do not allow importation and exportation of products from FMD-infected animals, Botswana invests greatly in the control of animal diseases including prevention and reduction of foot and mouth disease epidemic outbreaks. Control strategies for foot and mouth disease in Botswana include division of the country into veterinary zones (cordon fences) to minimize animal movement across border, public education, survey and testing, vaccination and culling. Since international trade of previously vaccinated animals is not permitted, prophylactic vaccination of cattle is carried out twice or three times a year only within zones deemed to be at highest risk of infection. Ring or reactive vaccination is also used as a control measure of FMD in these regions, but in the rest of the country vaccination is not used to control the disease. Highest-risk zones are mostly in the northern parts of Botswana where interaction between domestic animals and wild animals (especially the African buffalo) increases the possibility of outbreaks among cattle. Frequent re-importations of FMD into Botswana also result from mixing of animals across borders with neighboring countries such as Zimbabwe, Zambia and South Africa, during uncontrolled trade or smuggling of animals.

The first recorded case of FMD in Botswana was in the early 1930s. The disease was eradicated in the late 1930s only to reappear in the 1940s through to the 1950s. Well documented cases of FMD in Botswana include the 1970s and the 1990s outbreaks in the northern parts of the country. Recently documented cases were the 2002, 2005, 2006, 2007 and 2011 outbreaks that affected various areas of

Botswana. The 2011 outbreak mostly hit the north east of the country resulting in slaughtering of more than 30 000 cattle. Large epidemic outbreaks of FMD in Botswana often result in closure of some of Botswana meat commission's processing abattoirs, significant loss of profits and overall negative impact on farmers' general social welfare. Therefore, developing strategic means to prevent or control FMD outbreaks is one of Botswana government's top-priority tasks.

1.9 Models for control of infections by non-pharmaceutical interventions

Traditionally, mathematical models have been used to explore the control of human infectious diseases such as flu, measles, HIV, etc., by conventional control strategies including vaccination, isolation and drug-based therapy, and animal diseases such as foot and mouth disease using vaccination and/ or culling. Because much emphasis has been put on controlling diseases using these measures, there have been significant improvements in the development of more realistic control strategies such as optimal deployment of vaccination where vaccine coverage is constrained by logistical constraints, e.g. inadequate vaccine supply and shortage of skilled manpower. However, epidemiologists and the public in general, have always been aware that in addition to common disease control measures, certain human actions in response to infections, impact the course of infectious diseases. Examples of scenarios where neither drug nor conventional treatment-based methods, but human actions drive the pattern of spread of diseases include the following: the decision to main-

tain or increase the frequency of interactions with friends or colleagues by infected individuals during influenza outbreaks, promotes the spread of the disease, while avoidance of interaction decreases the disease spread; having multiple and/or concurrent sexual partners increases the risk of infection from HIV, while the decision to abstain from sexual interaction or engage in monogamous sexual relations reduces the chances of acquiring the disease. Despite limited resources, mobilization of the population to avoid risky behavior (e.g. reduction of casual sex encounters) has led to a 70% decline in HIV prevalence in Uganda since the early 1990s [120]. Other ways in which human actions can help reduce the rate of spread and magnitude of human infectious diseases include avoiding contacts (also known as social distancing), wearing masks (this has been used to curb infections such as SARS), and hand washing [45]. Below are some mathematical models for the control of infectious diseases by non-pharmaceutical interventions.

1.9.1 The spread of awareness and its impact on epidemic outbreaks. Funk et al, 2009

This article captures the idea that human behavioral response towards an infectious disease outbreak is determined by the amount and quality of information the population has about the infection. Thus, a large proportion of individuals who are aware of the occurrence or dangers of the disease translates to an increased number of people who make decisions to avoid transmission through preventative practices such as isolation, social distancing and vaccine uptake. Adoption of these precautionary measures leads to reduction of the overall impact of the disease. Members of

the host population generally acquire information about an infection through several means such as first-hand observation and word of mouth through interaction with other individuals, health personnel as well as media broadcast, e.g. television and radio. Below we illustrate one of the approaches that the authors propose to address the impact of human behavior on the spread of infectious diseases.

Here human behavior is described as a function of the level of information about the disease that individual members of the host population have. An individual-based model for the spread of awareness within the population is linked to a SIR model of the spread of the disease in such a way that more informed individuals are able to take precautionary measures and hence reduce their susceptibility better than less informed individuals. First we describe the model for the flow of information from one individual to another and then discuss the connection between this model and the epidemiological model.

Let X_i represent a member of the host population at information level i. The index i denotes the number of passages the information has undergone before arriving at the individual. Thus, X_0 represents an individual with first-hand information, X_1 represents an individual with second-hand information, X_2 represents an individual with third-hand information, etc. An individual denoted by X_0 is expected to be more informed and more capable of avoiding infection or transmission than an individual denoted by X_i where $i>0$. *Transmission of information* is assumed to take place from a X_i individual to a X_j individual, where $j>i+1$, and is denoted by

$$X_i + X_j \to X_i + X_{i+1}.$$

Fading of awareness is denoted by

$$X_i \to X_{i+1}.$$

Thus, as quality of information decreases at each information transmission event it is also lost within each individual, and it will eventually disappear from the entire population if it is not generated back. The authors assume that *generation of information* transforms an individual occupying any level of information to become a first-hand information bearer. That is, information generation is described by

$$X_i \to X_0.$$

The SIR epidemiological model is then constructed by assigning each individual a disease related status so that S_i, I_i and R_i denote susceptible, infectious and recovered individuals, respectively, at information level i. The events governing the disease dynamics are the usual *infection* and *recovery*. Note that this modeling framework implies that a susceptible individual with first-hand information S_0 is more capable of taking precautionary measures, and therefore less susceptible than a fellow susceptible who has second-hand information S_1; a susceptible individual with second-hand information S_1 is more capable of taking precautionary measures, and therefore less susceptible than a susceptible individual who has third-hand information S_2, etc.

1.9.2 Adaptive human behavior in epidemiological models. Fenichel et al, 2011

We discuss in general, the mechanism in which this article incorporates impacts of human behavior on the spread of infections diseases. The authors define human behavior in terms of varying tendencies to contact fellow members of the host population based on the disease statuses they possess. That is, while many epidemiological models in the literature infer that individuals of each health class are equally likely to come into contact, here person-to-person contact behavior is assumed to arise from the cost-benefit trade-offs such that, for instance, susceptible individuals benefit from avoiding contact with infectious individuals (since they will reduce the likelihood of contacting the disease) while infected or already recovered individuals may not have direct incentives from avoiding interactions with other members of the host population. Thus, susceptible individuals are likely to display more cautious behavior than the already infected or recovered members of the host population. The model developed in this paper is as follows.

$$\frac{dS}{dt} = -C(.)\beta SI/N$$
$$\frac{dI}{dt} = C(.)\beta SI/N - \nu$$
$$\frac{dZ}{dt} = \nu,$$

where S, I and Z are the numbers of susceptible, infectious and recovered individuals. $C(.)I/N$ is the rate at which susceptible individuals contact infectious individuals; β represents the probability that contact with an infectious individual results in disease transmission; the recovery rate is ν. The term describing contact behavior $C(.)$ takes

a form that assumes heterogeneous mixing of individuals with different health statuses because the expected benefits and costs of contact vary by health status. Contacts between $m-$type and $n-$type individuals, where m and n are individuals' health statuses (i.e. susceptible, infectious or recovered), are defined as

$$C^{mn}(.) = \frac{C^m C^n N}{SC^s + IC^i + ZC^z},$$

where the choice made by a type-m individual, C^m, is the expected number of contacts a type-m individual makes. Therefore, the equation above implies that mixing of members of the host population is conditional on the behaviors and the distribution of individuals of different health statuses.

1.10 Summary

In this chapter we introduced the general concept and goals of modeling the spread and control of infectious diseases using mathematical models. The choice of any type of a mathematical model is determined by, among others, the natural epidemiological features of the disease and aspects of the disease a researcher wishes to investigate. The development of the literature on mathematical models is mainly driven by the quest for extensions or improvement of previous models, by making realistic assumptions but also ensuring the models can be interpreted easily so as to inform policy on better disease control strategies. This chapter has provided a survey of modeling techniques as well as aspects of infectious diseases that are closely related to the type and the scope of mathematical models presented in the rest of this thesis: pair approximation models for the spread and control of foot and mouth

disease (FMD) in endemic or near-endemic settings, and the spread and control of a general infection by non-pharmaceutical interventions (NPIs).

Traditional spatially oriented models of FMD in the literature are tailored to the disease dynamics countries that rarely experience outbreaks. In Chapters 2 and 3, we fill up this gap in the literature by developing pair approximation models of foot and mouth disease that address issues relevant to endemic or near-endemic countries such as Botswana. Secondly, pair approximation models in the literature do not incorporate the regulation of infectious diseases by adoption of NPIs. Therefore, in Chapter 4 of this thesis we essentially introduce the study of impacts of adoption of NPIs on the dynamics of infectious diseases, to the theory and application of pair approximation models.

Chapter 2 presents a pair approximation model for the dynamics and control (by vaccination) of foot and mouth disease in endemic or near-endemic countries. The material from this chapter was published in the *Journal of Theoretical Biology* in 2014. Chapter 3 is about pair approximations modeling of impacts of constrained culling and vaccination on the control of foot and mouth disease in near-endemic countries. The material from this chapter was published in *Epidemics* in 2014. In Chapter 4 we develop a pair approximation model and explore impacts of adoption of NPIs on the dynamics of a general infectious disease. These chapters are connected through their use of pair approximation models to explore dynamics and control of infectious diseases. We present general conclusions and discussion of the thesis in Chapter 5.

Chapter 2

Dynamics and control of foot-and-mouth disease in endemic countries: a pair approximation model

Material from this chapter published in: Journal of Theoretical Biology, volume 357, pages 150-159 (2014)

Abstract

Previous mathematical models of spatial farm-to-farm transmission of foot and mouth disease (FMD) have explored the impacts of control measures such as culling and vaccination during a single outbreak in a country normally free of FMD. As a result, these models do not include factors that are relevant to countries where FMD is endemic in some regions, like long-term waning natural and vaccine immunity, use of prophylactic vaccination and disease re-importations. These factors may have implications for disease dynamics and control, yet few models have been developed for FMD-endemic settings. Here we develop and study an SEIRV (susceptible-exposed-infectious-recovered-vaccinated) pair approximation model of FMD. We focus on long term dynamics by exploring characteristics of repeated outbreaks of FMD and their dependence on disease re-importation, loss of natural immunity, and vaccine waning. We find that the effectiveness of ring and prophylactic vaccination strongly depends

on duration of natural immunity, rate of vaccine waning, and disease re-introduction rate. However, the number and magnitude of FMD outbreaks are generally more sensitive to the duration of natural immunity than the duration of vaccine immunity. If loss of natural immunity and/or vaccine waning happen rapidly, then multiple epidemic outbreaks result, making it difficult to eliminate the disease. Prophylactic vaccination is more effective than ring vaccination, at the same per capita vaccination rate. Finally, more frequent disease re-importation causes a higher cumulative number of infections, although a lower average epidemic peak. Our analysis demonstrates significant differences between dynamics in FMD-free settings versus FMD-endemic settings, and that dynamics in FMD-endemic settings can vary widely depending on factors such as the duration of natural and vaccine immunity and the rate of disease re-importations. We conclude that more mathematical models tailored to FMD-endemic countries should be developed that include these factors.

2.1 Introduction

Foot and mouth disease (FMD) is a highly transmissible viral infection affecting cloven-hoofed animals, including domestic livestock such as cattle, pigs, goats, sheep [10, 66, 131, 42] and some wild animals, e.g. buffalo. The disease agent of FMD belongs to the *picorna* virus family [19]. There are seven known serotypes of FMD virus, which vary according to geographical region [113, 3]. The serotypes of FMD are classified as: (a) European types O, A and C; (b) African types STA 1, STA 2 and STA 3 and (c) Asian type Asia 1 [29, 32], and there are several (more than 60)

subtypes of the virus [3, 5, 19]. Vaccination against one serotype does not provide protection against other serotypes. This makes it difficult to control the spread of FMD by vaccination alone, and adopting multiple control measures may offer better means of control.

The FMD virus can be found in secretions and excretions from infected animals, including expired air, saliva, milk, urine and semen. The virus is airborne and can also be transmitted through physical contact. Clinical symptoms of FMD include high fever, blisters inside the mouth, ruptured feet and stunted growth [113, 10, 42, 103]. However, animals rarely die from foot and mouth disease. Upon introduction, FMD virus spreads rapidly within a farm, and interaction between neighboring farms leads to a rapid spread of the disease to several kilometers (up to 6 km) from the source point [39]. Import-export routes also enhance the spread of FMD, potentially resulting in a highly damaging global economic impact.

FMD is one of the most economically important livestock diseases [19, 26]. Heavy import-export restrictions apply in countries that experience frequent FMD outbreaks [103]. Thus, the cost-benefit ratio of an investment business in FMD-affected animal species is greatly affected by frequent disease outbreaks. Due to its economic impact, FMD remains the greatest and most feared vesicular disease in India [83]. In livestock production, the economic loss due to FMD can be calculated by considering, e.g., milk loss, disease-induced abortions and treatment costs. By the time the 2001 UK FMD outbreak had been stopped, the government had spent nearly GBP 3 billion on the operation of containing and cleaning up after the disease [123]. Recent outbreaks in Botswana include in 2002, 2005, 2006, 2007, 2011 and

2012 [10, 75, 87].

There is no cure for FMD [98, 131]. Infected animals usually recover to a health-compromised status that renders them less profitable. Conventional control measures against FMD are movement restriction, public education, veterinary boundaries, quarantine, vaccination and culling (slaughtering animals in order to reduce the number of susceptible or infectious animals, and hence reduce spread of the disease [14]). Two basic forms of vaccination against foot and mouth disease are prophylactic vaccination (pre-outbreak: vaccination carried out to prevent introduction of the disease) and ring vaccination (during an outbreak: carried out on farms neighboring infected farms). The Cedivac-FMD Double Oil Emulsion (DOE) vaccines (one of many types of FMD vaccines) confer a duration of immunity of at least 6 months in cattle, sheep and pigs [25, 35]. Some vaccines can provide prolonged immunity for up to 12 months, depending on, among others, the species affected and the virus serotype. Cattle that have recovered from infection with one of the seven serotypes of the FMD virus remain protected against that serotype for up to 6 months to about 5 years, depending on the virus serotype [34]. Methods of culling include contagious premises (CP) culling (slaughtering farms based on their proximity to infected farms) and infected premises (IP) culling (slaughtering infected farms).

The availability of data for the 2001 FMD outbreak in the United Kingdom allowed the development of validated epidemiological models, making it possible to explore impacts of various control measures [126]. For instance, in [126] the authors used an individual-farm based transmission probability model, capturing spatiality by describing the probability of infection as a function of the distance between susceptible

farms and infection source (transmission kernel), and also explored impacts of ring vaccination strategies. In [65] the authors used a stochastic individual farm-based model to explore impacts of either national prophylactic vaccination campaigns, or combinations of reactive (during outbreak) vaccination and culling.

Compartmental models have also been used to study the dynamics and control of foot and mouth disease. In compartmental models, the host population is comprised of subdivisions called compartments such that the nature and time rates of transfer from one compartment to another are defined [21]. Each compartment represents the disease status of farms (e.g. susceptible, infectious or recovered). Compartmental models are sometimes referred to as mean-field approximations as they typically assume that members of the host population mix homogeneously [21]. Thus spatial spread of the disease is neglected [24], since it is assumed that an infectious farm is equally likely to infect any of the susceptible farms in the population. In [92] the authors adopt this approach to model the spread of FMD and impacts of vaccination, by dividing the population of farms into susceptible (S), vaccinated (V), latently infected (L) and infectious farms (I), and uses it to explore the impacts of births and deaths, culling, and vaccine waning.

Recently a number of foot and mouth disease transmission models have used moment closure approximations (pair approximation models in particular) to capture spatiality implicitly. In [95] the authors design and analyze an SEI (susceptible, exposed but not infectious, infectious) pair approximation model of foot and mouth disease and explore impacts of IP culling and CP culling. They assume that the disease spreads on a network of farms represented by nodes (farms) and edges

(links between farms). For many infectious diseases where spatiality is important for transmission and control, including foot and and mouth disease, spatially structured models may provide advantages over mean-field approximations such as conventional compartmental models [94, 15]. In [42] the authors present and analyze a pair approximation model of foot and mouth disease, employing data from the well-documented 2001 FMD out break in the United Kingdom, and explore impacts of ring culling and ring vaccination (both of which are applied during a single outbreak). In [42] the transmission rate is explicitly defined as a function of both local transmission between connected farms, and long range transmission due to transport since FMD virus can be transported to up to 60 km from the source point.

While mean field approximations are formulated under an assumption that individuals in the host population mix homogeneously, moment closure approximations capture the spatial spread of diseases by modeling states of neighboring members of the host population. This technique provides information about the spatial distribution of disease states on a network by employing pairs, triples, quadruples, and other higher-order correlations as state variables of ordinary differential equations [15, 24]. Each ordinary differential equation (also referred to as an equation of motion for a state variable) measures the expected rate of change of a state variable by averaging all possible events affecting the state variable [128]. To do this, the first step is to write the equations of motion for the number of neighboring pairs of individuals or groups of individuals of a given state on a network; these equations will have terms involving triples [15]. The equations of motion for triples will involve quadruples while the equations of motion for quadruples will have terms involving

five-order correlations. Essentially the procedure yields an infinite system of ordinary differential equations, each describing rates of change of state variables. However in order to solve the system analytically or using available computer software the system of equations needs to be finite. A closed, manageable system is obtained by truncating the hierarchy at some suitable level by a process known as *moment closure* [18, 15, 128, 57]. When the system is closed at the level of pairs, it is referred to as *pair approximations*. Pair approximations models track down the dynamics of neighboring pairs of members of the host population, capturing the correlations that develop when two individuals interact [15, 38]. Pair approximations also tend to be more analytically tractable than fully explicit network models.

Most models of FMD transmission are intended for epidemic settings, where control measures are designed to contain a single epidemic outbreak. However, FMD is an endemic problem in many countries. For example, in Botswana, FMD is endemic in some regions due to importation of FMD virus from wild African buffaloes and neighboring countries [10]. In endemic settings, long-term factors become important, such as waning of natural immunity, waning of vaccine immunity, and frequent disease re-introduction. Moreover, prophylactic and ring vaccination may become desirable control measures, under some circumstances. Despite the importance of such factors for FMD-endemic settings, they are not commonly included in spatial FMD transmission models. For example, to our knowledge there is no pair approximation FMD model that analyzes both ring and prophylactic vaccination. The same holds true for the impact of disease re-introduction. Our objective was to fill this gap in the literature by developing an SEIRV (susceptible, exposed but not infectious, in-

fectious, recovered and vaccinated) pair approximation model to explore the impacts of prophylactic and ring vaccination, vaccine waning and loss of natural immunity as well as disease re-introduction from an external source, on the dynamics of foot and mouth disease in a fixed population of farms.

2.2 Model

The state variables of pair approximation models are of the form $[XY]$, where X and Y represent the status of farms with respect to the disease so that $[XY]$ is defined as the expected number of status X and status Y pairs at a given time, t. The dynamics of state variables of pair approximation models are governed by the master equation:

$$\frac{dg(t)}{dt} = \sum r(\epsilon)\Delta g(\epsilon), \tag{2.1}$$

where $g(t)$ is the state variable of interest, $r(\epsilon)$ is the rate of event ϵ and $\Delta g(\epsilon)$ is the change this event causes in $g(t)$.

As an example of pair approximation derivation, in Appendix A.1 we derive the equation of motion for the number of susceptible-infectious, $S-I$ pairs, $\frac{d[SI]}{dt}$, for an SEIRV (susceptible, exposed but not infectious, infectious, recovered and vaccinated) pair approximation model of FMD. We show how ring and prophylactic vaccination as well as vaccine waning and loss of disease induced immunity are incorporated and observe that

$$\frac{d[SI]}{dt} = -\tau([ISI]+[SI])+\nu[SE]-\sigma[SI]-\psi_r([SI]+[ISI])-\psi_p[SI]+\omega[IR]+\theta[IV], \tag{2.2}$$

where τ, σ, ψ_r, ψ_p, ω and θ are the transmission rate, recovery rate, rate of ring vaccination, rate of prophylactic vaccination, rate of loss of natural immunity and rate of vaccine waning, respectively. The number of $I-S-I$ triples enters the equation of motion for $S-I$ pairs because it is possible that transmission from one infected farm to a susceptible farm can destroy a $S-I$ pair consisting of that susceptible farm and a second infected farm, creating an $E-I$ pair in its place. The sign in front of the triple term is negative because an $S-I$ pair is disappearing. The latent period of FMD is given by ν^{-1}, therefore $S-E$ is converted to $S-I$ (i.e. $S-I$ bond is *created*), at rate ν, leading to the term $+\nu[SE]$ on the RHS of this equation. The rest of the terms are developed in a similar manner.

If an equation of motion for $[ISI]$ is in turn formulated, it will involve quadruples and the hierarchy will go on to involve progressively higher order correlations. To truncate the hierarchy, we perform a moment closure approximation, a technique in which higher order correlations (order 3) are approximated in terms of lower order correlations (pairs and singletons). There exist various forms of moment closure approximations to the level of pairs, which vary in the assumptions they make about the distribution of neighbors around a farm. Here we adopt the ordinary pair approximation (OPA) [95], and approximate the number of triples in terms of pairs and singletons, and the number of neighbors of a farm, n, as

$$[XYZ] \approx \frac{(n-1)}{n}\frac{[XY][YZ]}{[Y]} \tag{2.3}$$

The ordinary pair approximation assumes that all individuals in the network have exactly n contacts. The approximation maintains pair correlations between X and

Y, and between Y and Z, but assumes higher order correlations between X and Z are negligible. In practice, X and Z could be correlated because they are directly connected, forming a triangle, or because X and Z have influenced one another via Y. The presence of triangles can be accounted for using a triangular approximation [95, 64]. In contrast, in a mean field approach $[XY]$ is approximated by $[X][Y]$ while $[XYZ]$ would be approximated by $[X][Y][Z]$.

2.2.1 Model equations

S, E, I, R and V respectively, represent epidemiological states of the host population (farms): susceptible, exposed, infectious, recovered and vaccinated. The

full model equations are given by

$$
\begin{aligned}
\frac{d[S]}{dt} &= -\tau[SI] - \psi_r[SI] - \psi_p[S] + \omega[R] + \theta[V] \\
\frac{d[E]}{dt} &= \tau[SI] - \nu[E] - \psi_r[EI] \\
\frac{d[I]}{dt} &= \nu[E] - \sigma[I] \\
\frac{d[R]}{dt} &= \sigma[I] - \omega[R] \\
\frac{d[V]}{dt} &= \psi_r([SI] + [EI]) + \psi_p[S] - \theta[V] \\
\frac{d[SS]}{dt} &= -2\tau[SSI] - 2\psi_r[SSI] - 2\psi_p[SS] + 2\omega[SR] + 2\theta[SV] \\
\frac{d[SE]}{dt} &= -\tau([ISE] - [SSI]) - \nu[SE] - \psi_r([ISE] + [SEI]) - \psi_p[SE] + \omega[ER] + \theta[EV] \\
\frac{d[SI]}{dt} &= -\tau([ISI] + [SI]) + \nu[SE] - \sigma[SI] - \psi_r([SI] + [ISI]) - \psi_p[SI] + \omega[IR] + \theta[IV] \\
\frac{d[SR]}{dt} &= -\tau[ISR] + \sigma[SI] - \psi_r[ISR] - \psi_p[SR] - \omega([SR] - [RR]) + \theta[RV] \\
\frac{d[SV]}{dt} &= -\tau[ISV] - \psi_r([ISV] - [SSI] - [SEI]) - \psi_p([SV] - [SS]) + \omega[RV] + \theta([VV] - [SV]) \\
\frac{d[EE]}{dt} &= 2\tau[ESI] - 2\nu[EE] - 2\psi_r[EEI] \\
\frac{d[EI]}{dt} &= \tau([ISI] + [SI]) + \nu([EE] - [EI]) - \sigma[EI] - \psi_r([EI] + [IEI]) \\
\frac{d[ER]}{dt} &= \tau[ISR] - \nu[ER] + \sigma[EI] - \psi_r[IER] - \omega[ER] \\
\frac{d[EV]}{dt} &= \tau[ISV] - \nu[EV] - \psi_r([IEV] - [ISE] - [EEI]) + \psi_p[SE] - \theta[EV] \\
\frac{d[II]}{dt} &= 2\nu[EI] - 2\sigma[II] \\
\frac{d[IR]}{dt} &= \sigma([II] - [IR]) + \nu[ER] - \omega[IR] \\
\frac{d[IV]}{dt} &= -\sigma[IV] + \nu[EV] + \psi_r([SI] + [ISI] + [EI] + [IEI]) + \psi_p[SI] - \theta[IV] \\
\frac{d[RR]}{dt} &= 2\sigma[IR] - 2\omega[RR] \\
\frac{d[RV]}{dt} &= \sigma[IV] + \psi_r([ISR] + [IER]) + \psi_p[SR] - \omega[RV] - \theta[RV] \\
\frac{d[VV]}{dt} &= 2\psi_r([IEV] + [ISV]) + 2\psi_p[SV] - 2\theta[VV].
\end{aligned}
\tag{2.4}
$$

The factor two in the equations of motion pairs of the form XX comes from the counting convention of same-status pairs, wherein pairs of type $X - X$ are counted twice. The ordinary pair approximation has been used to close the equations of

motion.

During an outbreak of foot and mouth disease, transmission at rate τ takes place between an infectious and a susceptible farm, moving the latter to the exposed compartment. A farm stays in the exposed state for ν^{-1} days (latent period), after which it becomes infectious. The recovery rate (transition from infectious state to recovered compartment) is given by σ. Loss of natural immunity (disease-induced immunity) takes place at rate ω, enabling transition of farms from R to S compartments. Prophylactic vaccination and ring vaccination at per capita rates ψ_p and ψ_r, respectively, transfer vaccinated susceptible and susceptible and/or exposed farms to the vaccinated compartment. The rate of loss of vaccine-induced immunity (vaccine waning) is given by θ (where farms lose protection from the vaccine, becoming susceptible again).

2.2.2 The basic reproduction number

The basic reproduction number, R_0, is defined as the expected number of secondary cases produced by a single infection in a completely susceptible population [56, 15, 76, 117]. An epidemic is expected if $R_0 > 1$ and the infection is expected to die out if $R_0 < 1$ [117, 54]. In Appendix A.2 we illustrate the derivation of a spatially-oriented basic reproduction number for a pair approximation model without control measures :

$$R_0 = \frac{\beta(n-1)^2}{\sigma n[(n-1) + (\frac{\beta}{\nu})]}, \tag{2.5}$$

where $\beta = \tau n$, n is the number of neighboring farms. The basic reproduction number increases with the number of neighbors, n, on account of decreased opportunities for localized clustering of infected individuals to interfere with further transmission.

The basic reproduction number with ring vaccination as the only control measure is:

$$\frac{m_3\tau(m_1\nu + m_2\psi_r)}{m_3\tau\psi_r + (m_1\nu + m_2\psi_r)(\frac{\sigma(m_4\nu+m_5\tau)}{\nu} + m_5\sigma\psi_r)},$$

where m_i, $i = 1...5$, are constants $\frac{n-1}{n} + 1$, $\frac{n-1}{n}Nq$, $n(n-1)^2$, $n(n-1)$ and n^2, respectively. In our model $n = 4$ neighbors per farm, $N = 40000$ farms. We assume that $q = 1.5$. We present the justification for this constant in Appendix A.3. Therefore $m_1 = 1.75$, $m_2 = 4.5 \times 10^4$, $m_3 = 36$, $m_4 = 12$ and $m_5 = 16$. The basic reproduction number with prophylactic vaccination only is:

$$\frac{m_3\tau}{\frac{\sigma(m_4\nu+m_5\tau)}{v} + \frac{m_6\nu+m_5\tau}{v}\psi_p},$$

where $m_6 = (n-1)^2 = 9$.

The basic reproduction number in the presence of prophylactic, ψ_p and ring, ψ_r vaccination (see Appendix A.2) is considerably more complicated and is given by:

$$R_0 \approx \frac{m_8\tau(n-1)^3 + m_7\tau n(n-1)^2}{m_9 n(n-1)^2 + (m_8\frac{n-1}{n} + m_7)[\sigma n(n-1) + m_{10}\sigma n^2 + \psi_p(n-1)^2 + m_{10}\psi_p n(n-1)]}, \quad (2.6)$$

where $m_7 = \nu + \psi_r + \psi_p$, $m_8 = \nu + \psi_r Nq$, $m_9 = \tau\psi_r$ and $m_{10} = \frac{\tau+\psi_r}{\nu}$.

2.2.3 Baseline parameters

Cattle, swine, sheep, goats and deer exhibit signs of clinical illness from FMD after an incubation period of about 2 to 14 days, [92]. The latent period of foot and mouth disease is 3.1 to 4.8 days in cattle [81]. Upon contact with the FMD virus, animals show clinical signs and are able to transmit the virus after 4 to 5 days [66]. Therefore we assume that the latent period is 4 days, thus $\nu = \frac{1}{4} = 0.25\ day^{-1}$. Once in the infectious compartment, cattle show symptoms and remain infectious for about 7 to 8 days before they recover, [95]. Our baseline choice of the recovery rate is $\sigma = \frac{1}{7} = 0.143\ day^{-1}$.

Cattle that have recovered from infection with one of the seven serotypes of FMD are not immune to other serotypes but remain protected against the first serotype for a considerable period of time. Laboratory experiments show that the length of natural protection may range from 6 months to 5.5 years, depending on the serotype [34]. Using this observation as a guide, and considering the possibility for transmission of multiple serotypes in the same population in succession, our baseline choice of the duration of natural immunity is 6 months (≈ 0.5 years, or $\omega = 0.0056$ day^{-1}), but we also explore scenarios of ≈ 1 year ($\omega = 0.0030\ day^{-1}$) and ≈ 2 years ($\omega = 0.0015\ day^{-1}$).

Cattle remain protected by FMD vaccine for up to 6 months [65], therefore $\theta = 0.0056\ day^{-1}$. We assume that per capita prophylactic and ring vaccination rates are $\psi_p = 0.005\ day^{-1}$ and $\psi_r = 0.005\ day^{-1}$, respectively. In some countries, foot and mouth disease can spread across borders through animal movement or trade. In some

parts of Botswana FMD is imported from Zimbabwe or South Africa resulting in a series of outbreaks almost every 2 years [87]. In our model simulations, the disease is re-introduced into the population of farms every $\delta = 800$ days (just over 2 years). The baseline transmission parameter is $\tau = 0.6\ day^{-1}$. In Appendix A.4 we estimate this parameter value from the expression of the basic reproduction number (equation 2.5). We present all baseline parameters in Table 2.1. Finally, to partially account for the effects of stochastic fadeout in our deterministic framework, when the total number of infectious farms falls below 1 in the simulation (less than one infected farm left), the infection is forced to die out, so that any subsequent outbreaks are the result of disease re-importation. The population size is $N = 40000$ farms.

In the model equations, prophylactic vaccination of the susceptible farm in a susceptible-infected pair occurs at rate ψ_p and converts SI to VI, creating the terms $-\psi_p[SI]$ in $\frac{d[SI]}{dt}$ and $+\psi_p[SI]$ in $\frac{d[VI]}{dt}$. However prophylactic vaccination is a pre-outbreak vaccination strategy and we assume that, in practice, authorities would switch all resources to ring vaccination in the event of an outbreak. To capture this in the model simulations, we assumed that ψ_p is set to zero whenever $[I] > 0$, and it remains zero for the duration of the outbreak, after which it is returned to baseline levels.

2.3 Results

Numerical analysis of our model was carried out in *MATLAB* using the ode45 solver. The quality of numerical solutions remained the same when we ex-

Table 2.1: Baseline parameters for our model

parameter	value	source
Transmission rate, τ	0.6 day^{-1}	[95]
Rate of moving from latent to infectious, ν	$0.25\,day^{-1}$	[66]
Rate of moving from infectious to recovered, σ	$0.143\,day^{-1}$	[95]
Rate of loss of disease-induced immunity, ω	$0.0056\,day^{-1}$	[34]
Rate of loss of vaccine-induced immunity, θ	$0.0056\,day^{-1}$	[34, 65]
Rate of ring vaccination, ψ_r	0.005 day^{-1}	assumption
Rate of prophylactic vaccination, ψ_p	0.005 day^{-1}	assumption
Frequency of disease re-introduction, δ	every 800 days	[87]

perimented with other ordinary differential equations solvers (ode15s and ode23) in *MATLAB*.

We focus on the impact of loss of natural immunity, ω, vaccine waning, θ, and disease re-introduction frequency, δ, on the number of outbreaks, average peak size of outbreaks, and cumulative number of infected farms over a given time period. We also consider impacts of prophylactic vaccination, ψ_p and ring vaccination, ψ_r, on disease incidence, cumulative infections and the basic reproduction number, R_0.

Figure 2.1 shows the impact of loss of natural immunity, ω, on disease re-introduction in the absence of control measures. For higher values of ω, natural immunity is short-lived causing the pool of susceptible farms to be rapidly replenished. Hence, epidemics do not fade out and the infection prevalence converges to an endemic equilibrium (Figure 2.1a, b). In contrast, if ω is low, corresponding to long-lived natural immunity, epidemics fade out and prevalence goes to zero after an outbreak. After some time, a subsequent disease introduction sparks a new outbreak. As a result, the epidemiology is characterized by sustained outbreaks every 3-5 years (Figure 2.1c, d). However, because the susceptible pool is relatively slow to replenish,

not every disease re-introduction is successful in starting an outbreak, meaning that outbreaks are spaced further apart when natural immunity wanes more slowly (Figure 2.1d versus 2.1c).

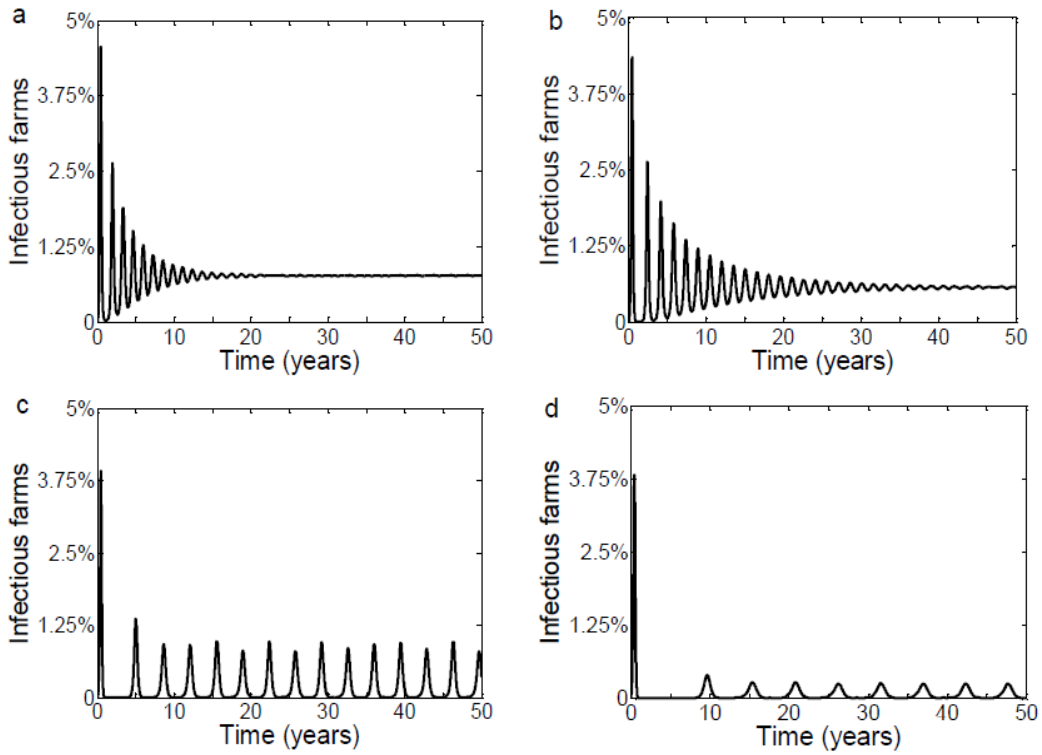

Figure 2.1: Time series of the number of infectious farms where rates of natural immunity waning, ω are 0.0055 day^{-1} (a), 0.0042 day^{-1} (b), 0.0014 day^{-1} (c) and 0.00055 day^{-1} (d). $\psi_p = \psi_r = 0$ day^{-1} and all other parameters are as in Table 2.1.

As a result of interactions between timing of disease re-introduction and rate of natural immunity waning, the dependence of the size and number of outbreaks on the natural immunity waning rate is not linear (Figure 2.2). As the rate of waning natural immunity, ω, increases, so does the number of outbreaks over a fixed time window of 20 years, through a series of plateaus (Figure 2.2a). The average peak

size of all outbreaks in this period of time also increases with ω, although beyond a certain point, further increases in ω do not change the average peak size (Figure 2.2b).

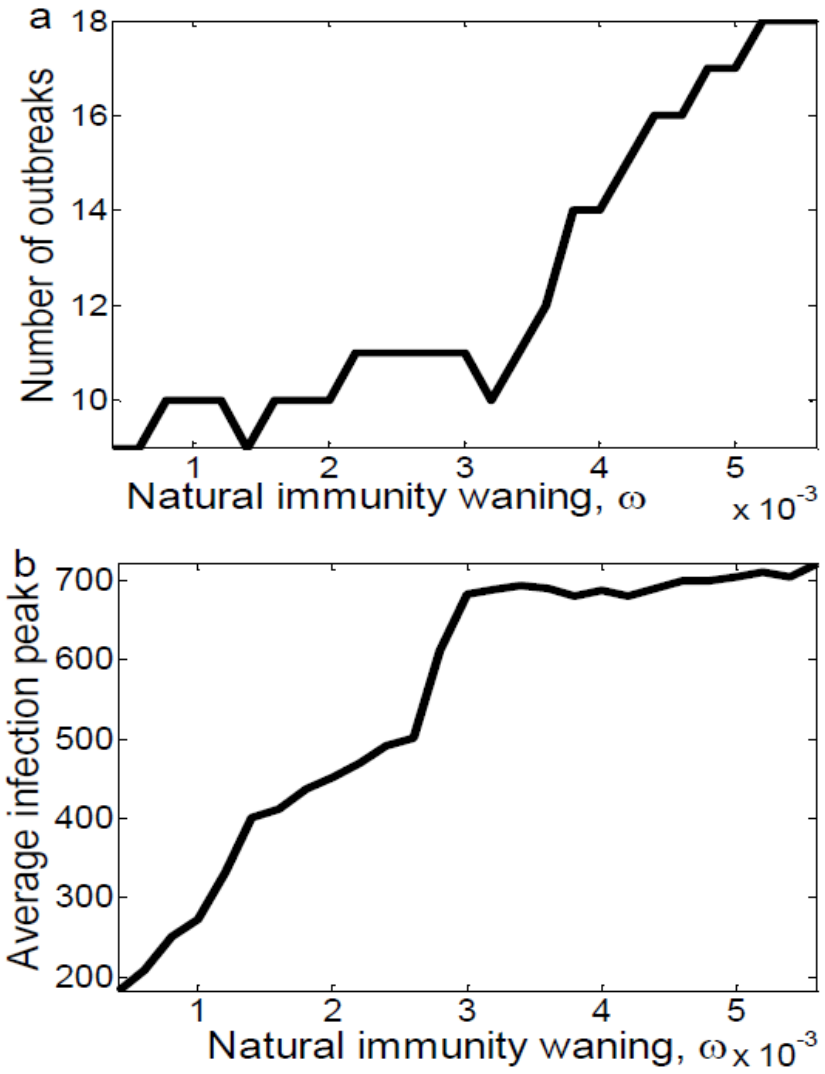

Figure 2.2: Number of outbreaks (a) and average infection peak (b) of outbreaks over a 20 year period versus rate of natural immunity waning, ω. $\psi_p = \psi_r = 0\ day^{-1}$ and all other parameters are as in Table 2.1.

The effectiveness of prophylactic vaccination, ψ_p and ring vaccination, ψ_r

is strongly determined by the presence or absence of vaccine waning, θ, and natural immunity waning, ω (Figure 2.3). If both vaccine immunity and natural immunity wane after 6 months, then a vaccination strategy with $\psi_p = 0.005\ day^{-1}$ and $\psi_r = 0.01\ day^{-1}$ fails to prevent the infection from becoming endemic (Figure 2.3a). However, if vaccines were to provide life-long immunity (i.e. $\theta = 0\ day^{-1}$), vaccination prevents future outbreaks (except for a small second outbreak due to re-importation) and eventually leads to eradication (Figure 2.3b). Similarly, if natural immunity were lifelong (Figure 2.3c) or if both natural and vaccine immunity were lifelong (Figure 2.3d), the infection is eradicated even more quickly.

Both prophylactic and ring vaccination decrease the cumulative number of infected farms (see surface plots of cumulative infections versus ψ_r and ψ_p, Figure 2.4). However, at similar per capita rates of vaccination, prophylactic vaccination appears to be more effective. This simply reflects the fact that more farms in total are vaccinated under prophylactic vaccination, for the same per capita vaccination rate. However, it may also reflect the fact that prophylactic vaccination is a preventive (pre-outbreak) form of vaccination that can delay or prevent outbreaks altogether. Almost all of the variation in the effectiveness of prophylactic vaccination occurs in a range of values from $\psi_p = 0\ day^{-1}$ to $\psi_p = 0.005\ day^{-1}$ (the upper limit corresponds to being able to vaccinate all farms after about 200 days).

Both vaccine waning, θ, and natural immunity waning, ω, affect the number of epidemics, average size of infection peaks and cumulative number of infected farms over a 20-year time window (Figure 2.5). The number of epidemics (Figure 2.5a), average infection peak (Figure 2.5b) and cumulative infections (Figure 2.5c)

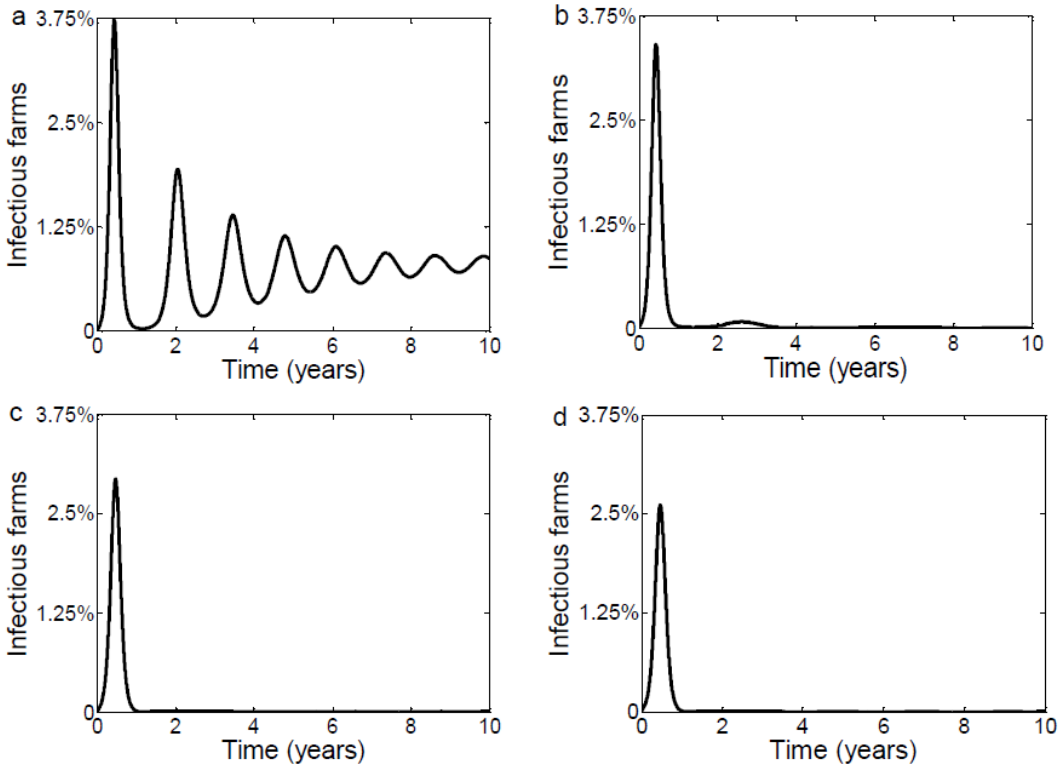

Figure 2.3: Time series for the number of infectious farms where $\omega = \theta = 0.0055$ day^{-1} (a), $\omega = 0.0055$ day^{-1} and $\theta = 0$ day^{-1} (b), $\omega = 0$ day^{-1} and $\theta = 0.0055$ day^{-1} (c) and $\omega = \theta = 0$ day^{-1} (d). $\psi_p = 0.005$ day^{-1}, $\psi_r = 0.01$ day^{-1} and all other parameters are as in Table 2.1.

are highest when both natural immunity and vaccine waning rates take values close to the baseline parameters ($\omega = \theta = 0.0055$ day^{-1}, corresponding to lowest immunity duration considered here: 6 months). Generally speaking, the number of epidemics, average infection peak and cumulative infections depend more sensitively on changes in the rate of natural immunity waning, ω, than they do on the rate of vaccine waning, θ (the height variation is greater along the ω axis than the θ axis).

When the frequency of disease importation δ is low (i.e. there is a long time

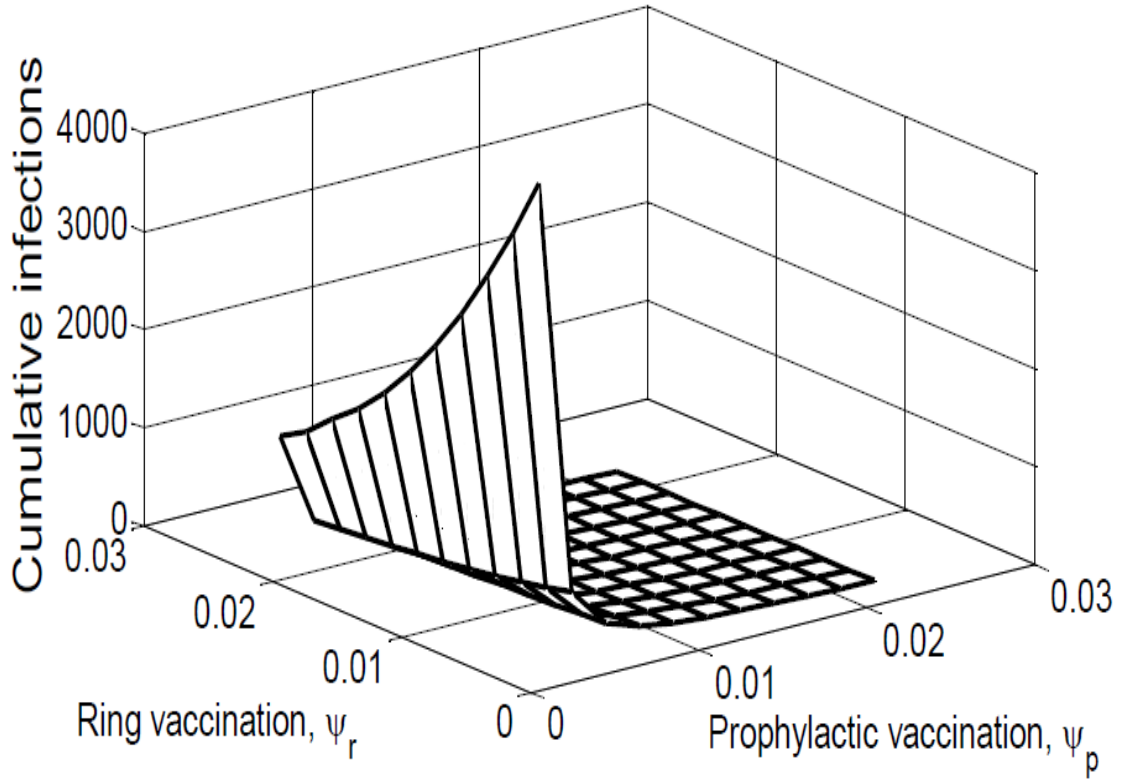

Figure 2.4: Cumulative number of infectious farms over 5 years as a function of prophylactic vaccination, ψ_p, and ring vaccination, ψ_r. All other parameters are as in Table 2.1.

interval between re-introductions), long periods of zero disease prevalence are interspersed with sharp epidemic outbreaks (Figure 2.6a). After an outbreak is finished, vaccination is sufficient to prevent FMD from becoming endemic, but not sufficient to prevent an outbreak after the next re-introduction. As the frequency of disease re-importation increases, outbreaks occur closer together, but they are smaller in magnitude (Figure 2.6a). However, despite the smaller magnitude of epidemic peaks, the cumulative incidence is nonetheless higher when re-introductions are close together

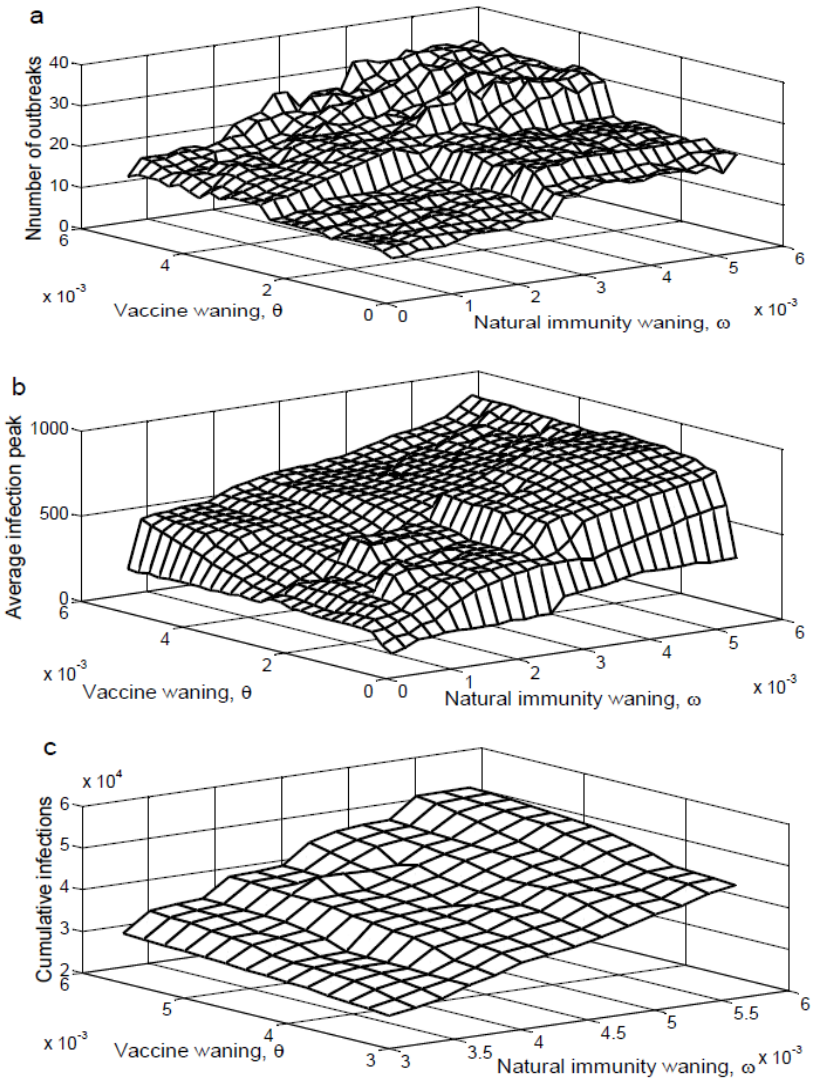

Figure 2.5: Number of outbreaks (a), average infection peak (b) and cumulative infections (c) over a 20 year period versus rate of natural immunity waning, ω, and vaccine waning, θ. $\psi_p = \psi_r = 0.001\ day^{-1}$ and all other parameters are as in Table 2.1.

(Figure 2.6b). Thus despite its capability to yield high-peak outbreaks, a lower rate of disease re-introduction produces fewer cumulative infections. Interestingly, when the rate of re-introduction is every 8 years, there is an outbreak every 8 years, but

when the rate of re-introduction is only 3 years (respectively, 0.5 years), there is an outbreak only every 4-5 years (respectively, 4 years), suggesting that re-introductions may prevent extinction of the pathogen in between outbreaks, thereby supporting endemic infection.

Both prophylactic vaccination, ψ_p, and ring vaccination, ψ_r also have a significant impact on the R_0 value as computed from equation 2.6 (Figure 2.7). However, prophylactic vaccination reduces R_0 below 1 more quickly than ring vaccination. This is similar to the observation for the relative impact of both forms of vaccination on the cumulative number of infected farms (Figure 2.4). Prophylactic vaccination appears to perform better that ring vaccination because it does not only delay occurrence of outbreaks, but it also reduces the sizes of subsequent outbreaks and guarantees disease eradication if well administered.

2.4 Discussion

Foot and mouth disease has both economic and social impacts in many countries. Even though it has since been eradicated or is under control in most developed countries, the occurrence of foot and mouth disease in the developing world can, and does, create global impacts. To avoid introduction of FMD into disease-free countries, heavy import-export restrictions apply on trade of animals and their products.

Here, we applied moment closure techniques to construct and analyze a pair approximation model of foot and mouth disease and explored impacts of loss of natural

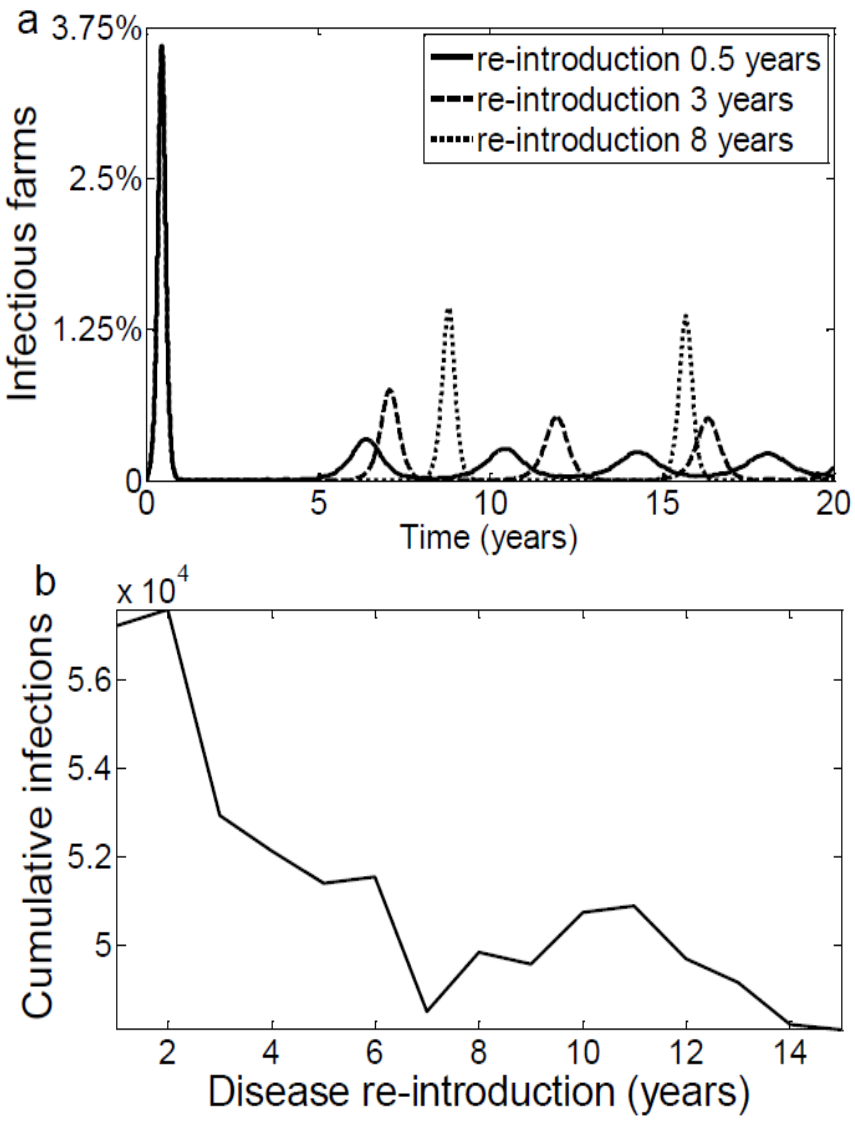

Figure 2.6: Time series for the number of infectious farms for varying rates of disease re-introduction (a) and cumulative number of infected farms versus disease re-introduction (b) over a 20 year period. $\psi_p = 0.00005\ day^{-1}$, $\psi_r = 0.0005\ day^{-1}$, $\theta = \omega = 0.0014\ day^{-1}$ and all other parameters are as in Table 2.1.

immunity, vaccine waning and disease re-introduction on infection dynamics and the basic reproduction number. At biologically plausible parameter values, both waning natural and vaccine immunity had significant impacts on the number and magnitude

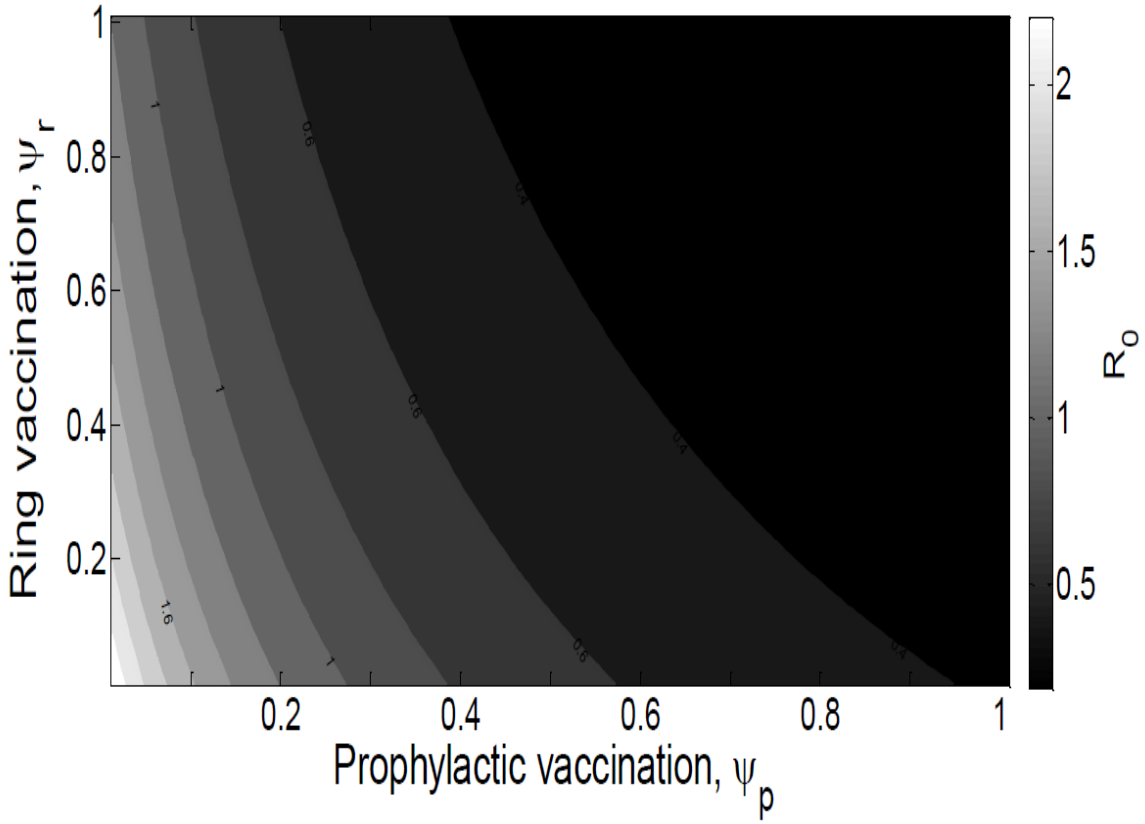

Figure 2.7: The basic reproduction number, R_0, versus prophylactic vaccination, ψ_p, and ring vaccination, ψ_r. All other parameters are as in Table 2.1.

of outbreaks, cumulative number of infections, and feasibility of disease control. The impact varied according to the precise parameter values, over biologically plausible parameter ranges. Hence, these factors are important to consider in any transmission model of FMD in an endemic country. These outcomes are somewhat more sensitive to the rate of waning natural immunity than the rate of waning vaccine immunity.

We also found that vaccination is more effective if loss of natural immunity is low (i.e. recovered farms remain in 'recovered' compartment longer due to longer-

lasting natural immunity). However, if farms lose natural immunity at a higher rate then it will be difficult to eliminate the disease. For the same per capita vaccination rate, prophylactic vaccination appears to be more effective than ring vaccination, partly because prophylactic vaccination better delays the occurrence of outbreaks, leading to smaller and less frequent subsequent outbreaks, and ensuring that the basic reproduction number stays below unity.

In most developing countries, vaccination capacity may be constrained by many factors including cost. Therefore as part of future work, this model can be modified to explore optimal and/or cost-effective prophylactic and ring vaccination strategies where control measures are forced to operate within constraints such as cost, availability of vaccine and manpower. Empirical data are generally lacking in FMD-endemic settings and this must also be addressed in order to better validate country-specific FMD models.

The outcomes of this analysis provide spatially oriented insight into the dynamics of foot and mouth disease and its control in FMD-endemic countries. The dependence of disease control effectiveness on loss of natural immunity and vaccine waning has not been well explored in the literature of foot and mouth disease models, but our analysis suggests that these factors are influential enough to necessitate inclusion in any mathematical model of FMD transmission and control in endemic countries.

Chapter 3

Impacts of constrained culling and vaccination on control of foot and mouth disease in near-endemic settings: a pair approximation model

Material from this chapter published in: Epidemics, volume 9, pages 18-30 (2014)

Abstract

Many countries have eliminated foot and mouth disease (FMD), but outbreaks remain common in other countries. Rapid development of international trade in animals and animal products has increased the risk of disease introduction to FMD-free countries. Most mathematical models of FMD are tailored to settings that are normally disease-free, and few models have explored the impact of constrained control measures in a 'near-endemic' spatially distributed host population subject to frequent FMD re-introductions from nearby endemic wild populations, as characterizes many low-income, resource-limited countries. Here we construct a pair approximation model of FMD and investigate the impact of constraints on total vaccine supply for prophylactic and ring vaccination, and constraints on culling rates and cumulative culls. We incorporate natural immunity waning and vaccine waning, which are important fac-

tors for near-endemic populations. We find that, when vaccine supply is sufficiently limited, the optimal approach for minimizing cumulative infections combines rapid deployment of ring vaccination during outbreaks with a contrasting approach of careful rationing of prophylactic vaccination over the year, such that supplies last as long as possible (and with the bulk of vaccines dedicated toward prophylactic vaccination). Thus, for optimal long-term control of the disease by vaccination in near-endemic settings when vaccine supply is limited, it is best to spread out prophylactic vaccination as much as possible. Regardless of culling constraints, the optimal culling strategy is rapid identification of infected premises and their immediate contacts at the initial stages of an outbreak, and rapid culling of infected premises and farms deemed to be at high risk of infection (as opposed to culling only the infected farms). Optimal culling strategies are similar when social impact is the outcome of interest. We conclude that more FMD transmission models should be developed that are specific to the challenges of FMD control in near-endemic, low-income countries.

3.1 Introduction

Foot and mouth disease (FMD) is a highly contagious, and non-curable viral disease of economically important cloven-hoofed animals such as cattle, pigs, goats and sheep [10, 66, 131, 42, 98], and more than 70 species of wild animals, e.g. deers, antelopes and buffaloes [33, 51]. The disease agent that causes FMD belongs to the *picorna* virus family [19, 33], and it exists in seven known immunologically distinct serotypes, which vary according to world geographical location [113, 3]: (a) European

types O, A and C; (b) African types STA 1, STA 2 and STA 3 and (c) Asian type Asia 1 [29, 32]. The FMD virus serotypes are further divided into several (more than 60) subtypes [3, 5, 19] and they all occur with little cross-protection between each other [67]. The virus is airborne and can also be transmitted through physical contact with infected animals' expired air, saliva, milk, urine, semen, animal feed and bedding, etc [42, 10, 51]. FMD is rarely fatal, but infected animals display high fever, depression, loss of weight and drop in milk production, as well as blisters on the tongue, lips, mouth, and between toes [113, 10, 42, 59].

Conventional control measures of FMD include movement restriction (e.g. through construction of 'veterinary boundaries', i.e. cordon fences erected to divide a country into multiple subregions to prevent movement of animals across the borders); public education; quarantine; vaccination and culling [14]. Control measures of FMD need to take into account the natural characteristics of the virus, mechanism of spread, as well as strategic implementation based on available resources [27, 112]. Because of their greater resources, most developed countries have managed to contain, eradicate and avoid importation of FMD virus into their territories. However the disease is still an impediment to more than 100 developing and transitional countries [23, 69, 114, 96], mostly in South America, Africa and the Middle East [68]. The types of animals affected by FMD have long been a source of food, transportation, medicine, entertainment, clothing, and financial security for humans [40]. Hence, the impact of FMD can extend beyond economics in many developing and transitional countries, where possession of domestic animals such as cattle in many cultural or religious groups is still seen as a symbol of wealth and high social status [40].

The rich database for the dynamics and control of the 2001 FMD outbreak in the United Kingdom (UK) has, of recent, inspired many researchers to develop and analyze mathematical models of the disease [125], with an intention to inform policy [46] on better disease control strategies. This had led to many studies focusing on dynamics of a single epidemic outbreak (characteristic of developed countries where FMD outbreaks are rare). Two basic forms of vaccination usually considered are prophylactic vaccination (pre-outbreak vaccination of farms in an at-risk population to prevent introduction of the disease) and ring vaccination (carried out during outbreaks on farms deemed to be at risk of infection due to their geographical proximity to infectious farms [65].

Methods of culling considered by most models include infected premises (IP) culling (slaughtering infected farms), dangerous contacts (DC) culling (culling in premises where animals may have been in direct or indirect contact with infected animals) and contagious premises (CP) culling (slaughtering of farms that border infected premises) [65, 124, 95]. However, few mathematical models of FMD have investigated impacts of constrained vaccination and culling in 'near-endemic' settings, where FMD outbreaks occur repeatedly due to re-introductions from nearby wild endemic populations.

In [125] the authors develop a probabilistic transmission model of FMD and explore an optimal deployment strategy of limited reactive ring vaccination of cattle in a single epidemic outbreak. In [93] the authors construct and numerically analyze single-outbreak, deterministic, mean-field equations (they assume homogeneous mixing of host population) based on an SEIR (susceptible, exposed, infected, recov-

ered) natural history of FMD to illustrate impacts of constrained vaccine supply on optimal vaccination schedule. In [106] the authors apply stochastic optimal control theory, and incorporate spatiality, to study impacts of constrained vaccination supply on an epidemic outbreak of FMD. In [52] the authors construct a compartmental SIR (susceptible,infectious, recovered) model that explores impacts of limited isolation resources and limited vaccination resources. This approach is also tailored to FMD-free settings. While they appreciate the benefits of investigating impacts of constrained vaccination in [101], the authors focus on benefits of vaccination given triggers such as change in location of epidemic outbreak, and delay in implementation of vaccination and develop a spatial premises based model using data from FMD situation in Scotland. In [42] the authors analyze data from the FMD epidemic outbreak in the United Kingdom in 2001 and parameterize a pair approximation model to capture spatial spread, and predict future outbreaks and potential impacts of vaccination (vaccination was not used during the UK 2001 FMD epidemic outbreak). In [95] the authors develop and study a pair approximation model of FMD that describes dynamics and control (by culling) of a single outbreak. They further present the derivation of a spatially oriented expression of the basic reproduction number (the expected number of secondary cases produced by a single infection in a completely susceptible population [15, 95, 21]), from which impacts of culling can be measured.

The following description of pair approximation (PA) models is adapted from [107, 15, 64, 95]. PA models are regarded to as the simplest extension of the mean field equations because while the latter are formulated under an assumption that members of the host population of farms mix homogeneously, such that an infectious farm can

transmit the virus to any susceptible farm in the population, the former implicitly incorporate spatiality by modeling pairs of neighbouring farms, and assume that events such as infection can take place only between connected farms. In the context of FMD, connection between farms can be described in terms geographical distance or other forms of interaction like business ties, which may enhance transmission of the virus. A PA model comprises of a system of ordinary differential equations called pair equations. The derivation of an equation of motion for a pair of farms will involve triples; equations of motion for triples will involve quadruples, etc. To obtain a manageable system of equations of motion we truncate this hierarchy by a technique called moment closure approximations (MCA). There exist several MCAs at the level of pairs (also known as pair approximations), but all of them are used to approximate the resulting triples in terms of lower order correlations, i.e. pairs and singletons. MCAs differ in their assumption of the distribution of farms in a network. The choice of a MCA depends on the intent of the studies or characteristics of the disease spread. For instance, for a triple involving nodes X, Y and Z the ordinary pair approximation (OPA) assumes conditional independence of disease statuses of farms such that a farm X is related to a farm Z, only because they are both directly connected to Y, i.e. no triangles. Another widely used MCA at the level of pairs is the triangular pair approximation (TPA). The distinguishing feature between the OPA and the TPA is that the latter allows for the existence of triangles in the population of farms.

Here we develop an SEIRVC (susceptible, exposed, infectious, recovered, vaccinated, culled) pair approximation model of FMD transmission in a near-endemic population, and explore the impact of constrained vaccination and culling on long-

term dynamics of the disease. The model is intended to apply to resource-limited countries subject to repeated disease re-introductions, such as Botswana. In Botswana, farms are dominated by cattle, seasonal movement of farm animals due to nomadism is minimal, veterinary boundaries are widely used, both vaccination and culling are applied (although only culling is applied in certain regions), and farming regions experience repeated re-introductions from neighbouring wild populations where FMD is endemic. The longer time horizon that repeated outbreaks and frequent disease re-introduction impose on disease control, and the wider use of vaccination in such countries, makes factors such as waning vaccine and natural immunity important [107]. Our objective is to illustrate features of FMD dynamics and control through vaccination and culling that are unique to resource-limited, near-endemic settings, in contrast to the broad literature on FMD modelling in higher-income, disease-free settings. Both the rates of culling and possible number of culls per epidemic outbreak may be dependent on the availability of resources such as manpower, equipment for culling and disposal of carcasses. Vaccine supplies are likewise limited by the stockpile available, and so authorities face a decision regarding when and how to vaccinate farms. As outcome measures, we explore both the final size of outbreaks, as well as social impacts. Social impact is defined by total animals culled or infected, and is intended to reflect the broader social significance of animals in some low-income countries [40]. The model structure is described in the following section.

3.2 Model description

We build on a previous pair approximation model of FMD [107]. Cattle are highly susceptible to FMD and this enables the virus to spread rapidly to the entire herd [30, 51]. Thus it is difficult to track down the spread of FMD from one animal to another within a farm. Hence, the farm is taken as the fundamental epidemiological unit in our model, in line with a common assumption in the literature on pair approximation FMD models [107, 95, 43].

The state variables of our model are singletons, $[X]$ and pairs, $[XY]$, representing the number of farms whose disease status is X, and the number of neighbouring pairs of farms comprising of status X and status Y farms, respectively. Transmission at a rate τ takes place between an infectious and a neighbouring susceptible farm, moving the latter to the exposed compartment. The population of farms is assumed to exist on a random contact network with Poisson-distributed neighbourhood size. However, the network is conceived to represent an underlying spatial point-process model with an infection kernel. Ref [17] shows that a properly parameterized network model can approximate epidemic dynamics of a spatial point-process model with an infection kernel, for parameters such that the infection is endemic in the absence of interventions. We also carried out the full analysis for a scenario where farms are distributed on a regular lattice, and we found that this did not qualitatively change the results.

A farm stays in the exposed state for ν^{-1} days on average (latent period), after which it becomes infectious. The recovery rate is σ. The natural immunity wan-

ing rate is ω, enabling transition of farms from R to S compartments. Prophylactic vaccination and ring vaccination occur at per capita rates ψ_p and ψ_r, respectively, and transfer vaccinated susceptible and exposed farms to the vaccinated compartment. The rate of loss of vaccine-induced immunity (vaccine waning) is θ (where farms lose protection from the vaccine, becoming susceptible again). We explore IP culling and DC culling (defined as slaughtering of non-infectious farms neighbouring an infected farm on the contact network) Whenever a DC cull occurs, the infected farm that prompted the cull is also culled (IP culling), but we refer to both processes inclusively as 'DC culling' throughout, for simplicity. The rates of IP and DC culling are μ_{IP} and μ_{DC}, respectively, and previously culled farms are replaced (joining the susceptible pool) at a rate η. Because links in a contact network can be taken to represent any kind of potentially effective contact between farms and because we do not model space explicitly, we interpret culling of a network neighbour as DC culling rather than CP culling, which is implemented in a geographically spatial environment.

The rates of transition between compartments are expressed mathematically so that the model is formulated as a system of ordinary differential equations. In Appendix B.1 we illustrate the derivation of the equation of motion for $[SI]$ and present the full pair approximation model. Two forms of the ordinary pair approximation (OPA) are usually used: the binomial OPA (applicable to regular networks where the number of contacts per farm is fixed) and the Poisson OPA (applies in random networks where the neighbourhood size varies from one individual farm to another). In this paper we approximate triples by the Poisson OPA, see Equation B.2.

3.2.1 The basic reproduction number.

The analytical tractability of pair approximation models enables the derivation and analysis of epidemiologically important features such as the basic reproduction number, R_0, defined as the expected number of secondary cases produced by a single infection in a completely susceptible population [15, 95, 21]. An epidemic is possible if $R_0 > 1$ but the infection will die out if $R_0 < 1$. Our expression of the basic reproduction number captures spatiality by virtue of the fact that its derivation uses the correlation function, C_{XY} between farms with disease statuses X and Y:

$$C_{XY} = \frac{N}{n}\frac{[XY]}{[X][Y]}, \tag{3.1}$$

where n is the average number of neighbours per farm and N is the total population size [64, 95]. $C_{XY} = 1$ corresponds to mass-action mixing; $C_{XY}>1$ aggregation and $C_{XY}<1$ avoidance of farm types X and Y. It is worth noting that under mean-field approximations where $n = N$ (because it is assumed that all susceptible individuals farms are equally likely to acquire the disease from any infectious farm in the population) and $[XY] = [X][Y]$, correlation between two farms remains constant at $C_{XY} = 1$, through time. However under pair approximations, it is possible to derive an expression for R_0 by taking advantage of biological intuition about the geometric structure of early invading clusters of infected farms. In particular, infected farms tend to cluster together on the network in the early stages of invasion, which has implications for the efficiency of disease transmission and hence the R_0. Such effects enable us to relate correlations between susceptible and infectious farms (C_{SI}) to correlations between exposed and infectious farms (C_{EI}) [15, 95]. A more detailed

description is provided in A.2 and the resulting expression for R_0 is

$$R_0 = \frac{\tau n C^*_{SI}}{(\psi_r + \mu_{DC}) n \left(\frac{[E]}{N} C_{EI}\right)^* + (\sigma + \mu_{IP})}. \tag{3.2}$$

C^*_{SI} and $\left(\frac{[E]}{N} C_{EI}\right)^*$ are defined explicitly in Appendix B.2.

At first glance, Equation 3.2 reveals that a high recovery rate σ, corresponds to a low value of the basic reproduction number. This is because increasing σ leads to a significant decrease of the number of infectious farms (therefore reducing the spread). Also from Equation 3.2 it is apparent that the transmission rate τ, increases the basic reproduction number while vaccination and culling reduce R_0. We point out, however, that the actual impacts of model parameters, including rates of control measures, can be modeled numerically using the full expression of the basic reproduction number presented in Appendix B.2.

3.2.2 Baseline parameters.

After contact with the virus, it takes between 2 and 14 days for cattle, swine, sheep, goats and deers to show symptoms of FMD [92]. According to Ref.[81] the latent period of FMD is 3.1 to 4.8 days in cattle. Ref. [66] claims this period is 4 to 5 days. Here we average over these values and assume that the latent period of FMD in cattle is 4 days, thus $\nu = 1/4 = 0.25\ day^{-1}$. Depending on animal species affected, infected animals remain symptomatic of FMD and infectious for about 7 to 10 days before they recover, [51]. Here we assume that the recovery rate is $\sigma = 1/7 = 0.143$ day^{-1}. Farms in Botswana tend to be dominated by cattle, hence our natural history

parameter values are those specific to cattle.

The length of natural and vaccine protection from FMD ranges from 6 months to 5.5 years, depending on species affected, the virus serotype, and type of vaccine administered [34, 65]. Our baseline choices of rates of natural immunity waning and vaccine waning are $\omega = 1/180 = 0.0056\ day^{-1}$ and $\theta = 1/180 = 0.0056\ day^{-1}$, respectively.

We fix the population size at $N = 40,000$ farms and assume that per capita vaccination rates of prophylactic and ring vaccination, ψ_p and ψ_r, take values between 0 day^{-1} and 0.006 day^{-1}. The predicted vaccination capacity in a higher-income country such as Scotland has been approximated as 136 farms per day [101]. For an absolute upper limit on ψ_p and ψ_r we choose 0.006 day^{-1}, which corresponds to vaccinating 240 farms per day in a population of 40,000 farms. We chose a relatively generous upper bound for the vaccination rate to illustrate what could be accomplished in resource-limited settings, if greater resources were eventually made available.

During the 7 month-long FMD outbreak in Great Britain in 2001, over 11,000 farms were culled [124]. This corresponds to 50 farms per day on average, although the rate was much higher during the peak of the epidemic. We assume that rates of IP culling, μ_{IP} and DC culling, μ_{DC}, take values between 0 day^{-1} and 0.25 day^{-1}. For a prevalence of 2.5 % in a population of 40,000 farms, this corresponds to an upper bound of 250 farms culled per day. As with vaccination, we chose a relatively generous upper bound to the culling capacities to illustrate what could be possible in resource-limited settings, if greater resources were eventually devoted to

FMD control.

We also assume that farmers are compensated for culled farms at a rate $\eta = 1/1464 = 0.00068\ day^{-1}$ (i.e. compensation is carried out after 4 years, which reflects the situation in near-endemic, resource-limited settings).

Our baseline value for the transmission rate is taken from a similar model in [107], where $\tau = 0.6\ day^{-1}$ was derived from the basic reproduction number. This value also yields epidemiologically plausible responses to realistic intervention levels [107]. However, we also explore scenarios with $\tau = 0.3\ day^{-1}$ (corresponding to a large average distance or low level of interaction between infectious and susceptible farms), and $\tau = 0.9\ day^{-1}$ (corresponding to a small average distance or high level of interaction between infectious and susceptible farms) in sensitivity analysis. Changes in the value of τ implicitly capture both changes in the spatial location of farms, with higher values corresponding to higher farm density, as well as any changes in average herd size or herd composition, though not between-farm heterogeneities.

In some countries, foot and mouth disease can spread across borders through animal movement or trade. In some parts of Botswana FMD is imported from Zimbabwe or South Africa resulting in a series of outbreaks almost every 2 years [87]. Model simulations in our study are run under a presumption that the disease is re-introduced into the population of farms every 800 days (just over 2 years). We summarize all baseline parameters in Table 3.1.

Table 3.1: Baseline parameters for our model

parameter	value	source
Transmission, τ	0.6 day^{-1}	[107]
Latency, ν	0.25 day^{-1}	[81, 92, 66]
Recovery, σ	0.143 day^{-1}	[95]
Natural immunity waning, ω	0.0056 day^{-1}	[34]
Ring vaccination, ψ_r	(0 - 0.006) day^{-1}	calibrated
Prophylactic vaccination, ψ_p	(0 - 0.006) day^{-1}	calibrated
Vaccine waning, θ	0.0056 day^{-1}	[34, 65]
IP culling, μ_{IP}	(0 - 0.25) day^{-1}	calibrated
DC culling, μ_{DC}	(0 - 0.25) day^{-1}	calibrated
Replacement of culled farms, η	0.00068 day^{-1}	assumption

3.2.3 Constraints of vaccination and culling capacity.

Let $X_p(t)$ and $X_r(t)$ be the cumulative number of farms prophylactically vaccinated and ring vaccinated since the beginning of the year, respectively, at any given time t. We define the 'vaccine capacity' as the total number of farms that can be vaccinated in a given year. Let V_i, $i = 1, 2, 3...$, be the vaccine capacity in a given year. Let ψ_p and ψ_r be the rates of prophylactic vaccination and ring vaccination, respectively. Also, let $\psi_p^{max}, \psi_r^{max} \in [0, 0.0060]^2$ describe maximal possible rates of prophylactic and ring vaccination. For each year, $\psi_p = \psi_p^{max}, \psi_r = \psi_r^{max}$ as long as $X_p + X_r \leq V_i$. However, as soon as the vaccine capacity V_i is reached, $\psi_p = \psi_r = 0$ day^{-1} for the remainder of the year. That is, each year, vaccination is deployed until maximum vaccine supply is reached, after which the outbreak progresses without additional control measures. At the beginning of the following year, $\psi_p = \psi_p^{max}, \psi_r = \psi_r^{max}$ and the process repeats. We assume that the vaccine is 100 % effective at the farm level and all vaccinated farms are protected from infection for the duration of vaccine immunity, although in reality the effectiveness at the level of the individual

animal can be less than 100 %, due to strain mismatch for example.

Culling rates can also be constrained. If C_i, $i = 1, 2, 3, ...$, is the maximum possible culling rate in a year, determined by available manpower, then corresponding rates of IP culling, μ_{IP}^{max}, and DC culling, μ_{DC}^{max}, depend on C_i and the network structure such that $(n+1)\mu_{IP}^{max} + \mu_{DC}^{max} = C_i$, where n is the average number of neighbours each farm has and $\mu_{IP}^{max}, \mu_{DC}^{max} \in [0, 0.25]^2$. The factor $(n+1)$ incorporates the idea that with DC culling the infected farm is also culled.

Finally, we also explore scenarios where the total number of culled farms is constrained. Let $Y_{IP}(t)$ and $Y_{DC}(t)$ be the cumulative number of farms IP-culled and DC-culled since the beginning of the year, respectively, at any given time and let Y_i, $i = 1, 2, 3...$ be the possible number of culled farms in a given year. Let $\mu_{IP}^{max}, \mu_{DC}^{max} \in [0, 0.25]^2$ describe the corresponding maximal possible rates of IP and DC culling. For each each year, if $Y_{IP} + Y_{DC} \leq Y_i$, then $\mu_{IP} = \mu_{IP}^{max}, \mu_{DC} = \mu_{DC}^{max}$, but once once Y_i is reached, then $\mu_{IP} = \mu_{DC} = 0\ day^{-1}$ for the remainder of the year.

3.3 Results and Discussion

Numerical analysis of our model was carried out in *MATLAB* using the ode45 solver. The quality of numerical solutions remained the same when we experimented with other ordinary differential equations solvers (ode15s and ode23) in *MATLAB*.

We first explore the impacts of constrained vaccination in the absence of culling. The total number of vaccines administered is constrained according to the

equation $X_p + X_r \leq V_i$. For any given rates of prophylactic vaccination ψ_p^{max}, and ring vaccination ψ_r^{max}, increasing the vaccine capacity, V_i, always brings about more vaccine coverage, leading to a decrease in cumulative infections over a 20 year period (Figure 3.1). Hence, as expected, increasing vaccine capacity is desirable whenever possible. However, if it is not possible to increase vaccine capacity, then a decision-maker faces the choice of how to optimize the rates of vaccination ψ_p^{max} and ψ_r^{max}. When vaccine capacity is relatively low (e.g. Figure 3.1a), the highest rates of prophylactic vaccination ψ_p^{max} actually produce more cumulative infections than intermediate rates falling within the darker regions of Figure 3.1a ($\psi_r^{max} = 0.0060\ day^{-1}$). The optimal ring vaccination rate remains at approximately $\psi_r^{max} = 0.0060\ day^{-1}$ (the maximum possible value in the range of values considered) while the optimal prophylactic vaccination rate increases gradually from $\psi_p^{max} = 0.0005\ day^{-1}$ (Figure 3.1a) to $\psi_p^{max} = 0.0022\ day^{-1}$ (Figure 3.1d) as V_i increases from 6000 per year to 18000 per year. At higher values of ψ_p^{max}, the supply of vaccine is used up before the year is finished, while at the lower, more optimal values of ψ_p^{max}, it lasts throughout the year. This observation implies that optimally controlling FMD when vaccine capacity is strongly constrained requires spreading out available supplies for prophylactic vaccination over the course of the year, while during outbreaks, ring vaccination should always be deployed as rapidly as possible.

Table 3.2 summarizes the optimal rates of prophylactic and ring vaccination for a range of values of vaccine capacity V_i. These results assume the baseline transmission rate $\tau = 0.6\ day^{-1}$. Decreasing the transmission rate ($\tau = 0.3\ day^{-1}$) decreases the overall number of cumulative infections, while increasing the transmission

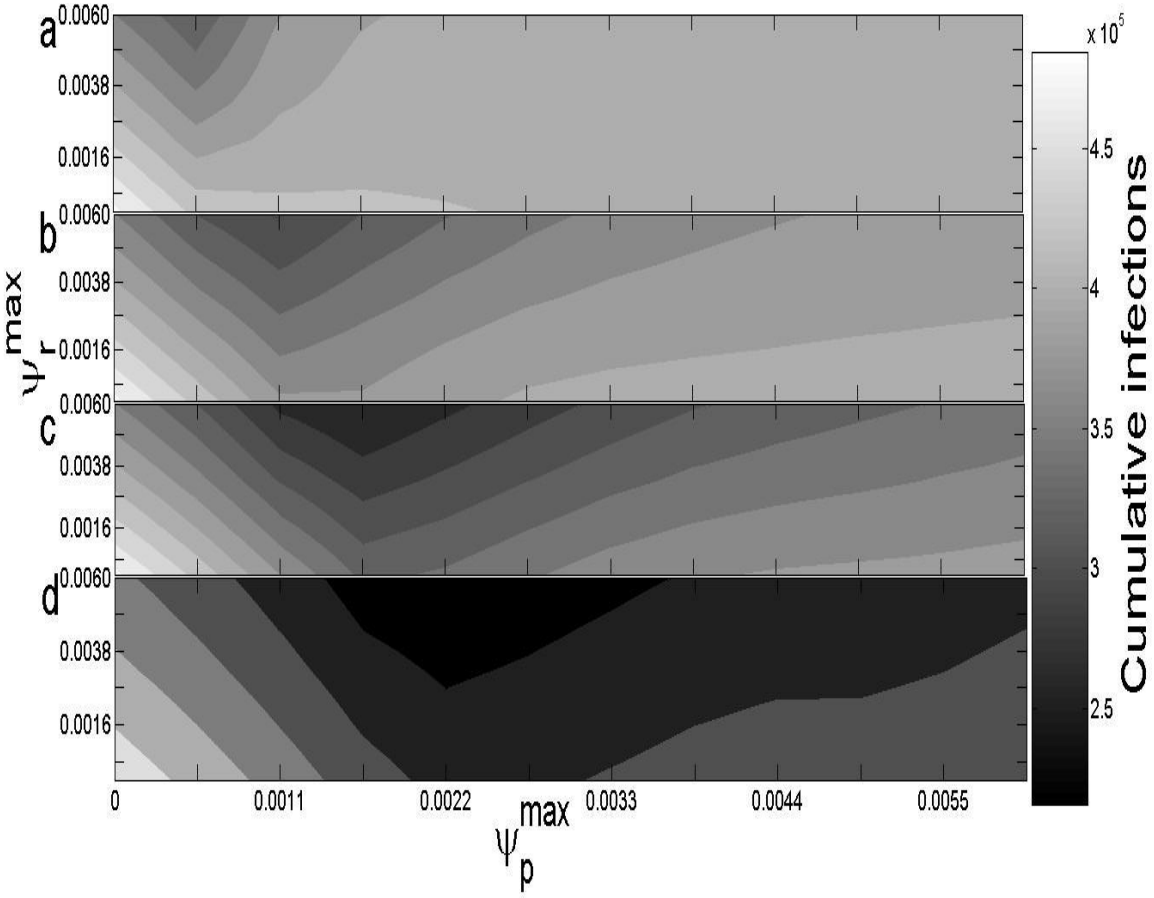

Figure 3.1: Cumulative infections in 20 years versus rates of prophylactic vaccination, ψ_p^{max}, and ring vaccination, ψ_r^{max}, for vaccine capacities $V_i = 6000$ per year (a), $V_i = 10000$ per year (b), $V_i = 14000$ per year (c) and $V_i = 18000$ per year (d). Model parameters are in Table 3.1.

parameter ($\tau = 0.9\ day^{-1}$) yields more cumulative infections (Online supplementary material Figure B.1). However, in agreement with the observation made from Figure 3.1, the conclusion that when vaccination capacity is strongly constrained, the optimal ring vaccination rate remains constant at the maximum possible value in the range of values considered, while the optimal prophylactic vaccination rate increases gradually from low to higher values as V_i increases, also holds for lower or higher

Table 3.2: Minimum cumulative infections in 20 years, corresponding optimal rates of prophylactic vaccination, ψ_p^{max}, and ring vaccination, ψ_r^{max}, varying vaccine capacities, V_i, and yearly average number of prophylactic and ring vaccines used. Model parameters are in Table 3.1.

V_i	min. cum. infec	ψ_p^{max}	ψ_r^{max}	avg. yearly proph.	avg. yearly ring
6000	323160	0.0005 day^{-1}	0.0060 day^{-1}	5599	401
8000	313059	0.0011 day^{-1}	0.0060 day^{-1}	7648	352
10000	296160	0.0011 day^{-1}	0.0060 day^{-1}	9675	325
12000	286434	0.0016 day^{-1}	0.0060 day^{-1}	11693	307
14000	258370	0.0016 day^{-1}	0.0060 day^{-1}	13711	289
16000	244865	0.0022 day^{-1}	0.0060 day^{-1}	15761	239
18000	215640	0.0022 day^{-1}	0.0060 day^{-1}	17782	218
20000	188626	0.0027 day^{-1}	0.0060 day^{-1}	19799	201
22000	167850	0.0027 day^{-1}	0.0060 day^{-1}	21814	186
24000	145680	0.0033 day^{-1}	0.0060 day^{-1}	23831	169

values of τ (Online supplementary material Figure B.1).

In agreement with Figure 3.1, the rate of prophylactic vaccination that yields minimum cumulative infections remains well below the maximum permissible value across a wide range of values of V_i, although the optimal value increases gradually with increasing V_i, up to a value of $\psi_p^{max} = 0.0033\ day^{-1}$ for $V_i = 24,000$ (Table 3.2). In contrast, the optimal rate of ring vaccination remains constant at the maximal value $\psi_r^{max} = 0.0060\ day^{-1}$. The total number of vaccines administered through ring vaccination is relatively small compared to the total number of vaccines administered prophylatically, since ring vaccination at a sufficiently high rate is sufficient to end an outbreak quickly, resulting in a relatively small number of ring-vaccinated farms (Table 3.2). Results are qualitatively similar for lower and higher transmission rates τ (Online supplementary material Tables B.1, B.2).

Time series of the number of infectious farms and number of vaccinated farms for various rates ψ_p^{max} show why it is better to spread out prophylactic vaccination over the course of the year (Figure 3.2). These time series illustrate the third row

of Table 3.2. We observe that when $\tau = 0.6\ day^{-1}$ then for $V_i = 10,000$ vaccines per year, the optimal rate of prophylactic vaccination $\psi_p^{max} = 0.0011\ day^{-1}$ prevents larger outbreaks, and the percentage of infectious farms remains below 1.5% (Figure 3.2a) and the vaccine supply lasts for most of the year (Figure 3.2b). However, at a higher rate $\psi_p^{max} = 0.0016\ day^{-1}$, the vaccine supply runs out much earlier in the year (Figure 3.2b). Every few years, this event is followed a few months later by large peaks in infection prevalence, surpassing 3%, and occurring before the supply is renewed the following year (Figure 3.2a).

We point out that waning of vaccine immunity plays a large role here. If vaccine immunity did not wane so quickly, a strategy of vaccinating at rate $\psi_p^{max} = 0.0016\ day^{-1}$ might work better, since vaccine protection would extend for a longer time, after the vaccine supply ran out. This is confirmed by sensitivity analysis (Online supplementary material, Table B.3). Thus the optimal rates of prophylactic and ring vaccination depend on the duration of natural immunity and vaccine immunity, such that when these durations are increased (i.e reduction of rates of natural immunity waning, ω and vaccine waning, θ), higher rates of prophylactic vaccination are optimal.

A decrease in the rate of disease importation causes a decrease in cumulative infections (Online supplementary material, Figure B.2). This signifies the importance of putting measures in place to avoid disease re-introduction, for instance by managing animal movement and erecting cordon fences around farms. It also illustrates how cumulative infections can be determined by nonlinear interactions between vaccine capacity and disease re-introduction rates, suggesting that vaccine programs and

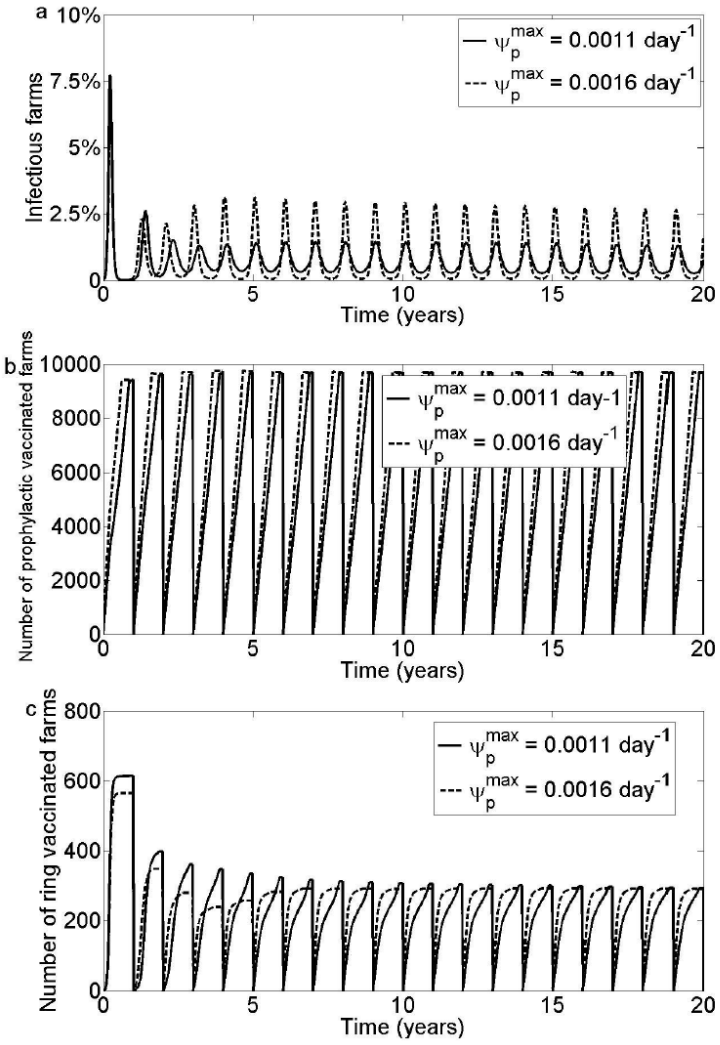

Figure 3.2: Time series for number of infectious farms (a), number of prophylactic vaccinated farms (b) and number of ring vaccinated farms (c) varying rates of prophylactic vaccination, ψ_p^{max}. $V_i = 10000$ per year, $\psi_r = 0.0060\ day^{-1}$ and parameters are in Table 3.1.

movement restrictions should be designed in an integrated way in near-endemic settings.

Next, we manipulated culling rates in the absence of vaccination, where culling rates ($\mu_{IP} = \mu_{IP}^{max}$ and $\mu_{DC} = \mu_{DC}^{max}$) are constrained by the equation ($n +$

1)$\mu_{IP}^{max}+\mu_{DC}^{max}=C_i$, where $\mu_{IP}^{max},\mu_{DC}^{max}\in[0,0.25]^2$ and n is the average neighbourhood size. (We remind the reader that, whenever a DC cull occurs, the infected premises that stimulated the DC cull is also culled.) As expected, increasing the culling rate capacity, C_i reduces cumulative infections and size of epidemic peaks (Figure 3.3).

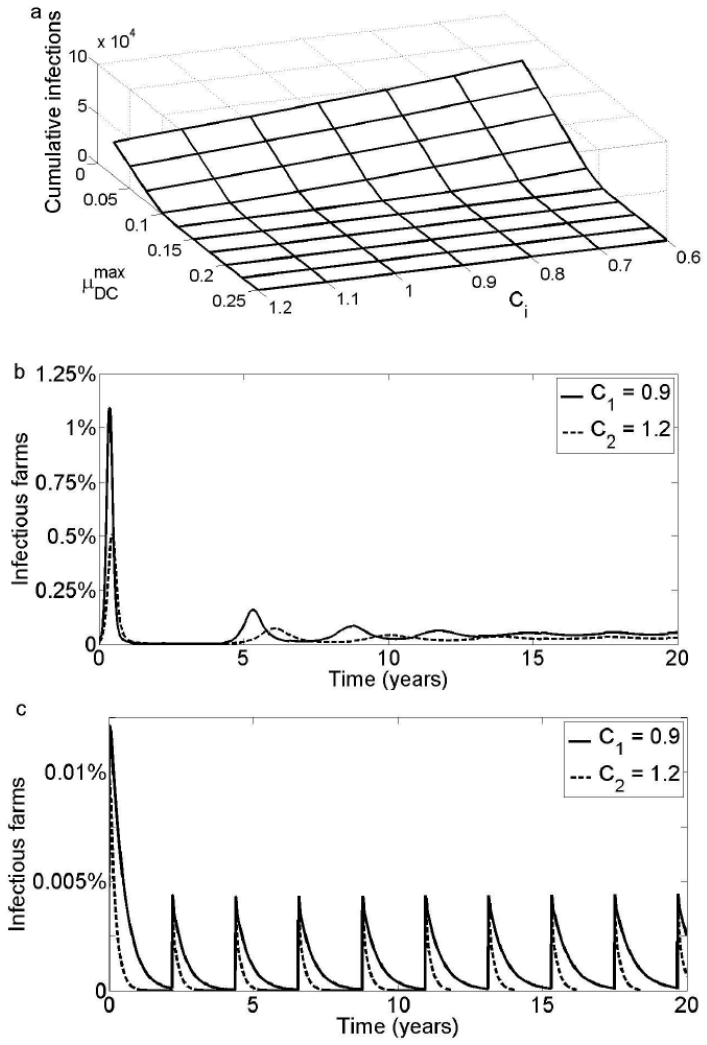

Figure 3.3: Cumulative number of infectious farms in 20 years as a function of **DC** culling, μ_{DC}^{max} (and IP culling, μ_{IP}^{max}), and culling rate capacity, C_i (a). Time series for infectious farms where $\mu_{DC}^{max}=0.025\ day^{-1}$ (b) and $\mu_{DC}^{max}=0.125\ day^{-1}$ (c). $n=4$ and other parameters are in Table 3.1.

However, the size of this reduction depends on the culling capacity. When the culling rate capacity C_i is small, the cumulative number of infections is smallest when μ_{DC} is large. For instance, when $C_i = 0.6$, then the cumulative number of infections is smallest when the rate of DC culling is $\mu_{DC}^{max} = 0.25\ day^{-1}$ (Figure 3.3a; we note that the corresponding rate of IP culling at this point is $\mu_{IP}^{max} = 0.07\ day^{-1}$). However, when the culling capacity is large, the cumulative number of infections is relatively small regardless of the value of μ_{DC}^{max} (Figure 3.3a). This implies that when culling capacity is small, it is better to concentrate resources into DC culling. However, if culling capacity is sufficiently large, then either IP or DC culling may be used, if their rates are high enough. The impact of changes in C_i is clear when culling rates are low (Figure 3.3b), but less apparent when culling rates are large, and the disease is essentially eradicated (Figure 3.3c: here rates of culling are so large that re-introduction of the disease every 800 days fails to set off an epidemic outbreak).

We also explored the impact of limiting the total number of culls allowed per year Y_i (described in Section 3.2.3). Increasing Y_i, decreases the number of cumulative infections (Figure 3.4).

We find that in agreement with Figure 3.3, when culling capacity Y_i is large, then the number of cumulative infections is relatively small across most possible rates of IP culling, μ_{IP}^{max} and DC culling, μ_{DC}^{max} and both forms of culling are relatively effective (Figure 3.4d). However, when Y_i is small, then the number of cumulative infections is only small when the rate of DC culling, μ_{DC}^{max} is sufficiently large, and the results are relatively insensitive to μ_{IP}^{max} (Figure 3.4a). Hence, when the total number of culls per year must be limited, it is better to put scarce resources into DC culling.

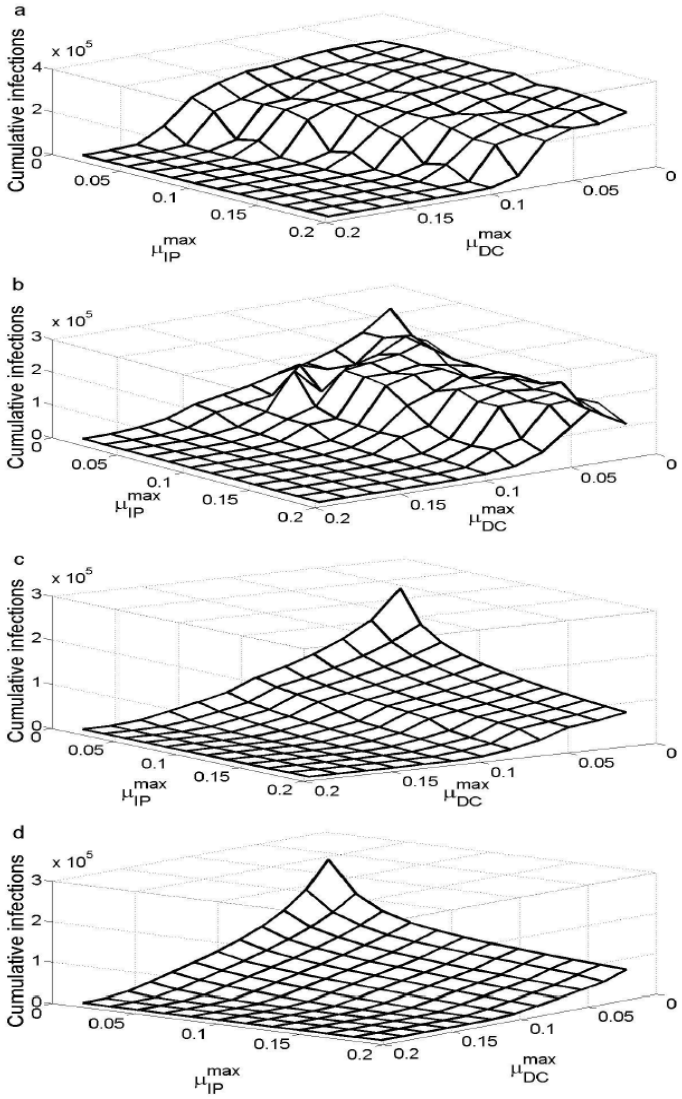

Figure 3.4: Cumulative number of infectious farms in 20 years as a function of IP culling, μ_{IP}^{max} and **DC** culling, μ_{DC}^{max} where upper boundaries of the number of culled farms are $Y_i = 1000$ per year (a), $Y_i = 2000$ per year (b), $Y_i = 4000$ per year (c) and $Y_i = 8000$ per year (d). Model parameters are in Table 3.1.

Along the same lines, another observation we can make from Figure 3.4 is that DC culling reduces cumulative infections faster than IP culling. For instance in Figure 3.4a, the number of cumulative infections decays rapidly with respect to

μ_{DC}^{max}, while the decrease in cumulative infections appears less steep with respect to μ_{IP}^{max}. This holds, but on different scales, even for large values of Y_i. The advantage of DC culling over IP culling is that the former helps get rid of potential new contacts, ensuring that initially infected farms do not have susceptible neighbours to whom they could transmit the disease. In contrast, unless it is applied promptly and rapidly, IP culling alone, may fail to prevent transmission to a neighbouring farm and thus a continued epidemic. The conclusions drawn from Figure 3.4 also hold under the high and low transmission rate scenarios ($\tau = 0.3, 0.9\ day^{-1}$), except that when the transmission rate is low or when Y_i is large enough then both forms of culling effectively bring the disease under control, and the results are less sensitive to variation of Y_i (Online supplementary material, Figure B.3).

A time series of the number of infectious farms in the situation where the number of farms culled is constrained below $Y_i = 1000$ per year shows how the fewest infections are obtained when culling rates are maximized, which results in rapid containment of the outbreak and thus fewer total culls in the long term (Figure 3.5d versus 3.5a). Confirming the observation established from Figure 3.4, when DC culling rates are very large, then the constraint $Y_i = 1000$ is never reached (Figure 3.5c, d) in contrast to the situation when culling rates are small (Figure 3.5a). Also in compliance with previous results, DC culling performs better than IP culling (Figure 3.5b versus Figure 3.5c).

Next, we evaluated the social impact of various control strategies, where social impact was defined as total number of farms infected or culled over a 20 year period. When the total number of annual culls Y_i is constrained, the social impact

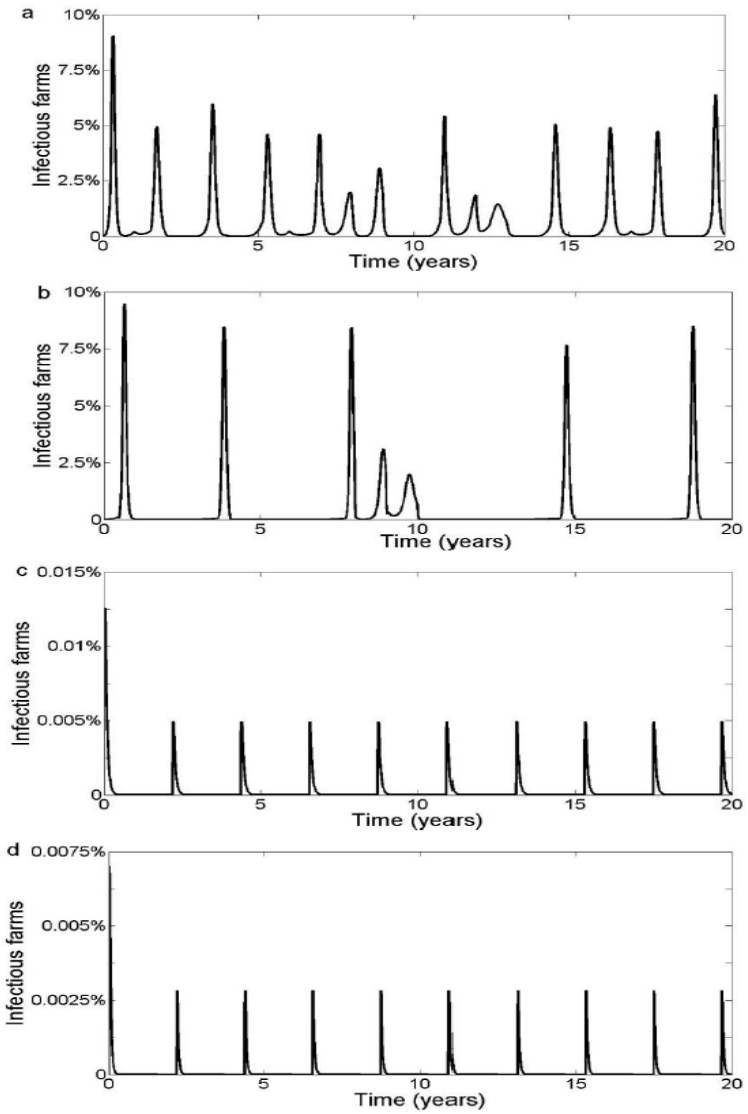

Figure 3.5: Time series for number of infectious farms where each year $\mu_{IP}^{max} = \mu_{DC}^{max} = 0.05\ day^{-1}$ (a), $\mu_{IP}^{max} = 0.25\ day^{-1}, \mu_{DC}^{max} = 0.05\ day^{-1}$ (b), $\mu_{IP}^{max} = 0.05\ day^{-1}, \mu_{DC}^{max} = 0.25\ day^{-1}$ (c) and $\mu_{IP}^{max} = \mu_{DC}^{max} = 0.25\ day^{-1}$ (d), before maximum culls, $Y_i = 1000$ per year is reached. Other parameters are in Table 3.1.

is smallest when DC culling rates are maximized and this applies across all values of Y_i (Figure 3.6). As before, results are less sensitive to changes in the IP culling rate. Hence, social impact at the global, population level is smallest when DC culling is

rapidly and vigorously applied at the local level. To permit this strategy to work, identification of infection point source and at-risk farms must be done early during the initial stages of an epidemic outbreak, so that DC culling not only successfully controls the disease but also results in fewer total culled farms, thereby minimizing social impact. While increasing the culling capacity Y_i generally reduces the number of cumulative infections and hence reduces social impact, its impacts are more profound when the transmission rate is large (Online supplementary material, Figure B.4).

In some regions of countries like Botswana, vaccination and culling can be applied simultaneously. Hence, we also explored a scenario where both control measures are applied, under constraints, and compared it to a scenario where only culling is applied. We found that the optimal culling strategy is to maximize the DC culling rate μ_{DC}^{max}, regardless of whether vaccination is also being applied (online supplementary material Figure B.5b versus B.5a). Additionally, at lower DC culling rates where culling is not perfectly effective in preventing epidemics, being able to deploy vaccination as well decreases cumulative infections by an order of magnitude, suggesting that the combination of both culling and vaccination is disproportionately more effective than either control measure on its own (online supplementary material Figure B.5b versus B.5a).

This model makes necessary simplifications that could influence results. Most notably, we assume that contacts between farms do not evolve over time, that the per-edge transmission rate and herd size are the same for each farm, and that the average farm density (reflected in average node degree of the Poisson distribution) does not change over the country. In reality, spatial and temporal heterogeneity

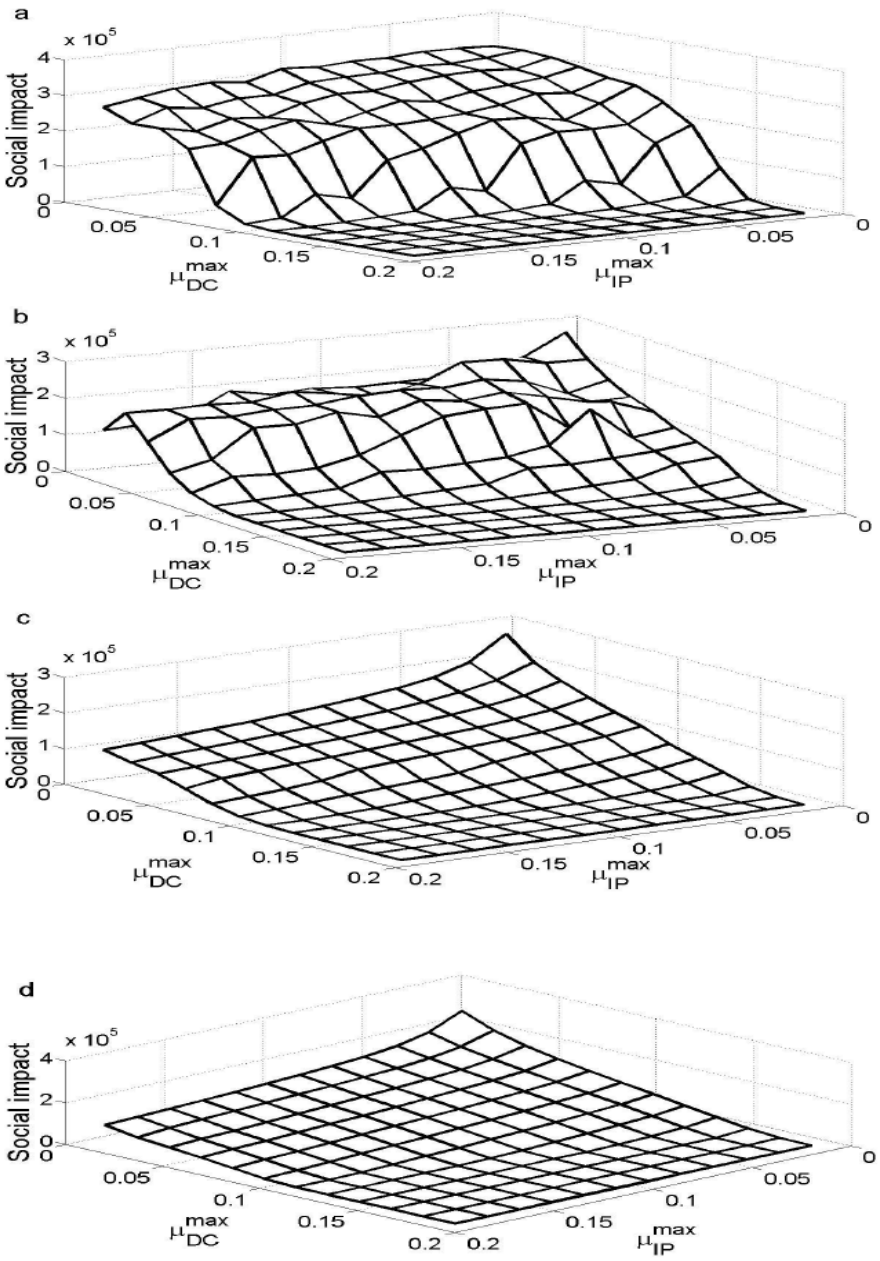

Figure 3.6: Social impact in 20 years as a function of IP culling, μ_{IP}^{max} and DC culling, μ_{DC}^{max} where upper boundaries of number of culled farms are $Y_i = 1000$ per year (a), $Y_i = 2000$ per year (b), $Y_i = 4000$ per year (c) and $Y_i = 8000$ per year (d). Model parameters are in Table 3.1.

could impact which control strategies are optimal. Seasonal movements of cattle due to nomadism, as occurs in some lower income countries, could also influence model predictions, although nomadism is not significant in Botswana.

Additionally, high resolution data are generally lacking in low income countries, making it difficult to create the kind of highly realistic country-specific models that were constructed for Great Britain in 2001 for example. However, the impact of heterogeneity on model predictions could be captured to some extent through carefully designed sensitivity analysis. And, even when high resolution data on current farm demographics is available, it is difficult to predict demographic changes over a longer period of time, as required for analyzing endemic or near-endemic situations. However, this is a problem for any model-based evaluation of long-term infectious disease dynamics, such as those undertaken for common endemic infections like measles.

3.4 Conclusions

Occurrence of repeated FMD epidemics in some developing countries poses a threat to international trade in animals and their products. Lack of resources such as skilled manpower, culling resources and vaccine supply, play a vital role in the dynamics and control of FMD in low-income countries with developing economies, as they cause difficulty in eradicating the disease and preventing future outbreaks. Decision-makers in these countries face tighter resource constraints when optimizing their control policies. In this paper we developed a spatially oriented pair approximation model that resembles the dynamics of FMD in some low-income countries

subject to near-endemic FMD. We investigated the impacts of constrained vaccination (prophylactic and ring) and culling (IP and DC) capacity on long-term dynamics of FMD.

We conclude that, if vaccine capacity is strongly constrained, then the strategy that minimizes the cumulative number of infections is rapid deployment of ring vaccination during outbreaks. In parallel with ring vaccination (and in contrast to the optimal ring vaccination approach), the rate of prophylactic vaccination must be carefully rationed such that vaccination is stretched out for as long as possible, in order to minimize cumulative long-term infections. This strategy avoids extended periods of time where no prophylactic vaccination is occurring, and during which populations are susceptible to outbreaks. With respect to optimal culling, the best approach is one that involves rapid identification of infected farms and their at-risk neighbours, followed by rapid culling of both infected and at-risk neighbouring premises. In contrast, putting resources into culling only the infected premises is usually less effective, even if more infected premises in total can be culled as a result. This is not sensitive to constraints on culling rates or on total annual culls, and results are similar when the outcome being minimized is total number of animals culled or infected (social impact).

Chapter 4

Spatially implicit modelling of disease-behaviour interactions in the context of non-pharmaceutical interventions

Material from this chapter has been submitted to Mathematical Biosciences

Abstract

Pair approximation models have been used to study the spread of infectious diseases in spatially distributed host populations, and to explore disease control strategies such as vaccination and case isolation. Here we introduce a pair approximation model of individual uptake of non-pharmaceutical interventions (NPIs) for an acute self-limiting infection, where susceptible individuals can learn the NPIs either from other susceptible individuals who are already practicing NPIs ("social learning"), or their uptake of NPIs can be stimulated by being neighbours of an infectious person ("exposure learning"). NPIs include individual measures such as hand-washing and respiratory etiquette. Individuals can also drop the habit of using NPIs at a certain rate. We derive a spatially defined expression of the basic reproduction number R_0 and we also numerically simulate the model equations. We find that exposure learning is

generally more efficient than social learning, since exposure learning generates NPI uptake in the individuals at immediate risk of infection. However, if social learning is pre-emptive, beginning a sufficient amount of time before the epidemic, then it can be more effective than exposure learning. Interestingly, varying the initial number of individuals practicing NPIs does not significantly impact the epidemic final size. Also, if initial source infections are surrounded by protective individuals, there are parameter regimes where increasing the initial number of source infections actually decreases the infection peak (instead of increasing it) and makes it occur sooner. The peak prevalence increases with the rate at which individuals drop the habit of using NPIs, but the response of peak prevalence to changes in the forgetting rate are qualitatively different for the two forms of learning. We conclude that pair approximation models of the impact of human behaviour on the spread and control of infectious diseases can help provide insights into infection control, and should be further developed.

4.1 Introduction

Mathematical models in epidemiology often make the assumption that successful control of epidemics is only determined by the availability and effective deployment of control measures such as vaccination and isolation, whose success largely depends on factors such as quantity of vaccine and logistical constraints. In recent years, some mathematical models are focusing on endogenously incorporating the impact of human behavioral patterns on the regulation of communicable diseases. Upon gaining awareness about an infectious disease outbreak, susceptible individuals

may decrease their infection risk by isolating themselves or reducing interactions with their friends, colleagues, etc, through staying at home and avoiding social contacts. This practice is known as social distancing [48, 79]. Along with social distancing, hand-washing, use of masks, and other respiratory etiquette are further examples of so-called 'non-pharmaceutical interventions' (NPIs) that can reduce infection spread [99]. While healthcare providers often advise the public on appropriate NPIs, behavioral choices of individual members of the host population partially determine the dynamics and feasibility to control an infectious disease outbreak.

Social distancing and other NPIs have assisted the control of infections such as flu, severe acute respiratory syndrome (SARS) and plague [16, 41, 122, 80, 44, 116, 45, 120, 78, 8]. However despite the availability of a large amount of information about the dangers and risks of sexually transmitted infections (STIs), actions like unsafe sexual behavior and needle sharing during intravenous drug use have been linked to the pandemic-scale dissemination of STIs such as HIV/AIDS [90, 84, 121, 86]. Generally, negligence or relaxation of precautionary measures is brought about by factors such as lack of awareness and engaging in infection-enhancing social practices such as handshakes, hug, kisses, sharing of food and concurrent sexual partner, as well as some cultural practices. The 2014 epidemic outbreak of Ebola in West Africa is an example of how cultural or religious practices, such as engaging in risky rituals and inappropriate handling of the sick or deceased, also influence the dynamics of infectious diseases [91].

Human behavior also plays a role in the regulation of some animal infectious diseases. For instance, the use of dogs in hunting and grazing cattle in countries such

as Kenya and Botswana, influences transmission of canine diseases between domestic dogs and the African wild dog [2]. Although culling (slaughtering of infectious or at-risk animals) has been found to effectively control foot and mouth disease, farmers' resistance towards this intervention measure (because of fear of loss of livestock) often makes it difficult to bring the disease under control.

In [41] the authors explore the impact of social distancing on the spread of an infection by incorporating health status-based contact behavior patterns into a mean-field equations epidemic model. Thus, the transmission dynamics are governed by differing contact levels between individuals of different health types. For example, due to the perceived risk of infection, susceptible individuals are likely to avoid contact with infected individuals, while maintenance contact with recovered individuals may have a less significant impact.

In [45] the authors explore the idea that the adoption of social distancing or other NPIs is driven by the level of information individuals have, such that members of the host population who possess first hand information become more cautious and therefore less susceptible than those who have second hand information. Similarly, individuals who have second hand information are less susceptible than those who posses third hand information, etc. This study was carried out by modeling information transmission and spread of an infection using mean-field equations and individual-based epidemic models. The research also discusses the significance of repeated re-generation of awareness into the population to ensure that most individuals have access to primary, or close-to-primary, information, which increases the number of individuals who exercise contact precautions and/or NPIs.

In [44] the authors capture the dynamic nature of individuals' decisions leading to adoption or non-practice of social distancing, by assuming that the network geometry within which the host population resides (particularly the neighborhood size) changes over time, depending on individuals' perceived risk of infection. Thus, adjustment of individuals' perceptions about the disease over time results in variation of contact pattens and, therefore, it affects the infection dynamics. Other researchers have explored game-theoretical [105] or rule-based simulation models [108, 118] of social distancing.

The spatial dimension of social distancing has been explored in some of this previous work [45, 44, 108, 118]. Spatial dynamics can be analytically intractable, hence the frequent decision to employ agent-based models. However, one method for implicitly capturing spatial dynamics that often permits analysis is moment closure approximation (MCA). MCAs employ pairs, triples, quadruples, etc., of connected individuals, as model state variables, such that transmission takes place only between connected susceptible and infectious individuals on the network. MCAs are usually comprised by a system of differential equations, where each equation describes time evolution of second order, third order, fourth order, etc., spatial correlations between individual members of the host population. Equations of motion for pairs involve terms in triples, equations of motion for triples involves terms in quadruples, etc. Therefore in order to obtain a closed system of equations, this hierarchy is truncated by techniques referred to as moment closures. Carrying out the closure at the level of pairs produces a pair approximation model [107, 18, 17, 15, 94, 95, 104, 42, 20, 64, 38, 57].

Here we develop and analyze a pair approximation model and explore the impacts of NPIs on the spread of an infectious disease. We incorporate impacts of NPIs by dividing the susceptible population into susceptible individuals who protect (S_p) (i.e., those who practice NPIs) and individuals who do not (S). State S individuals learn from state S_p and/or infectious (state I) individuals in their network neighborhood, and then decide whether or not to adopt NPIs. The dichotomy between adopting NPIs due to being next to an infectious person, versus learning NPIs from other individuals who adopt NPIs, captures the distinction between practicing NPIs reactively because of an immediate threat due to an infectious neighbour versus changing one's habits pre-emptively based on observing the actions of other individuals, and forming new habits (such as using hand sanitizers, or using a paper towel to open a bathroom door). We refer to learning NPIs from other state S_p contacts as "social learning", versus "exposure learning" that occurs from reacting to infection in an immediate network neighbour. We also derive the basic reproduction number and analyze the pair approximation equations to understand how control success depends on epidemiological and behavioral change parameters. The model is described in the following subsection.

4.2 Model

A state S individual who is neighbouring a state S_p individual transitions to the S_p state at a per capita rate ξ. Similarly, a state S individual neighbouring a state I individual transitions to the S_p state at a per capita rate ρ. These interactions

thereby result in susceptible individuals adopting NPIs. Switching from state S_p back to state S occurs at a per capita rate κ, representing forgetting, or complacency.

The rate of infection transmission from an infectious individual to a neighbouring state S_p individual is τ_p, whereas transmission to a neighbouring state S individual occurs at a rate $\tau > \tau_p$. Infected individuals recover at per capita rate σ. Thus, the state variables of the pair approximation model are numbers of susceptible, protective, infectious and recovered individuals denoted by $[S]$, $[S_p]$, $[I]$ and $[R]$, respectively, and numbers of paired individuals, $[XY]$ where, for instance $[S_pI]$ represents the number of edges comprising of susceptible protective and infectious individuals. We derive equations of motion for our model in Appendix C.1. We assume that the disease spreads on a regular network where the average node degree is n, in a population of size N, and we use the binomial ordinary pair approximation (Equation (C.2)), to approximate triples in terms of pairs and singletons, resulting

in:

$$
\begin{aligned}
\frac{d[S]}{dt} &= -\tau[SI] - \xi[S_pS] + \kappa[S_p] - \rho[SI] \\
\frac{d[S_p]}{dt} &= -\tau_p[S_pI] + \xi[S_pS] - \kappa[S_p] + \rho[SI] \\
\frac{d[I]}{dt} &= \tau[SI] + \tau_p[S_pI] - \sigma[I] \\
\frac{d[R]}{dt} &= \sigma[I] \\
\frac{d[SS]}{dt} &= -2\frac{n-1}{n}\frac{[SS]}{[S]}\Big((\tau+\rho)[SI] + \xi[S_pS]\Big) + 2\kappa[SS_p] \\
\frac{d[SS_p]}{dt} &= -\frac{n-1}{n}\Big((\tau+\rho)\frac{[SI][SS_p]}{[S]} + \tau_p\frac{[SS_p][S_pI]}{[S_p]} - \xi\frac{[SS_p][SS]}{[S]} - \rho\frac{[SI][SS]}{[S]}\Big) - \xi[SS_p] \\
&\quad + \kappa([S_pS_p] - [SS_p]) \\
\frac{d[S_pS_p]}{dt} &= -2\frac{n-1}{n}\Big(\tau_p\frac{[S_pI][S_pS_p]}{[S_p]} - \rho\frac{[SI][SS_p]}{[S]}\Big) + 2\xi[SS_p] - 2\kappa[S_pS_p] \\
\frac{d[SI]}{dt} &= \frac{n-1}{n}\Big(\frac{[SI]}{[S]}\Big(\tau[SS] - (\tau+\rho)[SI] - \xi[SS_p]\Big) + \tau_p\frac{[SS_p][S_pI]}{[S_p]}\Big) - (\tau+\sigma+\rho)[SI] + \kappa[S_pI] \\
\frac{d[S_pI]}{dt} &= \frac{n-1}{n}\Big(\frac{[SI]}{[S]}\Big((\tau+\xi)[SS_p] + \rho[SI]\Big) + \frac{[S_pI]}{[S_p]}\tau_p\Big([S_pS_p] - [S_pI]\Big)\Big) - (\tau_p+\sigma+\kappa)[S_pI] \\
&\quad + \rho[SI] \\
\frac{d[SR]}{dt} &= -\frac{n-1}{n}\frac{[SR]}{[S]}\Big((\tau+\rho)[SI] + \xi[SS_p]\Big) + \sigma[SI] + \kappa[S_pR] \\
\frac{d[S_pR]}{dt} &= -\frac{n-1}{n}\Big(\tau_p\frac{[S_pI][S_pR]}{[S_p]} - \frac{[SR]}{[S]}(\rho[SI] + \xi[S_pS])\Big) + \sigma[S_pI] - \kappa[S_pR] \\
\frac{d[II]}{dt} &= 2\frac{n-1}{n}\Big(\tau\frac{[SI]^2}{[S]} + \tau_p\frac{[S_pI]^2}{[S_p]}\Big) + 2\tau[SI] + 2\tau_p[S_pI] - 2\sigma[II] \\
\frac{d[IR]}{dt} &= \frac{n-1}{n}\Big(\tau\frac{[SI][SR]}{[S]} + \tau_p\frac{[S_pI][S_pR]}{S_p}\Big) - \sigma([II] - [IR]) \\
\frac{d[RR]}{dt} &= 2\sigma[IR].
\end{aligned}
\tag{4.1}
$$

4.2.1 The basic reproduction number

The basic reproduction number R_0 is the expected number of secondary infection cases produced by a single infectious individual upon introduction into a wholly susceptible population [31, 15, 9, 76, 92]. An epidemic may occur if $R_0 > 1$,

but the infection will die out if $R_0 \leq 1$. Therefore, effective disease control reduces R_0 below 1.

Here we use the pair approximation model above to derive an expression for R_0 that incorporates some effects of spatiality and allows us to study the impact of adoption of NPIs on the dynamics of the disease at the initial stage of an outbreak. For simplicity, we derive R_0 for a scenario where individuals start to learn and practice contact precautions during an outbreak ($S_p(0) \ll N$).

The condition under which the infection will spread is

$$\frac{d[I]}{dt} > 0 \Rightarrow \tau[SI] + \tau_p[S_pI] - \sigma[I] > 0, \tag{4.2}$$

which can be rearranged to yield

$$\frac{\tau[SI] + \tau_p[S_pI]}{\sigma[I]} > 1. \tag{4.3}$$

Therefore, we write R_0 in terms of (i) susceptibility of individuals who do not protect (captured by a high transmission parameter τ), (ii) susceptibility of individuals who practice NPIs (captured by a low transmission rate τ_p), (iii) the rate of recovery σ, and (iv) the numbers of $S - I$ and $S_p - I$ pairs as well as the overall number of infections individuals $[I]$:

$$R_0 = \frac{\tau[SI]}{\sigma[I]} + \frac{\tau_p[S_pI]}{\sigma[I]}. \tag{4.4}$$

Next we express pairs $[SI]$ and $[S_pI]$ in terms of the correlations between state S individuals and their infectious neighbors, and state S_p individuals and their infectious contacts, respectively. The correlation between individuals with status X

and Y is given by

$$C_{XY} = \frac{N}{n}\frac{[XY]}{[X][Y]}, \tag{4.5}$$

where n and N are the number of contacts each individual has and the total population size, respectively. $C_{XY}<1$ implies avoidance of interaction between state X and state Y individuals, $C_{XY} = 1$ assumes homogeneous mixing, while $C_{XY}>1$ implies strong correlation between state X and state Y individuals. Note that Equation (4.5) can be re-written as

$$[XY] = \frac{[n]}{N}[X][Y]C_{XY}, \tag{4.6}$$

therefore,

$$R_0 = \frac{n}{\sigma N}(\tau[S]C_{SI} + \tau_p[S_p]C_{S_pI}). \tag{4.7}$$

At the initial stage of an epidemic, we assume that the population is comprised mainly by susceptible individuals, only a few of whom practice NPIs:

$$[S] + [S_p] \approx N, \text{where } [S_p] << [S] \tag{4.8}$$

We define $s_p \equiv [S_p]/N$, thus the proportion of state S individuals at the beginning of the epidemic is $1 - s_p$, and R_0 becomes:

$$R_0 = \frac{n}{\sigma}\Big(\tau(1 - s_p)C_{SI} + \tau_p s_p C_{S_pI}\Big). \tag{4.9}$$

We use biological intuition to estimate the values C_{SI} and C_{S_pI}. There is a very small number of infectious individuals at the beginning of an outbreak, so $C_{SI} \approx 1$. However as the infection spreads, C_{SI} decreases and the clustering of infected individuals leads to a decrease in the rate of spread, and the disease may

die out if there are not enough susceptible individuals in the vicinity of the infected cluster to transmit the disease to. The dynamics of the disease at this point (referred to as the local minimum and denoted by C_{SI}^{min}) determine whether an epidemic will succeed or fail to take off. Thus, we need to evaluate C_{SI}^{min} [62]. Similar reasoning applies to $C_{S_pI}^{min}$. Hence

$$R_0 = \frac{n}{\sigma}\left(\tau(1-s_p)C_{SI}^{min} + \tau_p s_p C_{S_pI}^{min}\right). \tag{4.10}$$

The quantities C_{SI}^{min} and $C_{S_pI}^{min}$ are the solutions of $\frac{d}{dt}C_{SI} = 0$ and $\frac{d}{dt}C_{S_pI} = 0$, respectively.

The derivation of these quantities as well as the full expression of R_0 are presented in Appendix C.2. The full expression of R_0, Equation (C.5), is unwieldy but it depends on epidemiological parameters τ, τ_p and σ, NPIs-based parameters ξ, ρ and κ, as well as initial network configuration-dependent correlations C_{S_pS} and $C_{S_pS_p}$. It is clear from Equation (C.5) that a higher rate of recovery σ, reduces R_0, but the equation is too complicated to directly infer the impacts of other model components. Hence, numerical computations will be used to explore dependence of R_0 on model parameters and initial network configurations (Section 4.3).

We derive reduced versions of R_0 by considering special cases where individuals adopt NPIs through (a) social learning only (i.e. $\xi > 0\ day^{-1}$ and $\rho = 0\ day^{-1}$) and (b) exposure learning only (i.e. $\xi = 0\ day^{-1}$ and $\rho > 0\ day^{-1}$). For both of these scenarios we assumed that protective individuals consistently practice NPIs throughout the outbreak so that state S_p individuals do not switch back to state S (i.e. $\kappa = 0\ day^{-1}$). Furthermore, we assumed that the initial network configuration constitutes

one infectious (state I) individual with one protective (state S_p) neighbor who also has one state S_p contact, and the rest of the population is completely susceptible (i.e. state S) such that at the initial stage of the outbreak $[S] \approx N$, where the population size N is very large.

In Appendix C.2 we show that for case (a), where individuals adopt NPIs due to social learning only, if the protective behavior is highly effective as a control measure ($\tau_p << \tau$) and for typical model parameters ($N = 40000$, $s_p = 2/N$, $n = 4$, $\tau = 1\ day^{-1}$, $\tau_p = 0.0025\ day^{-1}$, $\sigma = 0.25\ day^{-1}$ and $\xi = 0.25\ day^{-1}$) then

$$R_0 \approx \frac{\tau n\chi - \xi + \sqrt{\tau^2 n^2 \chi^2 + \xi(\xi + 2\tau n\chi)}}{2\sigma}, \tag{4.11}$$

where

$$\chi \approx \frac{\tau(n-2) + \sqrt{\tau^2(n-2)^2 + 4\tau\tau_p(n-1)}}{2\tau n}. \tag{4.12}$$

Equation (4.11) confirms that social learning (ξ) reduces the initial spread of the infection. As expected, a highly transmissible infection (large τ) will increase R_0. We note that R_0 increases with χ. We discuss in Appendix C.2 that χ approximates the minimum of the correlation function C_{SI}^{min} between susceptible and infectious individuals. Therefore, factors that increase χ should also increase R_0. The quantity χ increases with the transmission rate to protective susceptible neighbours (τ_p), as well as the number of neighbours per individual (n), confirming the mitigating effects of spatially localized transmission.

We also show in Appendix C.2 that for case (b), where individuals adopt NPIs due to exposure learning only, if NPIs are highly effective ($\tau_p << \tau$), then for the same parameter regime (i.e. $N = 40000, s_p = 2/N, n = 4$, $\tau = 1\ day^{-1}$,

$\tau_p = 0.0025\ day^{-1}$, $\sigma = 0.25\ day^{-1}$ and $\rho = 0.25\ day^{-1}$) we have

$$R_0 \approx \frac{\tau n\chi + \sqrt{\left(\tau^2 n^2 \chi + 4\tau_p \rho n\right)\chi}}{2\sigma}, \tag{4.13}$$

where

$$\chi \approx \frac{\tau(n-2) - \rho + \sqrt{\tau^2(n-2)^2 - 2\tau\rho(n-2) + \rho^2 + 4\tau\tau_p(n-1)}}{2\tau n}.$$

Hence, more rapid adoption of NPIs due exposure learning (ρ) decreases χ, and therefore also decreases R_0. Spatial structure has a mitigating effect in this case as well.

In Appendix C.2 we show that when adopted NPIs are not strict (such that $\tau_p << \tau$ does not hold), then the corresponding expressions of R_0 for cases where individuals practice cautious behavior due to social learning only and exposure learning only are given by Equations (C.6) and (C.9), respectively.

4.3 Results

4.3.1 Dependence of R_0 on model parameters and network configuration

The spatial distribution of susceptible individuals (S) and individuals who practice NPIs (S_p) around the infection source at the initial stage of an epidemic have a strong influence on R_0, as computed from the full expression appearing in Appendix C.2, Equation (C.5) (Figure 4.1).

As expected, R_0 decreases with the proportion of protective individuals around the infection source cluster and in the entire population (Figures 4.1a ver-

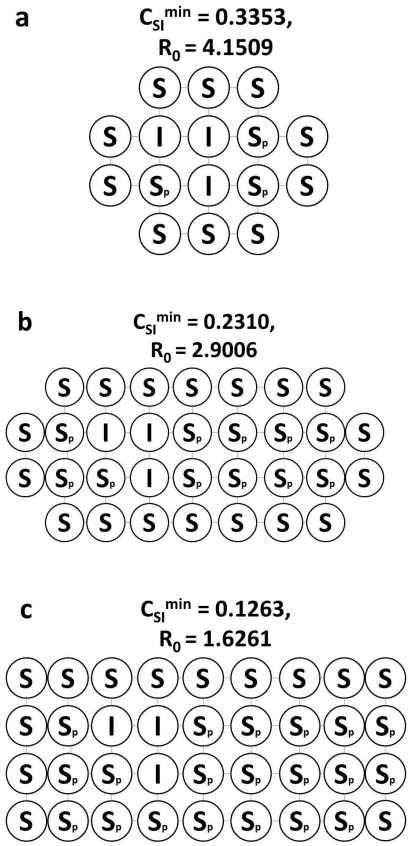

Figure 4.1: Typical network distributions of susceptible contacts, S, neighbors who practice social distancing techniques, S_p (as well as the respective calculations of the basic reproduction number) around the initial infection source, where all other members of the host population are fully susceptible (i.e. state S). The population size is $N = 40000$, each individual has $n = 4$ neighbors and model parameters are $\tau = 0.75\ day^{-1}$, $\tau_p = 0.1\ day^{-1}$, $\sigma = 0.25\ day^{-1}$, $\xi = \rho = 0.5\ day^{-1}$ and $\kappa = 0.01\ day^{-1}$.

sus 4.1c). This finding implies that upon inception of an outbreak it is crucial to identify the infection source promptly, and sensitize members of the host population about the disease and prevention measures, so that they can propagate awareness further through interactions with their spatial neighbours. We note that associating R_0 (and the overall disease dynamics) with specific network configurations in

which diseases and social interactions disseminate would not be possible under a homogeneous-mixing, mean-field equations approach.

Increasing the rate of adopting NPIs, either through exposure learning (ρ) or through social learning (ξ), decreases R_0. However, increasing the rate of adoption via infectious neighbours reduces R_0 more effectively than increasing the rate of adoption via protective susceptible neighbours (Figure 4.2a, b). This occurs because being next to infectious neighbors results in prompt adoption of preventative measures and avoidance of infection from that infectious neighbor, and hence it reduces R_0 better than a scenario where adoption of NPIs results from interaction with protective neighbors only, which may leave some infectious individuals in a part of the network with no protective individuals, while other parts of the network may have significant populations of protective individuals, but no infections. However, we note that this only applies when social learning can only begin at the start of an outbreak, and not beforehand as a pre-emptive measure.

4.3.2 Numerical analysis of pair approximation differential equations

Social and exposure learning during an outbreak

Numerical analysis of our model was carried out in *MATLAB* using the ode45 solver. The quality of numerical solutions remained the same when we experimented with other ordinary differential equations solvers (ode15s and ode23) in *MATLAB*. Similar to the results from the R_0 derivation, numerical simulation of Equation (4.1) shows that if both forms of learning can begin only during an out-

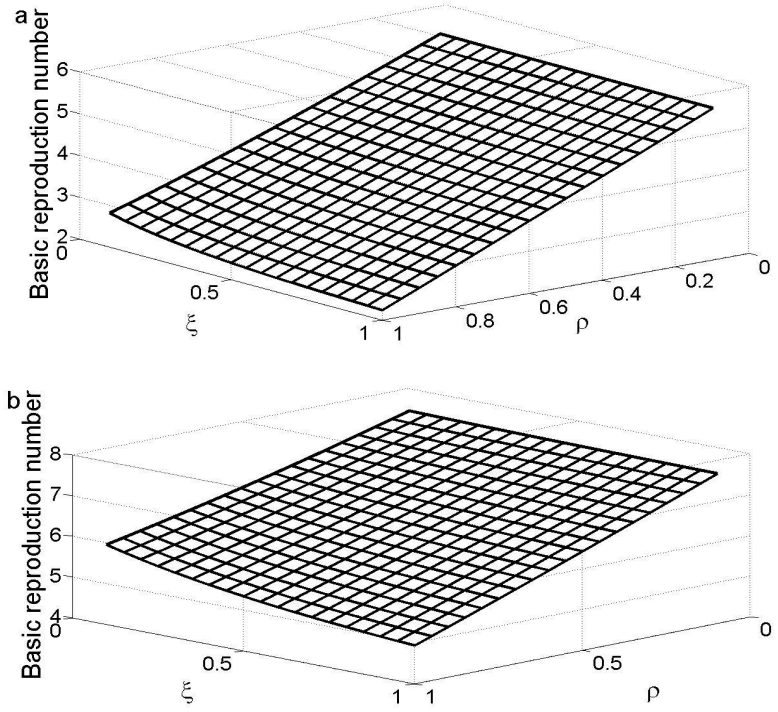

Figure 4.2: The basic reproduction number as a function of social learning from protective contacts at a rate ξ, and from infectious contacts at a rate ρ, where the transmission rate to protective individuals is $\tau_p = 0.1\ day^{-1}$ (a) and $\tau_p = 0.5\ day^{-1}$ (b). In all these plots $N = 40000, n = 4$, $\tau = 0.75\ day^{-1}$, $\sigma = 0.25\ day^{-1}$, $C_{S_pS_p} = 0, C_{S_pS} = 3/4$, $\kappa = 0\ day^{-1}$ and $s_p = 1/N$.

break, then NPIs adopted due to exposure learning (ρ) have a much larger impact on the size of the epidemic peak, than NPIs adopted due to social learning (ξ) (Figure 4.3i,l versus 4.3c,f). We also find that, adoption of NPIs stimulated by neighbouring infectious individuals leads to a higher number of protective individuals throughout and at the end of the epidemic, than practice of NPIs due to social learning (Figures 4.3h,k versus Figures 4.3b,e). This occurs because in this situation, learning from a neighbouring protective susceptible contact may not reach the parts of the network that need to be protected, resulting in those parts of the network being infected before

they can adopt NPIs.

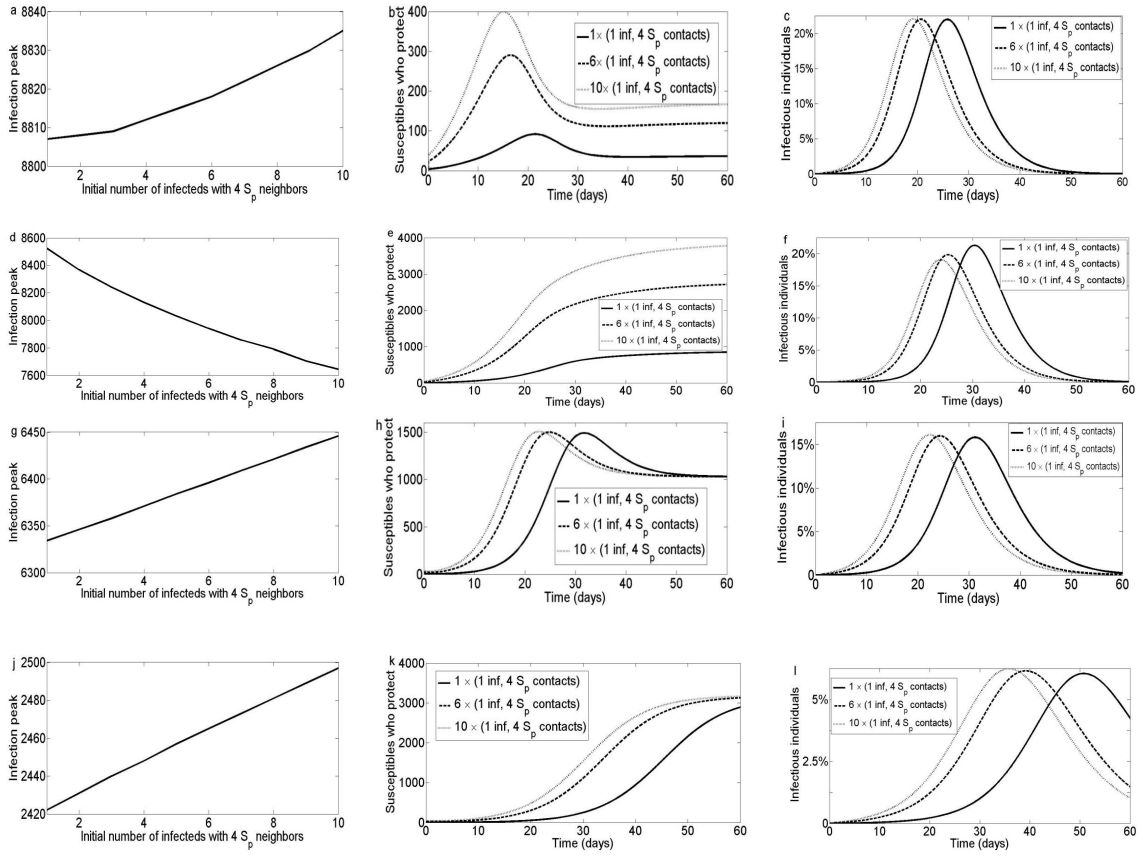

Figure 4.3: Infection peak versus initial distribution of *single infected individuals with 4 state S_p neighbors* (a, d, g, j), time series for susceptible individuals who protect (b, e, h, k) and time series for infectious individuals (c, f, i, l), varying the number of *1 infected node plus 4 S_p neighbors* at the beginning of the outbreak (the rest of the population is fully susceptible). In (a to f) $\xi = 0.25\ day^{-1}$, $\rho = 0\ day^{-1}$; in (g to l) $\xi = 0\ day^{-1}$, $\rho = 0.25\ day^{-1}$; in (a, b, c and g, h, i) $\tau_p = 0.6\ day^{-1}$; in (d, e, f and j, k, l) $\tau_p = 0.1\ day^{-1}$. Model parameters common to all graphs are $\tau = 0.8\ day^{-1}$, $\sigma = 0.25\ day^{-1}$ and $\kappa = 0\ day^{-1}$.

Increasing the initial number of infection source points with n protective neighbours (i.e. completely surrounded by individuals who practice NPIs) generally increases the infection peak (Figures 4.3a,g,j). This confirms intuition. However, con-

trary to phenomena normally observed in homogeneous-mixing models, increasing the number of infection source points who are surrounded by highly protective individuals can actually decrease the infection peak in other parameter regimes ($\tau_p = 0.1day^{-1}$, see Figures 4.3d and 4.3f). On the other hand, when NPIs are not strictly practiced (leading to a relatively high value of τ_p), increasing the number of infection source points will increase the infection peak, as usual, even when each of the initial infection sources are surrounded by a large proportion of protective contacts (see Supplementary Material, Figure C.1a).

Cumulative infections over a period of two months decrease with adoption of precautionary behavior due to social learning at a rate ξ, and exposure learning at a rate ρ, but, also as observed in Figures 4.2 and 4.3, the decrease in cumulative infections is more profound when individuals use exposure learning than social learning (Figure 4.4). Furthermore, adoption of NPIs only moderately decreases cumulative infections if upon learning about the disease and becoming protective, the new state S_p individuals practice less effective precautionary measures, resulting in an increased rate of transmission to state S_p individuals, τ_p (Figure 4.4a versus Figure 4.4b versus Figure 4.4c).

If individuals who practice NPIs lose this habit (captured by conversion from state S_p to state S at a 'forgetting' rate κ) then the population susceptibility increases, leading to a large number of infection cases and occurrence of large epidemic outbreaks, which are characterized by high infection peaks (Figure 4.5). However, the response of infection peaks to changes in the rates of forgetting is qualitatively different for the two types of learning, stemming from the fact that per capita success

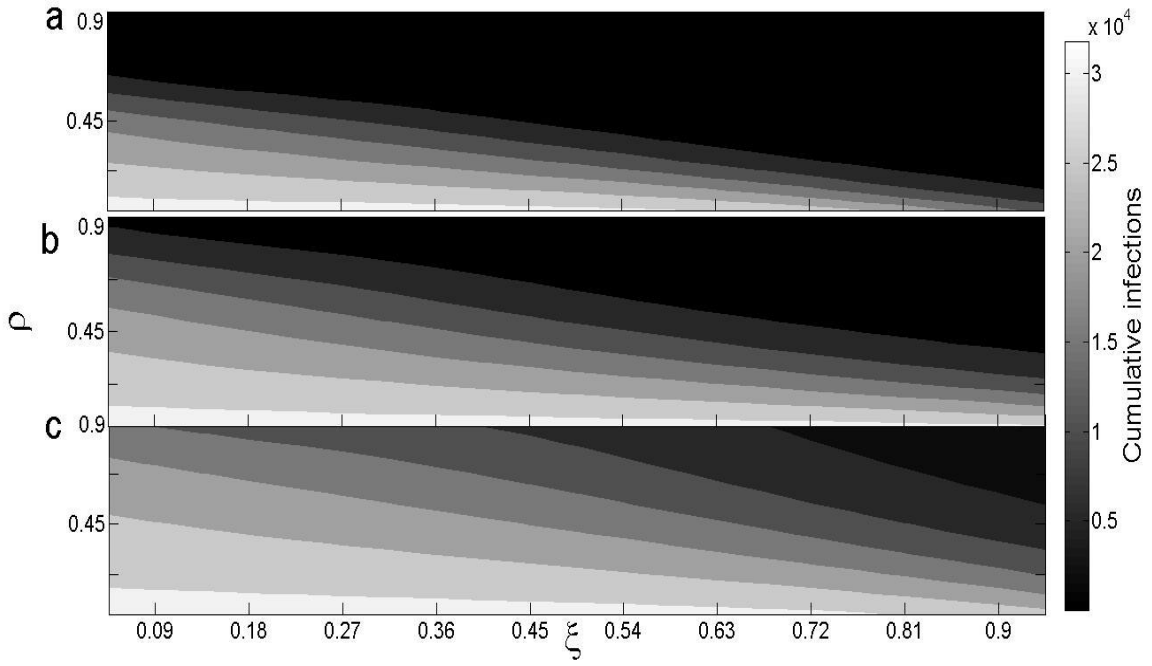

Figure 4.4: Cumulative infections as a function of social learning from both infectious and state S_p neighbors at rates ρ and ξ, respectively, where the initial conditions are *1 infected node and 1 state S_p neighbor* while the rest of the population is fully susceptible (i.e. state S), and $\tau_p = 0.1\ day^{-1}$ (a), $\tau_p = 0.2\ day^{-1}$ (b), $\tau_p = 0.3\ day^{-1}$ (c). Other model parameters are $\tau = 0.8\ day^{-1}$, $\sigma = 0.25\ day^{-1}$ and $\kappa = 0\ day^{-1}$.

of exposure learning–which operates only in immediate neighbours of an infected node–depends less on population prevalence than social learning. In particular, when the rate of forgetting is low, then the infection peak is roughly the same for both types of learning. However, when the rate of forgetting is high, then infection peaks are very high under social learning, but only moderately high under exposure learning. This occurs because effective social learning requires large parts of the network to be 'ready' for any infections which may enter the area by having high and stable populations of protective susceptible individuals, and large rates of forgetting prevent this from happening.

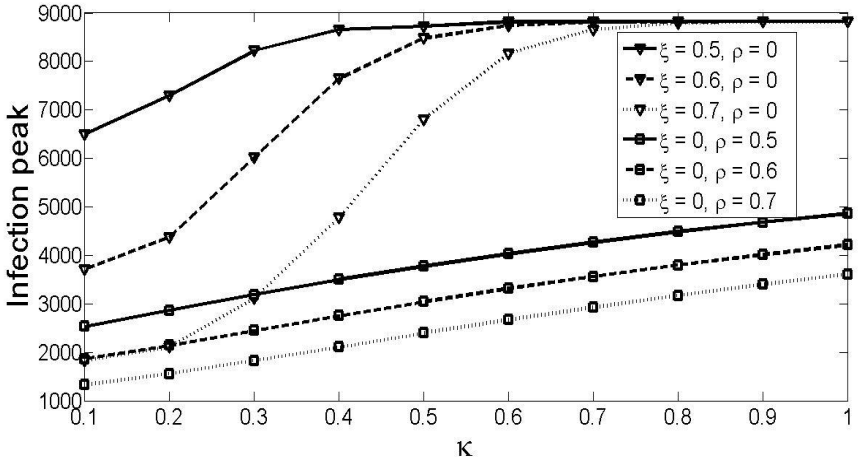

Figure 4.5: Infection peak versus the rate at which protective susceptible individuals forget, κ, varying regimes for social contagion parameters ξ and ρ. Initial conditions are *1 infected node and 2 state S_p neighbors* while the rest of the population is fully susceptible (i.e state S). Other model parameters are $\tau = 0.8\ day^{-1}$, $\tau_p = 0.3\ day^{-1}$ and $\sigma = 0.25\ day^{-1}$.

Social learning before and during an outbreak, and exposure learning during an outbreak

Many of the behaviours that fall under the rubric of NPIs, such as handwashing and respiratory etiquette, are learned preventively and are practiced in a population even before an epidemic. This builds up the proportion of protective individuals before introduction of the disease. Thus, the effectiveness of social learning may thus be considerably improved, although it is not clear how far in advance social learning must begin for it to be useful. In this subsection we consider scenarios where social learning can occur both prior to and after the introduction of an infection. In particular, we contrast a scenario where only social learning is practiced (but social learning begins to spread before the epidemic starts), to a scenario where only

exposure learning takes place, and we compare their performance.

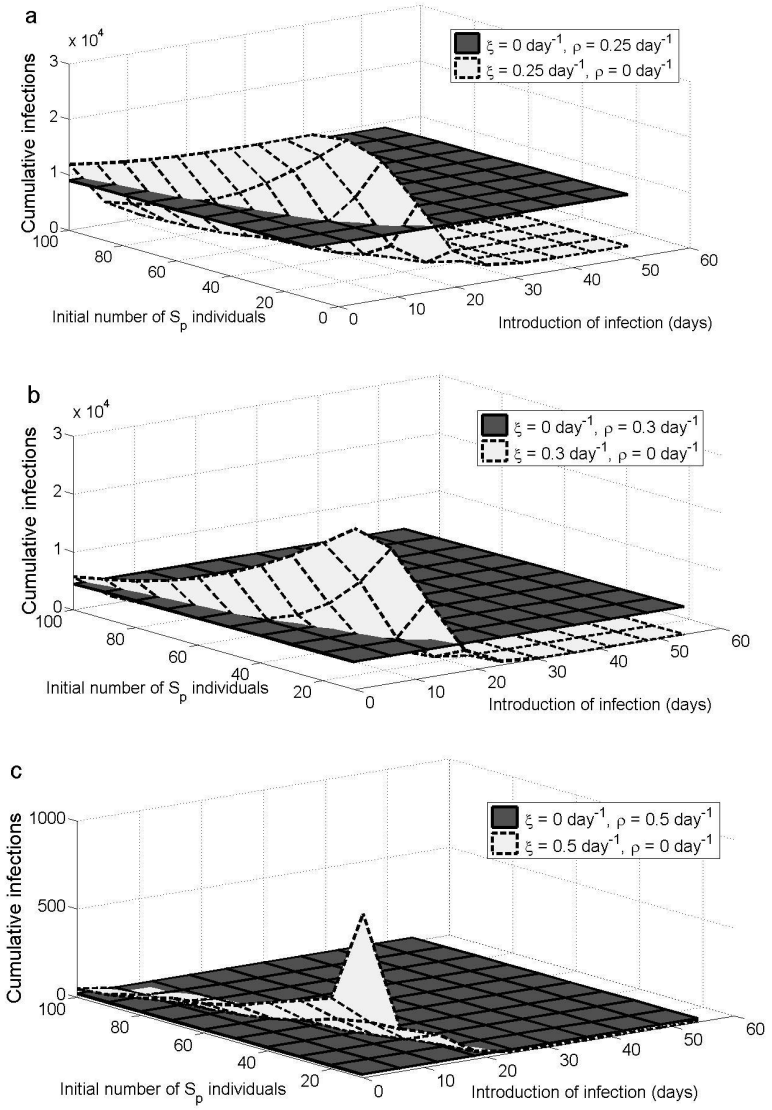

Figure 4.6: Cumulative infections as a function of the initial number of state S_p individuals and the time at which the infection is introduced, varying ξ and ρ, for the scenario of exposure learning only (dark grey surface) and social learning only (light grey surface). Other model parameters are $\tau = 0.8\ day^{-1}$, $\tau_p = 0.001\ day^{-1}$, $\sigma = 0.25\ day^{-1}$ and $\kappa = 0\ day^{-1}$.

In the absence of exposure learning ($\rho = 0$), model simulations confirm

how social learning before an epidemic creates large pools of protective individuals before the epidemic begins, leading to a decreased epidemic final size (Figure 4.6). At baseline parameter values, introducing social learning as early as possible is a highly effective way of decreasing the epidemic final size; increasing the initial number of protective individuals, S_p, also works but is less effective than stimulating social learning as early as possible (Figure 4.6a-c). Either of these measures is made more effective when social learning is more rapid (large ξ, Figure 4.6c versus b and a).

In contrast to observations made in most of the simulations in the previous subsections, social learning reduces the epidemic final size more effectively than exposure learning, except when social learning is not introduced soon enough before the epidemic, or when there are not enough initial protective individuals (Figure 4.6a-c). In either of these two exceptional cases, there is an insufficient pool of protective susceptible individuals in the population at the beginning of the epidemic, for social learning to be effective.

4.4 Discussion

NPIs partly determine the feasibility of infection control for many infectious diseases, especially ones where pharmaceutical interventions are not yet available. Here, we constructed a pair approximation model of a self-limiting infectious disease where individuals can choose to adopt NPIs either in response to learning it from other susceptible individuals, or having been stimulated to learn it from neighbouring an infectious person. The pair approximation model implicitly captures the underlying

spatial structure of the population.

We found that the impact of NPIs depends on the structure of the initial network configuration, particularly, the number and the neighborhood distribution of infectious, susceptible and individuals who practice NPIs, at the beginning of an outbreak. Both social learning and exposure learning lead to a decrease in the final size. At baseline parameter values, exposure learning is much more effective than social learning if social learning can only begin during the outbreak. However, social learning can outperform exposure learning if social learning begins early enough before the epidemic (although the initial number of protective individuals is not as important). While peak disease prevalence increases with the rate at which protective susceptible individuals stop the habit of practicing NPIs, the response of the infection peak to the rate of forgetting is qualitatively different for the two types of learning. We also found that, under certain parameter regimes, if infection source points are initially surrounded by protective individuals, increasing the number of infection source points at the beginning of an outbreak actually decreases the infection peak. This phenomena would not be revealed by the non-spatial, mean-field equations models.

Our model makes several simplifying assumptions. The model is based on the assumption that disease propagation and spatially localized learning take place only between connected neighbors on a regular network. In real life, networks within which infections spread are more complex, and mean-field effects (such as mass media) may be important. Future work could extend the pair approximation model to account for these effects. Also, in general, social networks are structurally different from networks in which infections spread. Thus, future work could also develop

pair approximations for dual-level networks consisting of both a social network and a disease spread network.

In conclusion, mathematical models that incorporate both spatial transmission of diseases and impacts of human NPI behaviour should be further developed, since they can help to develop more effective disease control strategies.

Chapter 5

Conclusions

5.1 Summary of the thesis

The capability of pair approximation models to describe spatial propagation of infectious diseases through contact networks by the use of ordinary differential equations ensures their relative tractability, and hence are more advantageous than the analytically tractable, but homogeneous-mixing, mean-field equations and the spatially explicit, but intractable, individual-based models. Pair approximation models have been used to describe and analyze fairly accurately, the spread and control of epidemic outbreaks of diseases such as measles, HIV/AIDS and foot and mouth disease. This thesis adds into the literature of pair approximation models, the study and analysis of spread and control (by vaccination and culling) of foot and mouth disease in endemic or near-endemic and often low-income resource-constrained countries, and the impact of adoption of non-pharmaceutical interventions on the control of a general infectious disease.

Foot and mouth disease is one of the most economically important livestock infectious diseases. International animal disease control bodies enforce adoption of strict control measures to contain foot and mouth disease in affected countries as

well as to prevent introduction of the disease into disease-free countries. While most developed countries have since eradicated foot and mouth disease, some low-income, developing countries still experience frequent epidemic outbreaks and struggle to control it due to lack of resources. Global eradication of foot and mouth disease will remain a far-fetched objective until measures are put in place to avoid or reduce the frequency of epidemic outbreaks in low-income countries. The pair approximation models of foot and mouth disease developed and discussed in this thesis incorporate aspects of the disease that are relevant to endemic settings. These factors include frequent re-importation of the disease from neighboring countries or infected wild animals neighboring livestock farms, loss of natural and vaccine-induced immunity and constrained culling and vaccination resources. Recently these factors have accounted for almost annual outbreaks of foot and mouth disease, mostly in cattle, in several parts of Botswana, and this has had a significant negative impact on the country's beef industry. The models of foot and mouth disease in this thesis were used to explore plausible ways of controlling the disease by several strategies of culling and vaccination in view of the situation of the disease in endemic or near-endemic settings.

In this thesis we also developed a pair approximation model for the spread of a single-outbreak human infectious disease, where propagation of adoption of non-pharmaceutical interventions (NPIs) into the population occurs through social learning (adoption of NPIs through social interaction with protective contacts) and exposure learning (adoption of NPIs due to being in the neighborhood of infected individuals).

5.2 Conclusions and discussion

We discuss the main findings and conclusions of the foot and mouth disease models developed in this thesis, and the outcomes of the model that explored impacts of adoption of NPIs on the course of an infection.

When disease transmission and deployment of vaccination to control FMD, are spatially localized processes then the optimal control strategy in endemic or near-endemic countries requires strategic administration of high-quality vaccines that are efficient and provide longer periods of protection, construction and maintenance of cordon fences around farms to prevent interaction between livestock and affected wild animals or avoid movement of animals across borders, and public education about the consequences of engaging in uncontrolled trade in livestock through non-gazetted means. Deployment of prophylactic vaccination is crucial in near-endemic countries because it protects animals from infection brought about by frequent disease re-importations. When vaccine supply is sufficiently limited, the most effective control means that minimizes effects of vaccine waning, natural immunity waning and disease re-importations, is rapid administration of ring vaccination during outbreaks coupled with careful rationing of prophylactic vaccination over the year.

Rapid culling in farms neighboring FMD-infected premises removes the *fuel* for potential new infections, therefore, it yields overall lower epidemic size than culling in infected farms only. To minimize impacts of re-importation of the FMD virus by culling, it is important to promptly identify the infection hot-spots and their neighborhoods and rapidly cull infected premises and their close contacts.

Adoption and maintenance of strict NPIs can lead to avoidance or prevention of large epidemic outbreaks. In fact, if the neighborhood of a source infection constitutes individuals who practice strict NPIs at all times, then the infection is mostly likely to die out before spreading into the rest of the population. In cases where individuals become aware and begin to learn and practice NPIs during an outbreak, exposure learning leading to avoidance of infection from infected spatial neighbors reduces the epidemic impact better than social learning from non-infectious contacts. However, adoption of NPIs through social learning becomes more efficient than exposure learning when more individuals adopt and practice NPIs both prior to and during infection outbreaks.

5.3 Future work

The overall goal of this thesis and the mathematical studies we wish to pursue in the near future, is to offer plausible disease control strategies, which could potentially eradicate human and animal infectious diseases, particularly in resource-constrained, low to middle-income countries. We want to make improvements on the models discussed in this thesis and design and analyze more accurate, disease-specific spatial models and apply them to situations of infectious diseases in the developing world.

The ability to gather accurate data explicitly describing the actual dynamics of foot and mouth disease in Botswana and most other resource-constrained FMD-endemic or near-endemic countries, is restricted. This has led to lack of valid data

and difficulty to devise means of bringing the disease under control. As part of future work, we will create a more accurate database of the FMD scenario in Botswana, including the spatial distribution of farms, and use the data to parameterize more accurate pair approximation models and explore more effective control strategies.

The decline of the prevalence of HIV in Uganda in the late 1990s resulted from wide-spread adoption of non-pharmaceutical interventions such as the use of condoms and social distancing measures such as reduction of multiple sexual partnerships. However, over the years, negligence and inadequate sexual behavior change have been linked to the escalation of HIV cases in Botswana, difficulty in controlling the disease and an overall negative impact on the country's economy. We wish to collect data and develop and analyze a pair approximation model for the spread of HIV in Botswana, coupled with a model of spread of awareness across the population, and explore NPIs and overall behavior change that could be enhanced to best reduce the prevalence rate of the disease.

Traditional pair approximation models, including those developed in this thesis, consider the spread of infectious diseases on fixed-edge networks where the spatial position and the number of neighbors per individual (or groups of individuals) are assumed to remain the same throughout the outbreak. While these assumptions are sufficient for short-lived or rarely occurring infection outbreaks, change of spatial location and dynamic neighborhood sizes play important roles in long-term infectious diseases such as HIV and FMD in endemic settings. Therefore, in addition to the future endeavors mentioned above, we want to explore pair approximation models (or other types of spatially oriented models) that describe the dynamic nature of

networks in which infectious diseases and awareness spread, and apply them to the situation of FMD and HIV in Botswana and elsewhere.

Bibliography

[1] L. Alberton. Graphs in the database: Sql meets social networks. *http : //www.alberton.info/graphs_in_the_database_sql_meets_social_networks.html*, Accessed: 27-11-2014.

[2] K.A. Alexander and J.W. McNutt. Human behavior influences infectious disease emergence at the humananimal interface. *Frontiers in Ecology and the Environment*, 8(10):522–526, 2010.

[3] A. Alonso, M.A. Martins, M.D. Gommes, R. Allende, and M.S. Sondahl. Foot and mouth disease viral typing by complement fixation and enzyme-linked immunosorbent assay monovalent and polyvalent antisera. *J Ver Diagn Invest*, 4:249–253, 1992.

[4] L. A. N. Amaral, A. Scala, M. Barthemelemy, and H. E. Stanley. Classes of small-world networks. *PNAS*, 97(21):11149–11152, 2000.

[5] E.C. Anderson, J. Anderson, and J. Doughty. The foot and mouth disease subtype variants in kenya. *J Hyg (London)*, 72(2):237–244, 1974.

[6] J.P. Aparicio and M. Pascual. Building epidemiological models from r0: an implicit treatment of transmission in networks. *Proc. R. Soc. B 22*, 274(1609):505–512, 2007.

[7] J. Arino, K.L. Cooke, and P. van den Driessche. An epidemiological model that includes a leaky vaccine with a general waning function. *Discrete and Continuous Dynamical Systems series B*, 4(2):479–495, 2004.

[8] M.C. Auld. Estimating behavioral response to the aids epidemic. *Contributions to Economic Analysis and Policy*, 5(12), 2006.

[9] N. Bacaer. Approximation of the basic reproduction number for vector-borne disease with periodic vector population. *Bulleting of Mathematical Biology*, 69:1067–1091, 2007.

[10] E.K. Baipoledi, G.Matlho, M. Letshwenyo, M. Chimbombi, E.K. Adom, M.V. Raborokgwe, and J.M.K. Hyera. Re-emergence of foot and mouth disease in botswana. *The Veterinary Journal*, 168:93–99, 2004.

[11] S. Bansal, B.T. Grenfell, and L. A. Meyers. When individual behaviour matters: homogeneous and network models in epidemiology. *J. R. Soc. Interface 22*, 4(16):879–891, 2007.

[12] S. Bansal, J. Read, B. Pourbohloul, and L. A. Meyers. The dynamic nature of contact networks in infectious disease epidemiology. *Journal of Biological Dynamics*, 4(5):478–489, 2010.

[13] A. Barrat and M. Weigt. On the properties of small-world network models. *Eur. Phys. J. B*, 13:547–560, 2000.

[14] S.J. Barteling. Development and performance of inactivated vaccines against foot and mouth disease. *Rev. sci. tech. Off*, 21(3):577–588, 2002.

[15] C.T. Bauch. The spread of infectious diseases in spatially structured populations: an invasory pair approximation. *Mathematical Biosciences*, 198:217–237, 2005.

[16] C.T. Bauch, A. d'Onofrio, and P. Manfredi. Behavioral epidemiology of infectious diseases: an overview: Modeling the interplay between human behavior and the spread of infectious diseases. *Springer-Verlag*, pages 1–19, 2013.

[17] C.T. Bauch and A.P. Galvani. Using network models to approximate spatial point-process models. *Mathematical Biosciences*, 184:101–114, 2003.

[18] C.T. Bauch and D.A. Rand. A moment closure model for sexually transmitted disease transmission through a concurrent partnership network. *The Royal Society*, 267:2019–2027, 2000.

[19] G.J. Belsham, S.M. Jamal, K. Tjϕrnehϕj, and A. Bϕtner. Rescue of foot-and-mouth disease viruses that are pathogenic for cattle from preserved viral rna samples. *PLoS ONE*, 6(1):1–10, 2011.

[20] J. Benoit, A. Nunes, and M. Telo da Gama. Pair approximation models for disease spread. *arXiv:q-bio/0510005*.

[21] F. Brauer. Some simple epidemic models. *Mathematical Biosciences and Engineering*, 3(1):1–15, 2006.

[22] F. Brauer. Mathematical epidemiology is not an oxymoron. *BMC Public Health*, 9(S2):1–11, 2009.

[23] G. Bruckner and V. E. Saraiva-Vieira. Oie strategy for the control and eradication of foot and mouth disease at regional and global level. *Conf. OIE*, pages 187–198, 2010.

[24] K. Bunwong. A new approach to pair approximation method for spatial model in ecology. *WSEAS Transactions on Mathematics*, 9(10):768–777, 2010.

[25] G. Chenard, P. Selman, and A. Dekker. Cedivac-fmd can be used according to a marker vaccine principle. *Veterinary Microbiology*, 128(1-2):65–71, 2008.

[26] E.M. Cottam, J. Wadsworth, A.E. Shaw, R.J. Rowlands, L. Goatley, S. Maan, N.S. Maan, P.P.C. Mertens, K. Ebert, Y. Li, E.D. Ryan, N. Juleff, N.P. Ferris, J.W. Wilesmith, D.T. Haydon, D.P. King, D.J. Paton, and N.J. Knowles. Transmission pathways of foot-and-mouth disease virus in the united kingdom in 2007. *PLoS Pathogens*, 4(4):1–8, 2008.

[27] M. Cruz-Aponte, E.C. McKiernan, and M.A. Herrera-Valdez. Mitigating effects of vaccination on influenza outbreaks given constraints in stockpile size and daily administration capacity. *BMC Infect Dis*, 11(207), 2011.

[28] L. Danon, A.P. Ford, T. House, C.P. Jewell, M.J. Keeling, G.O. Roberts, J.V. Ross, and M.C. Vernon. Networks and the epidemiology of infectious disease. *Interdisciplinary Perspectives on Infectious Diseases*, 2011:1–28, 2011.

[29] G. Davies. Foot and mouth disease. *Research in Veterinary Science*, 73:195–199, 2002.

[30] P. M. Depa, U. Dimri, M.C. Sharma, and R. Tiwari. Update on epidemiology and control of foot and mouth disease - a menace to international trade and global animal enterprise. *Vet. World*, 5(11):694–704, 2012.

[31] K. Dietz. The estimation of the basic reproduction number for infectious diseases. *Statistical methods in medical research*, 2(1):23–41, 1993.

[32] Y. Ding, H. Chen, J. Zhang, J. Zhou, L. Ma, L. Zhang, Y. Gu, and Y. Liu. An overview of control strategy and diagnostic technology for foot-and-mouth disease in china. *Virology Journal*, 10(78):1–6, 2013.

[33] E. Dion, L. Van Schalkwyk, and E.F. Lambin. The landscape epidemiology of foot-and-mouth disease in south africa : a spatially explicit multi-agent simulation. *Ecological Modelling*, 222(13):2059–2072, 2011.

[34] T.R. Doel. Natural and vaccine-induced immunity to foot and mouth disease: the prospects for improved vaccines. *Rev. sci. tech. Off. int. Epiz*, 15(3):883–911, 1996.

[35] J. Domenech, J. Lubroth, and K. Sumption. Immune protection of animals: the examples of rinderpest and foot and mouth disease. *Journal of Comparative Pathology*, 142:120–124, 2010.

[36] G. Consolo E. Barbera and G. Valenti. Spread of infectious diseases in a hyperbolic reaction-diffusion susceptible-infected-removed model. *American Physical Society*, 88(5):052719–1–052719–3, 2013.

[37] K.T.D. Eames and J.M. Read. Networks in epidemiology. *BIOWIRE 2007*, LNCS 5151:79–90, 2008.

[38] S.P. Ellner. Pair approximation for lattice models with multiple interaction scales. *Journal of Theoretical Biology*, 210:435–447, 2001.

[39] M. Enserink. Barricading u.s. boarders against a devastating disease. *Science*, 291:2298, 2001.

[40] B. Evans. The social and political impact of animal diseases. *Veterinaria Italiana*, 42(4):399–406, 2006.

[41] E.P. Fenichel, C. Castillo-Chavez, M.G. Geddia, G. Chowell, P.A. Gonzalez Parra, G.J. Hickling, G. Holloway, R. Horan, B. Morin, C. Perrings, M. Springborn, L. Velazquez, and C. Villalobos. Adaptive human behavior in epidemiological models. *PNAS*, 108(15):6306–6311, 2011.

[42] N.M. Ferguson, C.A. Donnelly, and R.M. Anderson. The foot and mouth epidemic in great britain: pattern of spread and impact of interventions. *Science*, 292:1155–1160, 2001.

[43] N.M. Ferguson, C.A. Donnelly, and R.M. Anderson. Transmission intensity and impact of control policies on the foot and mouth epidemic in great britain. *Nature*, 413(6855):542–548, 2001.

[44] M.J. Ferrari, S. Bansal, L.A. Meyers, and O.N. Bjϕrnstad. Network frailty and the geometry of head immunity. *Proc. R. Soc. B*, 273:2743–2748, 2006.

[45] S. Funk, E. Gilad, C. Watkins, and V.A.A. Jansen. The spread of awareness and its impact on epidemic outbreaks. *PNAS*, 106(16):6872–6877, 2009.

[46] G.P. Garnett. An introduction to mathematical models in sexually transmitted disease epidemiology. *Sex Transm Inf*, 78:7–12, 2002.

[47] A. Gelmana, I. Leenen, I.V. Mechelenb, P.D. Boeckb, and J. Poblomec. Bridges between deterministic and probabilistic models for binary data. *Statistical Methodology*, 7:187–209, 2010.

[48] R.J. Glass, L. M. Glass, W.E. Beyeler, and H.J. Min. Targeted social distancing designs for pandemic influenza. *Emerging Infectious Diseases*, 12(11):1671–1681, 2016.

[49] R.T. Greenlee. Measuring disease frequency in the marshfield epidemiologic study area (mesa). *Clin Med Res*, 1(4):273–280, 2003.

[50] R. Grima. A study of the accuracy of moment-closure approximations for stochastic chemical kinetics. *The journal of chemical physics*, 136:doi: 10.1063/1.3702848, 2012.

[51] M.J. Grubman and B. Baxt. Foot-and-mouth disease. *Clinical Microbiology Reviews*, 17(2):465–493, 2004.

[52] E. Hansen and T. Day. Optimal control of epidemics with limited resources. *J. Math. Biol.*, 62:432–451, 2011.

[53] T. Harko, F.S.N. Lobo, and M.K. Mak. Exact analytical solutions of the susceptible-infected-recovered (sir) epidemic model and of the sir model with equal death and birth rates. *Quantitative Biology*, 236:184–194, 2014.

[54] J.M. Heffernan, R.J. Smith, and L.M. Wahl. Perspectives an the basic reproduction ratio. *Journal of the Royal Society*, 2(4):281–293, 2005.

[55] H.W. Hethcote. Three basic epidemiological models. *Bioinformatics*, 18:120–144, 1989.

[56] H.W. Hethcote. The mathematics of infectious diseases. *Society for Industrial and Applied Mathematics*, 42(4):599–653, 2000.

[57] D. Hiebeler. Moment equations and dynamics of a household sis epidemiological model. *Bulletin of Mathematical Biology*, 68:1315–1333, 2006.

[58] W. Huang, M. Han, and K. Liu. Dynamics of an sis reaction-diffusion epidemic model for disease transmission. *Mathematical Biosciences and Engineering*, 7(1):51–66, 2010.

[59] A.D. James and J. Rushton. The economics of foot and mouth disease. *Rev Sci Tech*, 21(3):637–644, 2002.

[60] J. Jiang. Dynamics of a reaction-diffusion system of autocatalytic reaction. *Discrete and Continuous Dynamical Systems*, 21(1):245–258, 2008.

[61] A. Kandler and J. Steele. Innovation diffusion in time and space: effects of social information and of income nequality. *Journal for the Basic Principles of Diffusion Theory, Experiment and Application*, 11(4):1–17, 2009.

[62] M.J. Keeling. The effects of local spatial structure on epidemiological invasions. *Proceedings of The Royal Society of London*, B 22(266):859–867, 1999.

[63] M.J. Keeling and K.T.D. Eames. Networks and epidemic models. *J. R. Soc. Interface 22*, 2(4):295–307, 2005.

[64] M.J. Keeling, D.A. Rand, and A.J. Morris. Correlation models for childhood epidemics. *Proceedings of The Royal Society of London B 264*, pages 1149–1156, 1997.

[65] M.J. Keeling, M.E.J. Woolhouse, R.M. May, G. Davies, and B.T. Grenfel. Modeling vaccination strategies against foot and mouth disease. *Nature*, 421:136–142, 2003.

[66] M.J. Keeling, M.J. Woolhouse, D.J. Shaw, L. Matthews, M. Chase-Topping, D.T Haydon, S.J. Cornell, J. Kappey, J. Wilesmith, and B.T. Granfell. Dynamics of the 2001 uk foot and mouth disease: stochastic dispersal in a heterogeneous landscape. *Science*, 294(5543):813–817, 2001.

[67] P. Kitching, J. Hammond, M. Jeggo, B. Charleston, D. Paton, L. Rodriguez, and R. Heckert. Global fmd control - is it an option? *Vaccine*, 25(30):5660–5664, 2007.

[68] R.P. Kitching. recent history of foot and mouth disease. *J. comp. Pathol.*, 118:89–108, 1998.

[69] M. Kobayashi, T.E. Carpenter, B. F. Dickey, and R.E. Howitt. A dynamic, optimal disease control model for foot-and-mouth-disease: Ii. model results and policy implications. *Preventative Veterinary Medicine*, 79:274–286, 2007.

[70] J.S. Koopman. Infection transmission science and models. *Jpn. J. Infect. Dis.*, 58:S3–S8, 2005.

[71] L.H. Kuller. Epidemiology is the study of epidemics and their prevention. *American Journal of Epidemiology*, 134(10):1051–1056, 1991.

[72] M. Kuperman and G. Abramson. Small world effect in an epidemiological model. *Phys. Rev. Lett.*, 86:2909–2912, 2001.

[73] C.G Langton. Self-reproduction in cellular automata. *Physica*, 10D:135–144, 1984.

[74] C.H. Lee. A moment closure method for stochastic chemical reaction networks with general kinetics. *Communications in Mathematical and in Computer Chemistry*, 70:785–800, 2013.

[75] M. Letshwenyo, M. Fanikiso, and M. Chimbombi. The control of foot and mouth disease in botswana: special reference to vaccination. *Dev Biol (Basel)*, 119:403–413, 2004.

[76] J. Li, D. Blakeley, and R.J. Smith? The failure of r_0. *Computational and Mathematical Methods in Medicine*, 12:1–17, 2011.

[77] J. Li and X. Zou. Generalization of the kermack-mckendrick sir model to a patchy environment for a disease with latency. *Math. Model. Nat. Phenom.*, 4(2):92–118, 2009.

[78] C.N.L. Macpherson. Human behavior and the epidemiology of parasitic zoonoses. *International journal for parasitology*, 35(11-12):1319–1331, 2005.

[79] S. Maharaj and A. Kleczkowski. Controlling epidemic spread by social distancing: Do it well or not at all. *BMC Public Health*, 12(679):1–16, 2012.

[80] L. Mao and Y. Yang. Coupling infectious diseases, human preventive behavior, and networks–a conceptual framework for epidemic modeling. *Soc Sci Med*, 74(2):167–175, 2012.

[81] F. Mardones, A. Perez, J. Sanchez, M. Alkhamis, and T. Carpenter. Parameterization of the duration of infection stages of serotype o foot-and-mouth disease virus: an analytical review and meta-analysis with application to simulation models. *Vet Res*, 41(4):45, 2010.

[82] E. Massad, M.N. Burattini, F.A.B. Coutinho, and L.F. Lopez. The 1918 influenza a epidemic in the city of sao paulo, brazil. *Medical Hypotheses*, 68:442–445, 2007.

[83] L. Matthew and D.G. Menon. Economic impact of fmd in chazhoor panchayath. *Veterinary World*, 1(1):5–6, 2008.

[84] J.P. McGowan, S.S. Shah, C.E. Ganea, S. Blum, J.A. Ernst, K.L. Irwin, N. Olivo, and P.J. Weidle. Risk behavior for transmission of human immunodeficiency virus (hiv) among hiv- seropositive individuals in an urban setting. *CID*, 38:122–127, 2004.

[85] P. Merriman, M. Jones, G. Olsson, E. Sheppard, N. Thrift, and Y. Tuan. Space and spatiality in theory. *Dialogues in Human Geography*, 2(1):3–22, 2012.

[86] T. Modie-Moroka. Intimate partner violence and sexually risky behavior in botswana: implications for hiv prevention. *Health Care for Women International*, 30:230–231, 2009.

[87] M. Mokopasetso and N. Derah. Recent outbreaks of foot and mouth disease in botswana and zimbabwe. *Special Issues*, 23:8–12, 2005.

[88] D. Mollison and K. Kuulasmaa. Spatial epidemic models: theory and simulations. *Population dynamics of rabies in wildlife*, 1985.

[89] A. Morozov, S. Ruan, and B. Li. Patterns of patchy spread in multi-species reactiondiffusion models. *Ecological complexity*, 5:313–328, 2008.

[90] S.S. Morse. Factors in the emergence of infectious diseases. *Emerging Infectious Diseases*, 1(1):7–15, 1995.

[91] P. Moser. In nigeria, social mobilizers fight ebola - and misinformation. *http* : $//www.unicef.org/infobycountry/nigeria\_75929.html$, Accessed: 27-11-2014.

[92] S. Mushayabasa, C.P. Bhunu, and M. Dhlamini. Impact of vaccination and culling on controlling foot and mouth disease: a mathematical modeling approach. *World of Journal Vaccines*, 1:156–161, 2011.

[93] R.M. Neilan and S. Lenhart. An introduction to optimal control with an application in disease modeling. *American Mathematical Society*, 75:67–81, 2010.

[94] P.E. Parham and N.M. Ferguson. Space and contact networks: capturing of the locality of disease transmission. *Journal of Royal Society*, 3:483–493, 2005.

[95] P.E. Parham, B.K. Singh, and N.M. Ferguson. Analytical approximation of spatial epidemic models of foot and mouth disease. *Theoretical Population Biology*, 72:349–368, 2008.

[96] T.S. Patterson. Constraints: an integrated viewpoint. *Illuminare*, 7(1):30–38, 2001.

[97] G.A Pavlopoulos, M. Secrier, C.N. Moschopoulos, T.G. Soldatos, S. Kossida, J. Aerts, R. Schneider, and P.G. Bagos. Using graph theory to analyze biological networks. *BioData Mining*, 4(10), 2011.

[98] H.J. Pharo. Foot and mouth disease: an assessment of the risks facing new zealand. *New Zealand Veterinary Journal*, 50(2):46–55, 2002.

[99] F.M. Pillemer, R.J. Blendon, A.M. Zaslavsky, and B.Y. Lee4. Predicting support for non-pharmaceutical interventions during infectious outbreaks: a four region analysis. *DOI: 10.1111/disa.12089*, 2014.

[100] B. Planque, C. Loots, P. Petitgas, U. Lindstrom, and S. Vaz. Understanding what controls the spatial distribution of fish populations using a multi-model approach. *Fisheries Oceanography*, 20(1):1–17, 2011.

[101] T. Porphyre, H.K. Auty, M.J. Tildesley, G.J. Gunn, and M.E.J. Woolhouse. Vaccination against foot-and-mouth disease: do initial conditions affect its benefit? *PLoS ONE*, 8(10):e77616, 2013.

[102] A. Quarteroni. Mathematical models in science and engineering. *Notices of the AMS*, 56(1):10–19, 2009.

[103] A.N. Rae, C. Nixon, and P. Gardiner. Foot-and-mouth disease and trade restrictions: Latin america access to pacific rim beef. *The Australian Journal of Agriculture and Resource Economics*, 43(4):479–500, 1999.

[104] D.A. Rand. Correlation equations and pair approximations for spatial ecologies. *CWI Quarterly*, 12(3 and 4):329–368, 1999.

[105] C.T. Reluga. Game theory of social distancing in response to an epidemic. *Plos Computational Biology*, 6(5):e1000793, 2010.

[106] V. Rico-Ramirez, F. Napoles-Rivera, G. Gonzalez-Alatorre, and U.M. Diwekar. Stochastic optimal control for the treatment of a pathogenic disease. *Computer Aided Chemical Engineering*, 28:217–222, 2010.

[107] N. Ringa and C.T. Bauch. Dynamics and control of foot and mouth disease in endemic countries: a pair approximation model. *Journal of Theoretical Biology*, 357:150–159, 2014.

[108] A. Rizzo, M. Frasca, and M. Porfiri. Effect of individual behavior on epidemic spreading in activity-driven networks. *Physical Review E*, 90(042801), 2014.

[109] B. Roche, J.M. Drake, and P. Rohani. An agent-based model to study the epidemiological and evolutionary dynamics of influenza viruses. *BMC Bioinformatics*, 12(87):doi:10.1186/1471–2105–12–87, 2011.

[110] G. Rose and D.J.P. Barker. What is epidemiology? *British Medical Journal*, 2:803–804, 1978.

[111] P.K. Roy, J. Mondal, R. Bhattacharyya, S. Bhattacharya, and T. Szabados. Extinction of disease pathogenesis in infected population and its subsequent recovery: a stochastic approach. *Journal of Applied Mathematics*, http://dx.doi.org/10.1155/2013/381286, 2013.

[112] S. Roy, T.F. McElwain, and Y. Wan. A network control theory approach to modeling and optimal control of zoonoses: case study of brucellosis transmission in sub-saharan africa. *PLoS Negl Trop Dis*, 5(10):e1259, 2011.

[113] N.M. Rweyamamu. Foot and mouth disease control strategies in africa. *Preventative Veterinary Medicine*, 2:329–340, 1984.

[114] M. Rweyemamu. Global perspective for foot and mouth disease control. *Rev. Sci. Tech. Off. Int. Epizoot*, 21:765–773, 2002.

[115] A.H. Salas, L.J.H. Martinez, and O.S. Fernandez. Reaction-diffusion equations: a chemical application. *Scientia et Technica Ano*, XVII(46):134–137, 2010.

[116] M. Salathe and S. Bonhoeffer. The effect of opinion clustering on disease outbreaks. *J. R. Soc. Interface*, 5:1505–1508, 2008.

[117] P.H.T. Schimit and L.H.A. Monteiro. On estimating the basic reproduction number in distinct stages of a contagious disease spreading. *Ecological Modelling*, 240(2012):156–160, 2012.

[118] L.B. Shaw and I.B. Schwartz. Fluctuating epidemics on adaptive networks. *Physical Review E*, 77(066101), 2008.

[119] P. Smadbeck and Y.N. Kaznessis. A closure scheme for chemical master equations. *PNAS*, 110(35):14261–14265, 2013.

[120] R.L. Stoneburner and D. Low-Beer. Population-level hiv decline and behavioral risk avoidance in uganda. *Science*, 304:714–718, 2004.

[121] R.R. Swenson, W.S. Hadley, C.D. Houck, S.K. Dance, and L.K. Brown. Who accepts a rapid hiv antibody test? the role of race/ethnicity and hiv risk behavior among community adolescents. *Journal of Adolescent Health*, 48:527–529, 2011.

[122] J.M. Tchuenche and C.T. Bauch. Dynamics of an infectious disease where media coverage influences transmission. *ISRN Biomathematics*, 2012.

[123] D. Thompson, P. Muriel, D. Russell, P. Osborne, A. Bromley, M. Rowland, S. Creigh-Tyte, and C. Brown. Economic costs of the foot and mouth disease outbreak in the united kingdom in 2001. *Rev Sci Tech*, 21(3):675–687, 2002.

[124] M.J. Tildesley, P.R. Bessell, M.J. Keeling, and M.E.J. Woolhouse. The role of pre-emptive culling in the control of foot-and-mouth disease. *Proceedings of the Royal Society B 22*, 276(1671):3236–3248, 2009.

[125] M.J. Tildesley, N.J. Savill, D.J. Shaw, R. Deardon, S.P. Brooks, M.E. Woolhouse, B.T. Grenfell, and M.J. Keeling. Optimal reactive vaccination strategies for a foot-and-mouth outbreak in the uk. *Nature*, 440(7080):83–86, 2006.

[126] M.J. Tildesley, N.J. Savill, D.J. Shaw, R. Deardon, S.P. Brooks, M.E.J. Woolhouse, B.T. Grenfell, and M.J. Keeling. Economic costs of the foot and mouth disease outbreak in the united kingdom in 2001. *Rev Sci Tech*, 21(3):675–687, 2001.

[127] H. Trottier and P. Philippe. Deterministic modeling of infectious diseases: theory and methods. *The Internet Journal of Infectious Diseases*, 1(2), 2000.

[128] M. van Baalen. Pair approximations for different spatial geometries. *The geometry of ecological interactions: simplifying spatial complexity*, pages 359–387, 2000.

[129] T. Virgl, A. Kaminskas, L. Majercak, and A. Maris. Conway's game of life. *https : //www.doc.ic.ac.uk/project/examples/*2012/163/*g*1216326/*game.php*, Accessed: 27-11-2014.

[130] D.J. Watts and S.H. Strogatz. Collective dynamics of small-world networks. *Nature*, 394:440–442, 1998.

[131] U. Wernery and J. Kinne. Foot and mouth disease and similar virus infections in camelids: a review. *Rev. sci. tech. Off. int. Epiz.*, 31(3):907–918, 2012.

[132] S. Wolfram. Cellular aotomata as models of complexity. *Nature*, 311:419–423, 1984.

[133] Y. Zhang and X. Zhao. A reaction-diffusion lyme disease model with seasonality. *SIAM J. APPL. MATH*, 73(6):2077–2099, 2013.

Appendix A

Derivation of model equations, the basic reproduction number, parameter q and the transmission rate for Chapter 2

A.1 Derivation of the equation of motion for [SI]

We illustrate the derivation of a SEIRV pair approximation model of FMD by demonstrating the derivation of the equation of motion for [SI].

The dynamics of [SI] are governed by the equation:

$$\frac{dg(t)}{dt} = \sum r(\epsilon)\Delta g(\epsilon),$$

where $g(t)$ is the state variable of interest (i.e. [SI]), $r(\epsilon)$ is the rate of event ϵ and $\Delta g(\epsilon)$ is the change this event causes in $g(t)$ (i.e. [SI]).

As the disease progresses, [SI] is affected by the following events.

Infection of the susceptible farm by the infectious farm in the S-I edge converts S into E, i.e. $SI \mapsto EI$, where $\mapsto$ means 'transformed to'. This adds $-\tau[SI]$ into the equation of motion for [SI]. The *negative* sign,-, in the coefficient is a result of this

event 'destroying' S-I edges.

Infection of the susceptible farms 'from the left' in a triple I-S-I, i.e. $I \leftrightarrow SI$ gives rise to $SI \mapsto EI$, contributing the term $-\tau[ISI]$ into the equation of motion for [SI].

Latent period is $\frac{1}{\nu}$, therefore $SE \mapsto SI$ and the process 'creates' SI (hence *positive* coefficient). Thus we add $\nu[SE]$ into the equation of motion for [SI].

A infectious farm recovers at rate, σ, therefore $SI \mapsto SR$ contributing $-\sigma[SI]$ into the equation of motion for [SI].

Ring vaccination (defined as vaccination of exposed and susceptible farms that have links with infected farms) in the susceptible farm in a pair S-I, at rate ψ_r converts SI to IV and adds $-\psi_r[SI]$ to $\frac{d[SI]}{dt}$.

Ring vaccination in the susceptible farm in a triple I-S-I, at rate ψ_r converts SI to IV and adds $-\psi_r[ISI]$ to $\frac{d[SI]}{dt}$.

A recovered farm in an I-R pair loses natural immunity at rate ω to form an S-I pair, thus adding $\omega[IR]$ to $\frac{d[SI]}{dt}$.

A vaccinated farm in an I-V pair loses vaccine protection at rate θ to form an S-I pair, thus adding $\theta[IV]$ to $\frac{d[SI]}{dt}$.

Therefore the equation of motion for [SI] is

$\frac{d[SI]}{dt} = -\tau([ISI]+[SI]) + \nu[SE] - \sigma[SI] - \psi_r([SI]+[ISI]) - \psi_p[SI] + \omega[IR] + \theta[IV]$.

A.2 Derivation of the basic reproduction number

We derive the expression of the basic reproduction number for a pair approximation model of foot and mouth disease without control measures. The equations of motion for the number of exposed and infectious farms are important in the derivation of the basic reproduction number. An epidemic is expected if $\frac{d}{dt}[E]+\frac{d}{dt}[I]>0$ and the disease is expected to die out if $\frac{d}{dt}[E] + \frac{d}{dt}[I]<0$. Using the correlation function between susceptible and infectious farms, $C_{SI} = \frac{N}{n}\frac{[SI]}{[S][I]}$, we re-write the equation of motion for the number of exposed farms as

$\frac{d}{dt}[E] = \frac{\beta}{N}[S][I]C_{SI} - \nu[E]$, where $\beta = \tau n$.

At the beginning of an epidemic almost all farms are susceptible, i.e. $[S] \approx N$. Therefore we simplify the equation of motion for the number of exposed farms further:

$\frac{d}{dt}[E] = \beta[I]C_{SI} - \nu[E]$.

An epidemic is expected if $\frac{d}{dt}[E] + \frac{d}{dt}[I] = \beta[I]C_{SI} - \nu[E] + \nu[E] - \sigma[I]>0$, i.e.

$\beta[I]C_{SI} - \sigma[I]>0$.

Thus there will be an epidemic if $\frac{\beta}{\sigma}C_{SI} > 1$. Therefore the expression of the ba-

sic reproduction number is

$$R_0 = \frac{\beta}{\sigma} C_{SI}. \tag{A.1}$$

The correlation between susceptible and infectious farms, C_{SI} is not constant but it changes from $C_{SI} \approx 1$ at the beginning of the infection, decreasing as more individuals become infected [15]. An increase in the number of infected farms leads to reduction of the infection rate in the long run, and at this point the epidemic may fade out. This is a local minimum of C_{SI}. The dynamics of the disease at this point are important in deriving an explicit form of the basic reproduction number. Therefore we seek C_{SI}^{min}, the local minimum value of C_{SI}, obtained by solving $\frac{d}{dt} C_{SI} = 0$.

The derivative of the correlation function between the number of susceptible and infectious farms is given by

$$\frac{d}{dt} C_{SI} = \frac{N}{n} \frac{1}{[S][I]} \frac{d}{dt}[SI] + \frac{N}{n}[SI] \frac{d}{dt} \frac{1}{[S][I]}.$$

This expression is equivalent to:

$$\frac{d}{dt} C_{SI} = \frac{N}{n} \frac{1}{[S][I]} \frac{d}{dt}[SI] + C_{SI}(-\frac{1}{[I]} \frac{d}{dt}[I] - \frac{1}{[S]} \frac{d}{dt}[S]).$$

Substituting the equations of motion for $[SI]$, $[I]$ and $[S]$, into the equation above, applying the ordinary pair approximation to express the number of triples as pairs and singletons, and noting that at the initial stages of the disease there are no recovered farms (i.e. $[R] \approx 0$), yields

$$\frac{d}{dt} C_{SI} = -\tau(n-1)\frac{[I]}{N} C_{SI}^2 - \tau C_{SI} + \nu \frac{[E]}{[I]} C_{SE} - \nu \frac{[E]}{[I]} C_{SI} + \tau n \frac{[I]}{N} C_{SI}^2.$$

Note that at the initial stages of the infection $[S] \approx N$; a simple analysis of terms involving $\frac{[I]}{N}C_{SI}^2$ shows that they are too small to have significant impact on the correlation between susceptible and infectious farms. We let $\frac{[I]}{N}C_{SI}^2 \to 0$ so that the equation of motion for C_{SI} becomes

$$\frac{d}{dt}C_{SI} = -\tau C_{SI} + \nu\frac{[E]}{[I]}C_{SE} - \nu\frac{[E]}{[I]}C_{SI}.$$

To solve for C_{SI}^{min} explicitly, we need simpler representation for C_{SE} and $\frac{[E]}{[I]}$.

In a network where there are no 'triangles', when a susceptible farm becomes exposed, this newly exposed farm inherits the neighborhood of the susceptible [95, 64]. Thus

$$C_{SE} \approx \frac{(n-1)}{n}C_{SS}.$$

Adopting arguments by [95] we assume further that the host population space is such that $C_{SS} \approx 1$, so that

$$C_{SE} \approx \frac{(n-1)}{n}.$$

The process of a farm moving from the exposed to the infectious state implies that the farm now inherits a fraction $(n-1)/n$ of the neighborhood it had previously [95, 64]. Thus

$\frac{[E]}{[I]} \approx (\frac{n-1}{n})$.

Therefore the equation of motion for C_{SI} is

$$\frac{d}{dt}C_{SI} = -\tau C_{SI} + \nu\frac{(n-1)}{n}\frac{(n-1)}{n} - \nu\frac{(n-1)}{n}C_{SI}.$$

We obtain C_{SI}^{min} by letting the left hand side of the equation above equal zero and solve for C_{SI}. It follows that

$C_{SI}^{min} = \frac{(n-1)^2}{n[(n-1)+(\frac{\beta}{\nu})]}$ where $\beta = \tau n$.

But $R_0 = \frac{\beta}{\sigma}C_{SI}^{min}$, therefore

$$R_0 = \frac{\beta(n-1)^2}{\sigma n[(n-1)+(\frac{\beta}{\nu})]}$$

where $\beta = \tau n$. Under mean field approximations, the corresponding expression of the basic reproduction number is $R_0 = \frac{\tau}{\sigma}$. This overestimates the true R_0 in a spatially structured population of farms because it does not take into account the slowing effects of spatially localized transmission [15]. On the other hand, the expression of the basic reproduction number derived under moment closure techniques provides a better estimation of the true value of R_0 because of the pair approximations' capacity to capture the time evolution of local spatial structure. Here transmission can only take place between neighboring farms.

A.3 Derivation of a constant q

We present the derivation of a constant q in the expressions of the basic reproduction number in Chapter 2. This constant represents a ratio $\frac{[EI]}{[E]}$. Suppose the population is distributed on a square grid and that initially only one farm is exposed (state E) and the rest of the farms are susceptible (state S). At this stage of the outbreak none of the farms are infectious, therefore $\frac{[EI]}{[E]} = \frac{0}{1} = 0$ (see Figure A.1a). For simplicity, we assume that at every time step exposed farms become infectious

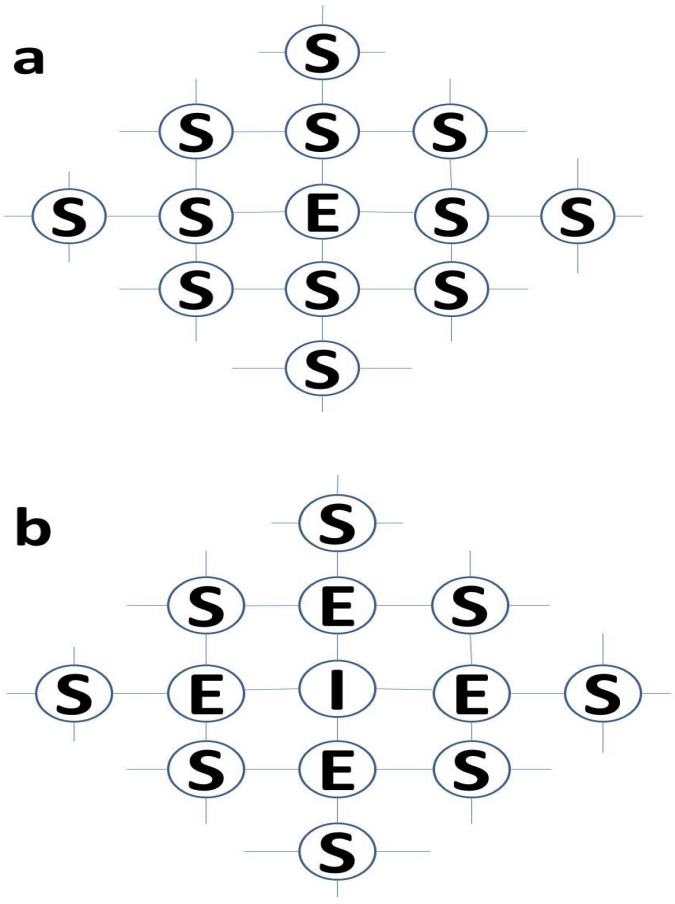

Figure A.1: Illustration of the derivation of a constant q

and pass on the virus to susceptible neighbors such that the latter transition from state S to state E, while the rest of the population remains susceptible. Thus, the network configuration during the second time step is represented by Figure A.1b (here $\frac{[EI]}{[E]} = \frac{4}{4} = 1$). The same procedure shows that in the next 7 time steps this ratio will take values, 1.5, 1.6..., 1.75, 1.8, 1.83..., 1.85, 1.87, 1.8... and 1.9. In the 1000^{th} time step $\frac{[EI]}{[E]} = 1.9...$. Thus, on a square grid $0 < \frac{[EI]}{[E]} < 2$. Since the basic reproduction number is determined by the disease dynamics at the initial stages of an infection we claim that at this point $\frac{[EI]}{[E]} \approx 1.5$, hence $q = 1.5$.

A.4 Derivation of the transmission parameter, τ

We derive the baseline transmission rate τ from the expression of the basic reproduction number, Equation (2.5). Substituting $n = 4$, $\beta = \tau n = 4\tau$, $\nu = 1/4$ and $\sigma = 1/7$ into this expression yields

$R_0 = \frac{63\tau}{3+16\tau}$.

Changing the subject of this formula to τ gives

$\tau = \frac{3R_0}{63-16R_0}$.

τ takes positive values only when $R_0>0$ and $63 - 16R_0>0$. Thus transmission will take place when

$0<R_0<\frac{63}{16}$, i.e. $0<R_0<3.9375$.

The corresponding baseline choice of τ should be based on the choice of R_0 in this interval.

Also, on a square-grid if recovery rate is $\sigma = 0$ then an infected farm can infect no more than $n-1$ neighbors, none of whom ever recover (the farm became infected through one of its neighbors, so no more than $n-1$ neighbors can be susceptible) [15]. Thus $R_0 \leq n-1$. If infectious farms recover (to recovered compartment), i.e. $\sigma>0$, then the susceptible denominator is still at most $n-1$, i.e. $R_0 \leq n-1$.

Thus, if each farm has $n = 4$ neighbors, then $R_0 \leq n-1 = 3$, for all τ and σ.

Therefore, on a square-grid torus, an infected farm can infect at most 3 of its 4 neighbors.

If $R_0 = 1$, then $\tau = \frac{3\times1}{63-16\times1} = \frac{3}{47} \approx 0.064$;
If $R_0 = 2$, then $\tau = \frac{3\times2}{63-16\times2} = \frac{6}{31} \approx 0.194$;
If $R_0 = 3$, then $\tau = \frac{3\times3}{63-16\times3} = \frac{9}{15} \approx 0.600$.

Our baseline choice of the transmission rate is $\tau = 0.600$.

Appendix B

Derivation of model equations, basic reproduction number and supplementary Tables and Figures for Chapter 3

B.1 Derivation of the equation of motion for [SI], and the full model.

Here we demonstrate the derivation of the equation of motion for [SI] in a SEIRVC pair approximation model of FMD using an approach similar to the one in [64, 104, 15, 107], and then present the model in full.

In moment closure approximations the equation of motion for any state variable, $g(t)$, is determined by summing over all events that affect the state variable. Thus the dynamics of $g(t)$ are governed by the master equation:

$$\frac{dg(t)}{dt} = \sum_{\epsilon \in events} r(\epsilon)\Delta g(\epsilon), \tag{B.1}$$

where $r(\epsilon)$ is the rate of event ϵ and $\Delta g(\epsilon)$ is the change this event causes in $g(t)$. As will be observed in the following illustration, at each node on the network the rates

$r(\epsilon)$ and change $\Delta g(\epsilon)$ are expressed in terms of their population-averaged values as well as the deviations of those values from the expected means at a given node. The summation over each node is carried out in such a way that any significant stochasticity is incorporated in the evaluation of a state variable while the remaining stochasticity can be treated as random noise and may be discarded. We illustrate this concept below.

Before we proceed to the derivation of the equation on motion for $[SI]$, we first list all events in the model that affect this state variable:

Infection at a rate τ of a susceptible farm by its infectious neighbour (in a $S-I$ pair) converts S into E, i.e. $SI \mapsto EI$, where $\mapsto$ means 'transformed to'. This process *destroys* a $S-I$ pair. Similarly, infection at a rate τ of a susceptible farm 'from the left' in a triple $I-S-I$, i.e. $I \leftrightarrow SI$ also *destroys* a $S-I$ pair.

Transition of a farm from the exposed to the infectious state in a pair $S-E$ at a rate ν (NB: latent period is $\frac{1}{\nu}$) *creates* a $S-I$ pair, i.e. $SE \mapsto SI$.

Recovery of an infectious farm at a rate, σ in a pair $S-I$ implies $SI \mapsto SR$. Therefore the process *destroys* $S-I$.

Ring vaccination (defined as vaccination of exposed and susceptible farms that have links with infected farms) in the susceptible farm in a pair $S-I$, at rate ψ_r *destroys* $S-I$ by a transformation $SI \mapsto IV$. Similarly ring vaccination in the susceptible farm in a triple $I-S-I$, *destroys* $S-I$.

DC culling (defined as culling on farms neighbouring infectious farms) at a rate μ_{DC} in the susceptible farm in a pair $S-I$ and a triple $I-S-I$, similarly transforms $S-I$ into $I-C$, thereby *destroying* $S-I$.

IP culling (defined as culling on infectious farms) at a rate μ_{IP} in the infectious farm in a pair $S-I$ *destroys* $S-I$ to form $S-C$.

A recovered farm in an $I-R$ pair loses natural immunity at rate ω to *create* a $S-I$ pair.

A vaccinated farm in an $I-V$ pair loses vaccine protection at rate θ, and the process *creates* a $S-I$ pair.

Replacement of previously culled farms at a rate η *creates* $S-I$ by transforming $I-C$ into $S-I$.

The following notations will be adopted to proceed with the derivation of the equation of motion for $[SI]$:

$n_x(i)$: number of state i neighbours of a node x;

$n_{xy}(i)$: number of state i neighbours of a node x, which has node y as a neighbour;

ζ_x: disease state of node x;

ζ_{xy}: disease state of an edge involving x and y.

Therefore, the master equation for $[SI]$ is given by

$$\begin{aligned}\frac{d[SI]}{dt} = &\sum_{\zeta_{xy}=SI} \tau(n_{xy}(I))(-1) + \sum_{\zeta_x=S} \nu(n_x(E))(+1) + \sum_{\zeta_x=S} \sigma(n_x(I))(-1) \\ &+ \sum_{\zeta_{xy}=SI} \psi_r(n_{xy}(I))(-1) + \sum_{\zeta_x=R} \omega(n_x(I))(+1) + \sum_{\zeta_x=V} \theta(n_x(I))(+1) \\ &+ \sum_{\zeta_{xy}=SI} \mu_{DC}(n_x(I))(-1) + \sum_{\zeta_x=S} \mu_{IP}(n_x(I))(-1) + \sum_{\zeta_x=C} \eta(n_x(I))(-1).\end{aligned}$$

The *positive* $+$ and *negative* $-$ signs in this formulation indicate *creation* or *destruction* of the $S-I$ pair, respectively. The next step is to replace quantities $n_x(I)$, $n_{xy}(I)$ and $n_x(E)$ by their population-averaged values (means) plus the stochastic fluctuations of those quantities from the means at the node x and pairs xy. We introduce more notations to illustrate this step. Let $n(i|j)$ be the population-averaged value of $n_x(i)$ when $\zeta_x = j$ and let $n(i|jk)$ be the population-averaged value of $n_{xy}(i)$ when $\zeta_{xy} = jk$. For example here $n_{xy}(I)$ is replaced by $n(I|SI) + \rho_{xy}(I|SI)$ where $\rho_{xy}(I|SI)$ represents the stochastic fluctuation from the mean. The resulting expression is then simplified by taking out constants such as $n(I|SI)$ and the model parameters out of the sums and further noting that terms such as $\sum_{\zeta_x=S} \rho_x(I|S)$, which represent fluctuations, are zero by definition. Furthermore the following identities, which apply to all network types,

$n(i|jk) = \frac{[ijk]}{[jk]}$; $n(i|ji) = 1 + \frac{[iji]}{[ji]}$; $n(i|j) = \frac{[ij]}{[j}$ and $n(i|i) = 1 + \frac{[ii]}{[i]}$,

enable us to write the equation of motion for $[SI]$ as

$$\frac{d[SI]}{dt} = -\tau([ISI] + [SI]) + \nu[SE] - \sigma[SI] - \psi_r([SI] + [ISI]) - \psi_p[SI] + \omega[IR] + \theta[IV] - \mu_{DC}([SI] + [ISI]) - \mu_{IP}[SI] + \eta[IC].$$

Since farms are distributed on a random network in which the neighbourhood size is assumed to obey a Poisson distribution, and because there are *no triangles*, third order correlations take the form

$$[ijk] = \frac{[ij][jk]}{[j]} \text{ and } [iji] = \frac{[ij]^2}{[j]}. \tag{B.2}$$

This is approximation of triples into pairs and singletons is referred to as the Poisson ordinary pair approximation.

The full model (before approximating triples into lower-order correlations) is

B.1.1 The model

$$
\begin{aligned}
\frac{d[S]}{dt} &= -\tau[SI] - \psi_r[SI] - \psi_p[S] + \omega[R] + \theta[V] - \mu_{DC}[SI] + \eta[C] \\
\frac{d[E]}{dt} &= \tau[SI] - \nu[E] - \psi_r[EI] - \mu_{DC}[EI] \\
\frac{d[I]}{dt} &= \nu[E] - \sigma[I] - \mu_{IP}[I] \\
\frac{d[R]}{dt} &= \sigma[I] - \omega[R] \\
\frac{d[V]}{dt} &= \psi_r[SI] + \psi_r[EI] + \psi_p[S] - \theta[V] \\
\frac{d[C]}{dt} &= \mu_{DC}[SI] + \mu_{DC}[EI] + \mu_{IP}[I] - \eta[C] \\
\frac{d[SS]}{dt} &= -2\tau[SSI] - 2\psi_r[SSI] - 2\psi_p[SS] + 2\omega[SR] + 2\theta[SV] - 2\mu_{DC}[SSI] + 2\eta[SC] \\
\frac{d[SE]}{dt} &= -\tau([ISE] - [SSI]) - \nu[SE] - \psi_r([ISE] + [SEI]) - \psi_p[SE] + \omega[ER] + \theta[EV] \\
&- \mu_{DC}([ISE] + [SEI]) + \eta[EC] \\
\frac{d[SI]}{dt} &= -\tau([ISI] + [SI]) + \nu[SE] - \sigma[SI] - \psi_r([SI] + [ISI]) + \omega[IR] + \theta[IV] \\
&- \mu_{DC}([SI] + [ISI]) - \mu_{IP}[SI] + \eta[IC] \\
\frac{d[SR]}{dt} &= -\tau[ISR] + \sigma[SI] - \psi_r[ISR] - \psi_p[SR] - \omega([SR] - [RR]) + \theta[RV] - \mu_{DC}[ISR] + \eta[RC] \\
\frac{d[SV]}{dt} &= -\tau[ISV] - \psi_r([ISV] - [SSI] - [SEI]) - \psi_p([SV] - [SS]) + \omega[RV] + \theta([VV] - [SV]) \\
&- \mu_{DC}[ISV] + \eta[VC] \\
\frac{d[SC]}{dt} &= \mu_{DC}([SSI] + [SEI] - [ISC]) + \mu_{IP}[SI] - \eta[SC] + \eta[CC] \\
\frac{d[EE]}{dt} &= 2\tau[ESI] - 2\nu[EE] - 2\psi_r[EEI] - 2\mu_{DC}[EEI] \\
\frac{d[EI]}{dt} &= \tau([ISI] + [SI]) + \nu([EE] - [EI]) - \sigma[EI] - \psi_r([EI] + [IEI]) - \mu_{DC}([EI] + [IEI]) - \mu_{IP}[EI] \\
\frac{d[ER]}{dt} &= \tau[ISR] - \nu[ER] + \sigma[EI] - \psi_r[IER] - \omega[ER] - \mu_{DC}[IER] \\
\frac{d[EV]}{dt} &= \tau[ISV] - \nu[EV] - \psi_r([IEV] - [ISE] - [EEI]) + \psi_p[SE] - \theta[EV] - \mu_{DC}[IEV] \\
\frac{d[EC]}{dt} &= \mu_{DC}([ISE] + [EEI] - [IEC]) + \mu_{IP}[EI] - \eta[EC] \\
\frac{d[II]}{dt} &= 2\nu[EI] - 2\sigma[II] - 2\mu_{IP}[II] \\
\frac{d[IR]}{dt} &= \sigma([II] - [IR]) + \nu[ER] - \omega[IR] - \mu_{IP}[IR] \\
\frac{d[IV]}{dt} &= -\sigma[IV] + \nu[EV] + \psi_r([SI] + [ISI] + [EI] + [IEI]) - \theta[IV] - \mu_{IP}[IV]r \\
\frac{d[IC]}{dt} &= \mu_{DC}([ISI] + [SI] + [IEI] + [EI]) - \mu_{IP}[IC] - \eta[IC] \\
\frac{d[RR]}{dt} &= 2\sigma[IR] - 2\omega[RR] \\
\frac{d[RV]}{dt} &= \sigma[IV] + \psi_r([ISR] + [IER]) + \psi_p[SR] - \omega[RV] - \theta[RV] \\
\frac{d[RC]}{dt} &= \mu_{DC}([ISR] + [IER]) + \mu_{IP}[IR] - \eta[RC] \\
\frac{d[VV]}{dt} &= 2\psi_r([IEV] + [ISV]) + 2\psi_p[SV] - 2\theta[VV] \\
\frac{d[VC]}{dt} &= \mu_{DC}([ISV] + [IEV]) + \mu_{IP}[IV] - \eta[VC] \\
\frac{d[CC]}{dt} &= 2\mu_{DC}([ISC] + [IEC]) + 2\mu_{IP}[IC] - 2\eta[CC].
\end{aligned}
\tag{B.3}
$$

The factor 2 in the equations of motion pairs of the form $[XX]$ comes from the counting convention of same-status pairs such that, e.g. $[II]$ denotes twice the number of infected-infected pairs [104, 15].

B.2 Derivation of the basic reproduction number

Here we present the derivation of the basic reproduction number for our pair approximation model of foot and mouth disease.

At the initial stage of the infection an outbreak is expected to take off if the numbers of exposed, $[E]$ and infectious, $[I]$ farms increase. That is, an epidemic is expected if $\frac{d}{dt}[E] + \frac{d}{dt}[I] > 0$ or the disease will to die out if $\frac{d}{dt}[E] + \frac{d}{dt}[I] < 0$. Substituting the equations of motion for $[E]$ and $[I]$ from Equation (B.3) into either of the inequalities above shows that the disease will spread if

$$\tau[SI] - (\psi_r + \mu_{DC})[EI] - (\sigma + \mu_{IP})[I] > 0.$$

The definition of the correlation between any two farms given by Equation 3.1 implies that $[SI]$ and $[EI]$ in the expression above can be written in terms of the correlation between susceptible and infectious farms, and between the exposed and infectious farms, respectively, so that the condition under which the disease will spread is now

$$\tau n \tfrac{[S][I]}{N} C_{SI} - (\psi_r + \mu_{DC}) n \tfrac{[E][I]}{N} C_{EI} - (\sigma + \mu_{IP})[I] > 0.$$

We divide this inequality by $[I]$ and use the convention that at the beginning of

an epidemic (initial inoculation) there is only one or very few infected farms such that almost the entire population is susceptible, i.e. $[S] \approx N$, to rewrite the condition for the spread of the disease as

$\tau n C_{SI} - (\psi_r + \mu_{DC}) n \frac{[E]}{N} C_{EI} - (\sigma + \mu_{IP}) > 0$ or

$\frac{\tau n C_{SI}}{(\psi_r + \mu_{DC}) n \frac{[E]}{N} C_{EI} + (\sigma + \mu_{IP})} > 1.$

The left hand side of the expression above is essentially the basic reproduction number. That is, the basic reproduction number is a function of the transmission rate, the average neighbourhood size, vaccination, culling, correlation between susceptible and infectious farms and correlation between exposed and infectious farms:

$$R_0 = \frac{\tau n C_{SI}}{(\psi_r + \mu_{DC}) n \frac{[E]}{N} C_{EI} + (\sigma + \mu_{IP})}. \tag{B.4}$$

Note that in the absence of control measures Equation B.4 transforms to a simpler expression of the basic reproduction number:

$R_0 = \frac{\tau n C_{SI}}{\sigma}$.

While in the case of mean-field equations, C_{SI} and $\frac{[E]}{N} C_{EI}$ are assumed to remain constant over time, here these correlations are variables and their critical values are crucial in the derivation of the basic reproduction number [15, 95]. For instance, at the beginning of an epidemic when almost the entire population is susceptible, then $C_{SI} \approx 1$. C_{SI} decreases as more farms become infected and the subsequent clustering of infected farms creates a situation where the infection is *wasted*, resulting in reduc-

tion of the infection rate, and at this point the epidemic may die out if there are no susceptible farms in the neighbourhood to acquire and transmit the disease further. This point is a local minimum of C_{SI}, and is denoted by C^*_{SI}. Thus the disease dynamics at this point will determine whether or not the disease will spread. This value is obtained by solving $\frac{d}{dt}C_{SI} = 0$. In a similar manner the basic reproduction number is defined by the critical value $(\frac{[E]}{N}C_{EI})^*$, obtained by solving $\frac{d}{dt}\frac{[E]}{N}C_{EI} = 0$. Therefore we need to evaluate C^*_{SI} and $(\frac{[E]}{N}C_{EI})^*$ and substitute them into Equation (B.4) to give an explicit form of the basic reproduction number.

First we evaluate C^*_{SI}. The equation of motion for the the correlation between susceptible and infectious farms is given by

$$\frac{d}{dt}C_{SI} = \frac{N}{n}\frac{1}{[S][I]}\frac{d}{dt}[SI] + C_{SI}(-\frac{1}{[I]}\frac{d}{dt}[I] - \frac{1}{[S]}\frac{d}{dt}[S]).$$

Substituting the equation of motion for $[SI]$ from Equations (B.3) into the equation above, applying the Poisson OPA (Equation B.2) to express terms involving triples as pairs and singletons and expressing pairs in terms of their correlation functions, show that the first term of the equation of motion for C_{SI} is given by

$$\frac{N}{n}\frac{1}{[S][I]}\frac{d}{dt}[SI] = -\tau n\frac{[I]}{N}C^2_{SI} - \tau C_{SI} + \nu\frac{[E]}{[I]}C_{SE} - \sigma C_{SI} - \psi_r n\frac{[I]}{N}C^2_{SI} - \psi_r C_{SI} - \psi_p C_{SI} - \mu_{DC} n\frac{[I]}{N}C^2_{SI} - \mu_{DC}C_{SI} - \mu_{IP}C_{SI} + \omega\frac{[R]}{[S]}C_{IR} + \theta\frac{[V]}{[S]}C_{IV} + \eta\frac{[C]}{[S]}C_{IC}.$$

The remaining terms of the equation of motion for C_{SI} are

$$C_{SI}(-\tfrac{1}{[I]}\tfrac{d}{dt}[I] - \tfrac{1}{[S]}\tfrac{d}{dt}[S]) = -\nu\tfrac{[E]}{[I]}C_{SI} + \sigma C_{SI} + \mu_{IP}C_{SI} + \tau n\tfrac{[I]}{N}C^2_{SI} + \psi_r n\tfrac{[I]}{N}C^2_{SI} +$$

$\psi_p C_{SI} + \mu_{DC} n \frac{[I]}{N} C_{SI}^2 - \omega \frac{[R]}{[S]} C_{IR} - \theta \frac{[V]}{[S]} C_{IV} - \eta \frac{[C]}{[S]} C_{IC}.$

Therefore

$\frac{d}{dt} C_{SI} = -(\tau + \psi_r + \mu_{DC} + \nu \frac{[E]}{[I]}) C_{SI} + \nu \frac{[E]}{[I]} C_{SE}.$

We use a convention also adopted in [104, 95, 64], that on a network where nodes X and Z in a triple $X - Y - Z$ are conditionally independent, i.e. no triangles, then when a susceptible farm becomes exposed, this newly exposed farm inherits the neighbourhood of the susceptible, and this means C_{SE} is related to C_{SI} such that $C_{SE} \approx \frac{(n-1)}{n} C_{SS}$. However at the beginning of an infection almost all farms are susceptible, therefore $C_{SS} \approx 1$, so that $C_{SE} \approx \frac{(n-1)}{n}$ Similar arguments can be made to approximate $\frac{[E]}{[I]}$. That is the process of a farm moving from the exposed to the infectious state implies that the farm now inherits a fraction $(n-1)/n$ of the neighbourhood it had previously so that $\frac{[E]}{[I]} \approx (\frac{n-1}{n})$.

Therefore the equation of motion for C_{SI} now becomes

$\frac{d}{dt} C_{SI} = -(\tau + \psi_r + \mu_{DC} + \nu \frac{n-1}{n}) C_{SI} + \nu \frac{(n-1)^2}{n^2}$

and the value of C_{SI} associated to R_0 is

$C_{SI}^* = \frac{\nu(n-1)^2}{n[(n-1)\nu + (\tau + \psi_r + \mu_{DC})n]}.$

Another critical value of the basic reproduction number $(\frac{[E]}{N} C_{EI})^*$, is obtained by

solving

$\frac{d}{dt}\frac{[E]C_{EI}}{N} = \frac{1}{n}(-\frac{[EI]}{[I]^2}\frac{d}{dt}[I] + \frac{1}{[I]}\frac{d}{dt}[EI])$.

Substituting the equations of motion for $[I]$ and $[EI]$ and employing similar assumptions to those applied in the derivation of C^*_{SI} above, and further noting that in a large population the initial disease dynamics are characterized by very small values of terms such as $\frac{[I]}{N}C^2_{SI}$ (i.e. $\frac{[I]}{N}C^2_{SI} \to 0$ as $N \to \infty$), we show that the equation of motion for $\frac{[E]}{N}C_{EI}$ can be written as

$$\frac{d}{dt}\left(\frac{[E]}{N}C_{EI}\right) = \tau C_{SI} - \nu\frac{n-1}{n}\left(\frac{[E]}{N}C_{EI}\right) + \nu\frac{n-1}{n}\left(\frac{[E]}{N}C_{EE}\right) - \nu\left(\frac{[E]}{N}C_{EI}\right) - \psi_r\left(\frac{[E]}{N}C_{EI}\right) - \psi_r q\left(\frac{[E]}{N}C_{EI}\right) - \mu_{DC}\left(\frac{[E]}{N}C_{EI}\right) - \mu_{DC}q\left(\frac{[E]}{N}C_{EI}\right),$$

where $q = \frac{[EI]}{[E]}$. We carried out a separate study to show that q varies with the structure of the network. Furthermore we argue that when all correlations are at their quasi-equilibria then $\frac{[E]}{N}C_{EI}$ (proportional to the expectation of an exposed farm given that there is an infectious farm within its neighbourhood) will always be much higher than $\frac{[E]}{N}C_{EE}$ (proportional to the expectation of finding an exposed farm given that an exposed farm resides nearby). That is there is a higher probability of becoming becoming infected when nearest neighbours are infectious. This allows us to approximate the equation of motion for $\frac{[E]}{N}C_{EI}$ by

$$\frac{d}{dt}\left(\frac{[E]}{N}C_{EI}\right) =$$

$$\tau C_{SI} - \left(\nu\frac{n-1}{n} + \nu + \psi_r + \psi_r q + \mu_{DC} + \mu_{DC}q\right)\left(\frac{[E]}{N}C_{EI}\right)$$

Therefore

$$\left(\frac{[E]}{N}C_{EI}\right)^* = \frac{\tau n C_{SI}^*}{(2n-1)\nu+n(q+1)(\psi_r+\mu_{DC})}.$$

We simplify this expression further by replacing C_{SI}^* by its explicit form derived above, and write

$$\left(\frac{[E]}{N}C_{EI}\right)^* = \frac{\tau\nu(n-1)^2}{[(n-1)\nu+(\tau+\psi_r+\mu_{DC})n][(2n-1)\nu+n(q+1)(\psi_r+\mu_{DC})]}.$$

In summary the expression of the basic reproduction number for our model is given by

$$R_0 = \frac{\tau n C_{SI}^*}{(\psi_r+\mu_{DC})n\left(\frac{[E]}{N}C_{EI}\right)^*+(\sigma+\mu_{IP})},$$

where C_{SI}^* and $\left(\frac{[E]}{N}C_{EI}\right)^*$ are as presented above.

B.3 Online supplementary material.

Table B.1: Minimum cumulative infections in 20 years, corresponding optimal rates of prophylactic vaccination, ψ_p^{max}, and ring vaccination, ψ_r^{max}, varying vaccine capacities, V_i, and yearly average number of prophylactic and ring vaccines used. $\tau = 0.3$ day^{-1} and other parameters are in Table 3.1.

V_i	min. cum. infec	ψ_p^{max}	ψ_r^{max}	avg. yearly proph.	avg. yearly ring
6000	185080	0.0005 day^{-1}	0.0060 day^{-1}	5664	336
8000	178148	0.00075 day^{-1}	0.0060 day^{-1}	7765	235
10000	152640	0.0011 day^{-1}	0.0060 day^{-1}	9770	230
12000	138290	0.0011 day^{-1}	0.0060 day^{-1}	11808	192
14000	111110	0.0016 day^{-1}	0.0060 day^{-1}	13829	171
16000	83303	0.0016 day^{-1}	0.0060 day^{-1}	15848	152
18000	58175	0.0016 day^{-1}	0.0060 day^{-1}	17902	98
20000	36631	0.0022 day^{-1}	0.0060 day^{-1}	19921	79
22000	12870	0.0022 day^{-1}	0.0060 day^{-1}	21952	48
24000	6168	0.0027 day^{-1}	0.0060 day^{-1}	23963	37

Table B.2: Minimum cumulative infections in 20 years, corresponding optimal rates of prophylactic vaccination, ψ_p^{max}, and ring vaccination, ψ_r^{max}, varying vaccine capacities, V_i, and yearly average number of prophylactic and ring vaccines used. $\tau = 0.9$ day^{-1} and other parameters are in Table 3.1.

V_i	min. cum. infec	ψ_p^{max}	ψ_r^{max}	avg. yearly proph.	avg. yearly ring
6000	375630	0.0005 day^{-1}	0.0060 day^{-1}	5447	553
8000	359990	0.00075 day^{-1}	0.0060 day^{-1}	7622	378
10000	350150	0.0011 day^{-1}	0.0060 day^{-1}	9694	306
12000	333240	0.0011 day^{-1}	0.0060 day^{-1}	11704	296
14000	313920	0.0016 day^{-1}	0.0060 day^{-1}	13726	274
16000	301210	0.0022 day^{-1}	0.0060 day^{-1}	15739	261
18000	271060	0.0022 day^{-1}	0.0060 day^{-1}	17741	259
20000	252700	0.0027 day^{-1}	0.0060 day^{-1}	19756	244
22000	224090	0.0027 day^{-1}	0.0060 day^{-1}	21774	226
24000	202960	0.0033 day^{-1}	0.0060 day^{-1}	23789	211

Table B.3: Minimum cumulative infections in 20 years, corresponding optimal rates of prophylactic vaccination, ψ_p^{max}, and ring vaccination, ψ_r^{max}, varying vaccine capacities, V_i, and yearly average number of prophylactic and ring vaccines used. $\omega = \theta = \frac{1}{270}$ day^{-1} and other parameters are in Table 3.1.

V_i	min. cum. infec	ψ_p^{max}	ψ_r^{max}	avg. yearly proph.	avg. yearly ring
6000	202750	0.00075 day^{-1}	0.0060 day^{-1}	5771	229
8000	181049	0.0011 day^{-1}	0.0060 day^{-1}	7802	198
10000	159040	0.0016 day^{-1}	0.0060 day^{-1}	9821	179
12000	137902	0.0016 day^{-1}	0.0060 day^{-1}	11841	159
14000	110740	0.0022 day^{-1}	0.0060 day^{-1}	13868	132
16000	87843	0.0022 day^{-1}	0.0060 day^{-1}	15898	102
18000	59802	0.0027 day^{-1}	0.0060 day^{-1}	17909	91
20000	33367	0.0033 day^{-1}	0.0060 day^{-1}	19946	54
22000	17661	0.0055 day^{-1}	0.0060 day^{-1}	21977	23
24000	14568	0.0055 day^{-1}	0.0060 day^{-1}	23991	9

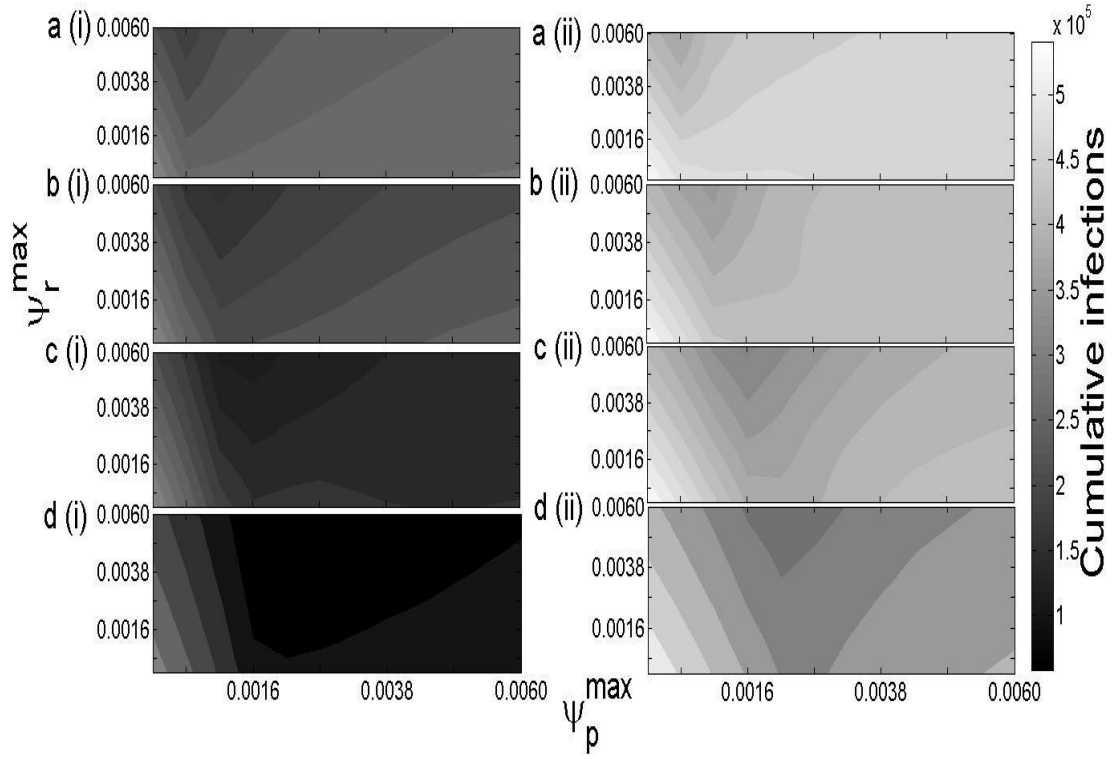

Figure B.1: Cumulative infections in 20 years versus rates of prophylactic vaccination, ψ_p^{max}, and ring vaccination, ψ_r^{max}, for vaccine capacities $V_i = 6000$ per year (a), $V_i = 10000$ per year (b), $V_i = 14000$ per year (c) and $V_i = 18000$ per year (d). In a(i), b(i), c(i) and d(i) $\tau = 0.3\ day^{-1}$; in a(ii), b(ii), c(ii) and d(ii) $\tau = 0.9\ day^{-1}$; other parameters are in Table 3.1.

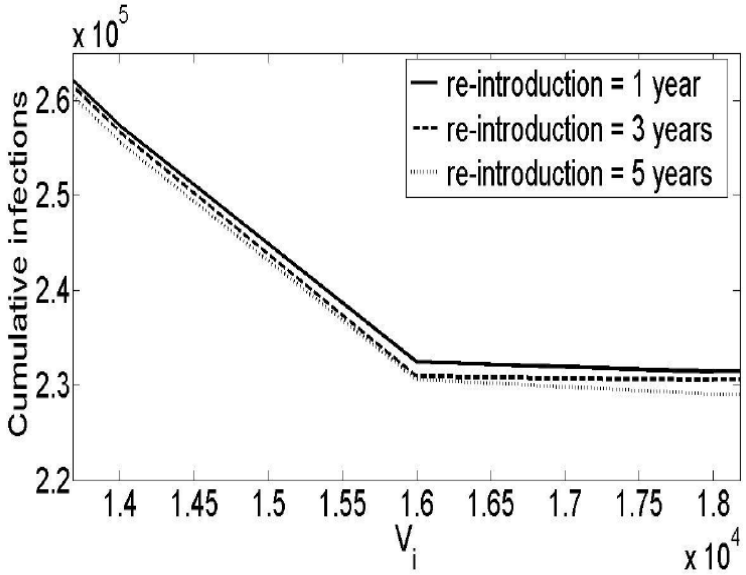

Figure B.2: Cumulative number of infectious farms in 20 years as a function of vaccine capacity, V_i, for varying rates of disease re-introduction. $\psi_p = 0.0016\ day^{-1}$, $\psi_r = 0.0060\ day^{-1}$ and other parameters are in Table 3.1.

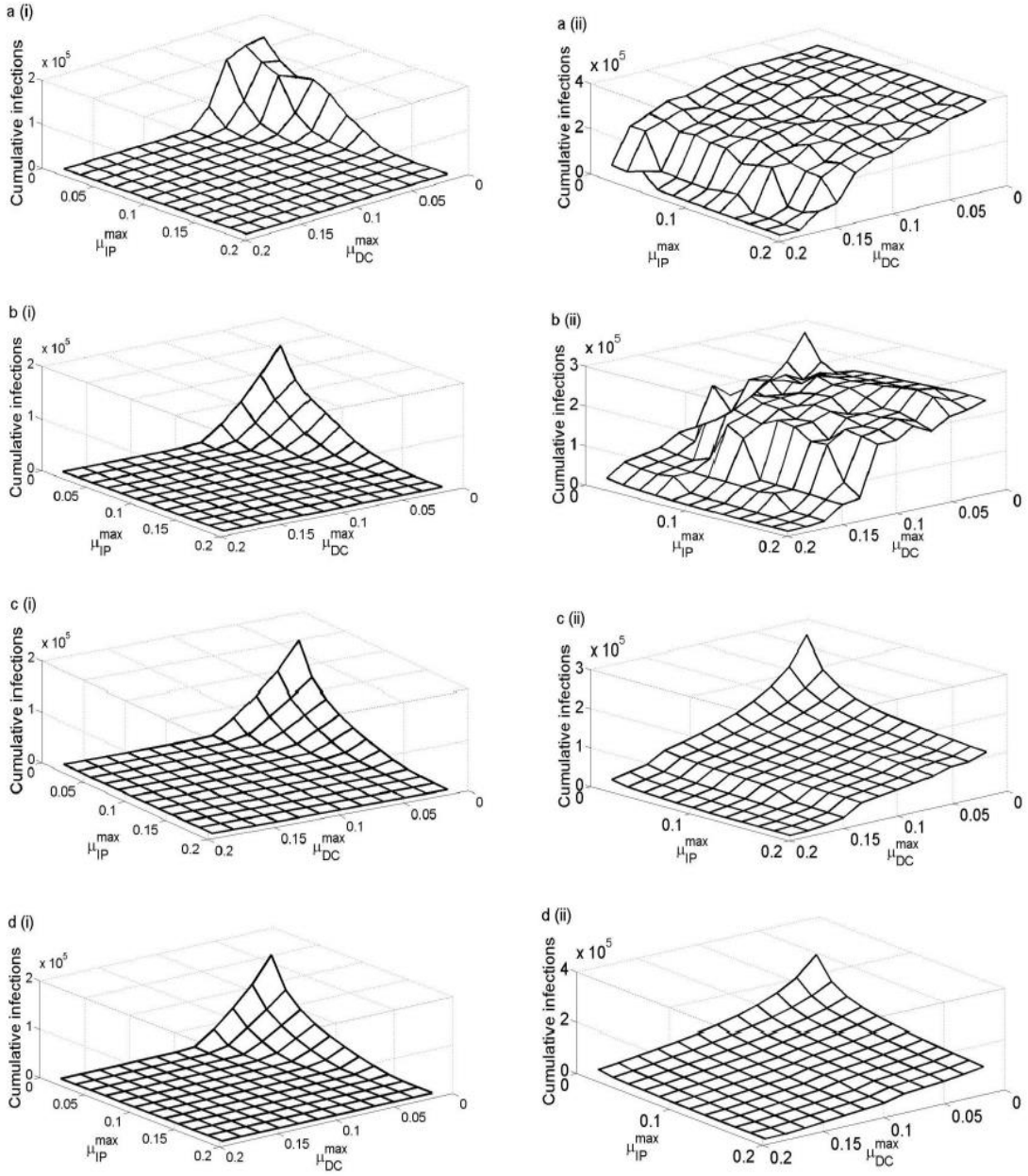

Figure B.3: Cumulative number of infectious farms in 20 years as a function of IP culling, μ_{IP}^{max} and DC culling, μ_{DC}^{max} where upper boundaries of the number of culled farms are $Y_i = 1000$ per year (a), $Y_i = 2000$ per year (b), $Y_i = 4000$ per year (c) and $Y_i = 8000$ per year (d). In a(i), b(i), c(i) and d(i) $\tau = 0.3\ day^{-1}$; in a(ii), b(ii), c(ii) and d(ii) $\tau = 0.9\ day^{-1}$; other parameters are in Table 3.1.

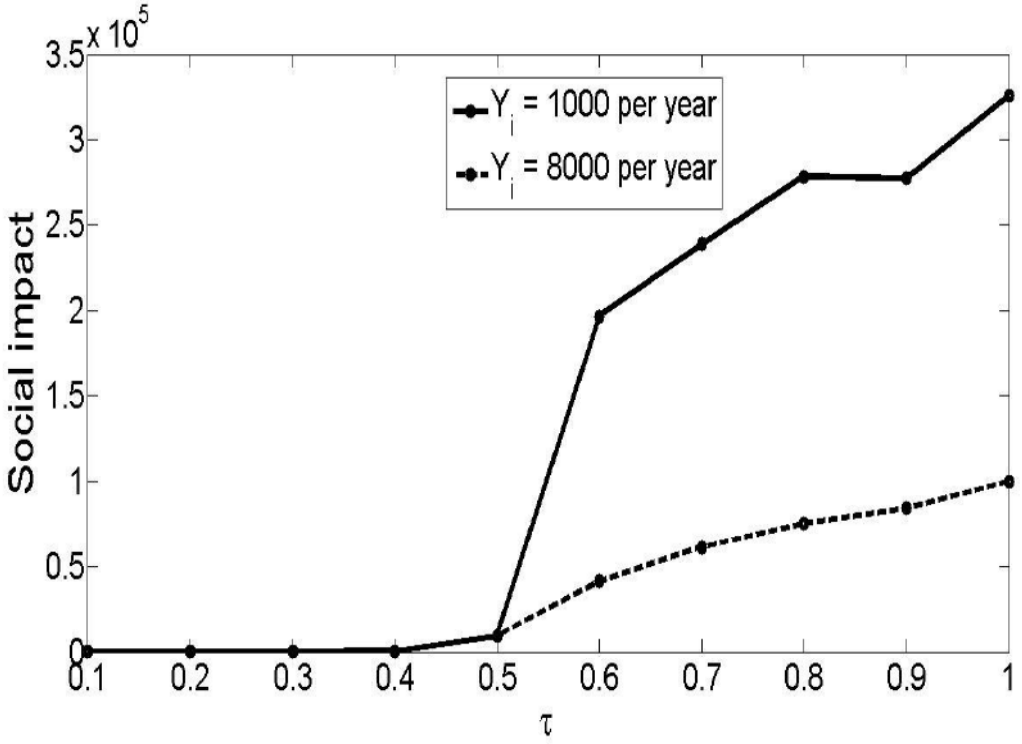

Figure B.4: Social impact in 20 years as a function the transmission rate, τ, where possible number of culls, Y_i is varied. $\mu_{IP}^{max} = \mu_{DC}^{max} = 0.1\ day^{-1}$ and other parameters are in Table 3.1.

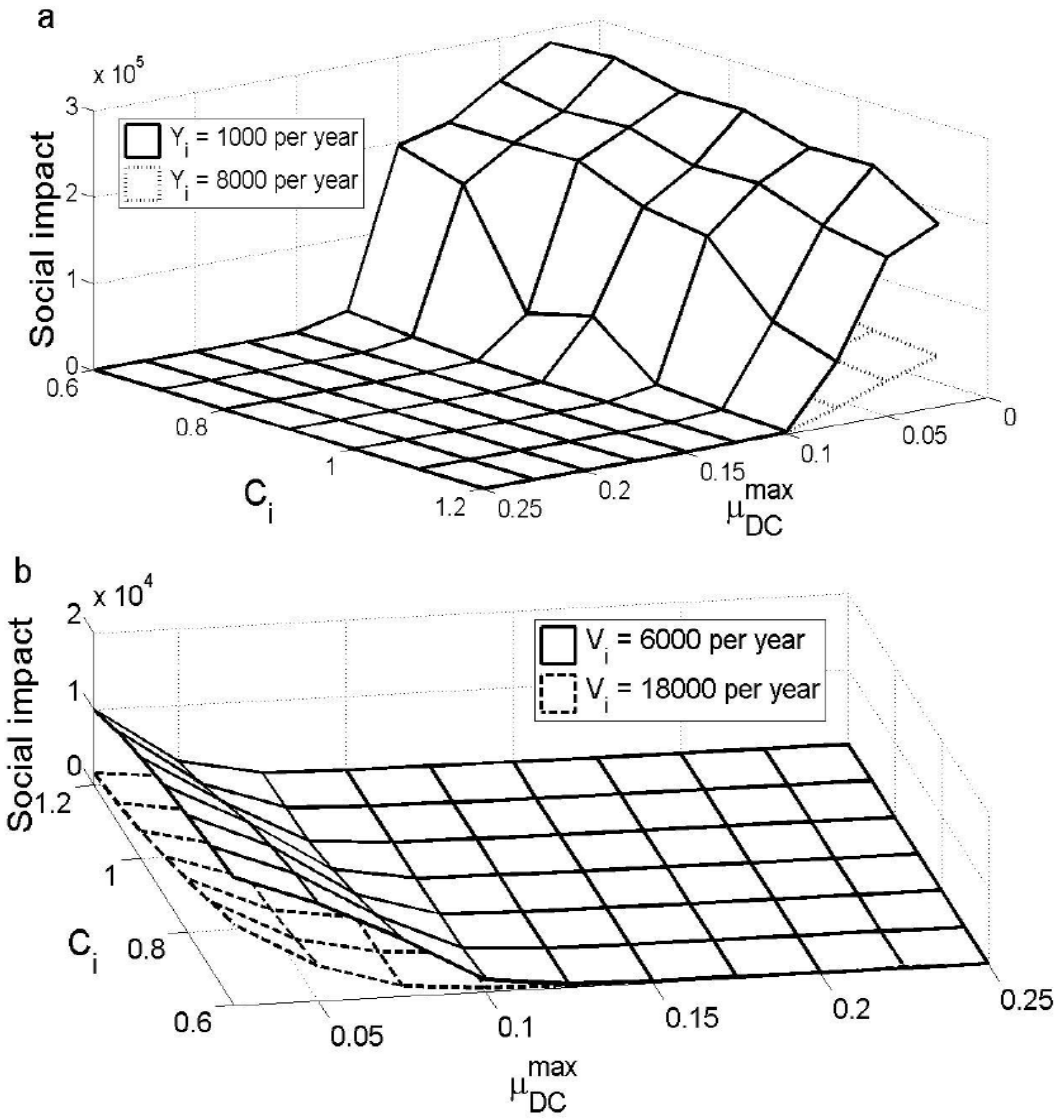

Figure B.5: Social impact in 20 years as a function of DC culling, μ_{DC}^{max} and culling capacity C_i, where each year: $(n+1)\mu_{IP}^{max}+\mu_{DC}^{max} = C_i$ before reaching yearly maximum culls Y_i (a) and culling rates are constrained such that $(n+1)\mu_{IP}^{max} + \mu_{DC}^{max} = C_i$ while vaccination is deployed at rates $\psi_p = 0.0016\ day^{-1}$ and $\psi_r = 0.0060\ day^{-1}$ before reaching yearly maximum vaccine capacity V_i (b). Other parameters are in Table 3.1.

Appendix C

Derivation of model equations, basic reproduction number and supplementary Figure for Chapter 4

C.1 Derivation of the equation of motion for $[SI]$

Here we demonstrate the construction of equations of motion for pair approximation models by deriving $\frac{d[SI]}{dt}$.

In moment closure approximations the equation of motion for a state variable $g(t)$, is determined by expressing $\frac{dg(t)}{dt}$ as a function of the sum of all events that affect the state variable. That is

$$\frac{dg(t)}{dt} = \sum_{\epsilon \in events} r(\epsilon)\Delta g(\epsilon), \tag{C.1}$$

where $r(\epsilon)$ is the rate of event ϵ and $\Delta g(\epsilon)$ is the change this event causes in $g(t)$. Equation (C.1) is referred to as the master equation. As illustrated below, at each node on the network the rates $r(\epsilon)$ and change $\Delta g(\epsilon)$ are expressed in terms of their population-averaged values and the deviations of those values from the expected means at a given node. The summation over each node is carried out in such a way that any significant stochasticity is incorporated in the evaluation of a state variable while the remaining stochasticity can be treated as random noise and may be discarded. We illustrate this concept below.

The time evolution of the number of $S-I$ pairs is determined by the following events.

Infection at a rate τ of a susceptible, S individual by their infectious, I neighbour (in a $S-I$ pair) converts S into I, i.e. $SI \mapsto II$, where $\mapsto$ means 'transformed to'. This process *destroys* a $S-I$ pair. Similarly, infection at a rate τ of a susceptible individual 'from the left' in a triple $I-S-I$, i.e. $I \leftrightarrow SI$ also *destroys* a $S-I$ pair. However a $S-I$ pair is *created* as a susceptible individual is infected at the same rate, τ, in a triple $I-S-S$.

Transmission of the disease from an infectious, I individual to their protective contact, S_p at a rate τ_p in a triple $S-S_p-I$ transforms S_p to I, and therefore *create* a $S-I$ pair.

Recovery of the infectious individual at a rate, σ in a pair $S-I$ implies $SI \mapsto SR$. Therefore the process *destroys* $S-I$.

Adoption of NPIs at a rate ξ, by a state S individual as a result of social learning from their state S_p neighbor in a triple S_p-S-I converts S to S_p, and therefore it *destroys* a $S-I$ link.

Adoption of NPIs at a rate ρ, by a state S individual due to being in the neighborhood of a state I individual in a pair $S-I$ or a triple $I-S-I$ converts S to S_p, and therefore it *destroys* a $S-I$ link.

Stopping the use of NPIs by a protective individual at a rate κ in a S_p-I pair increases their susceptibility, i.e. S_p converts to S, and the process *creates* a $S-I$ pair.

To demonstrate the next steps of the derivation of the equation of motion for $[SI]$, the following notations will be useful:

$n_x(i)$: number of state i neighbours of a node x;

$n_{xy}(i)$: number of state i neighbours of a node x, which has node y as a neighbour;

ζ_x: disease state of node x;

ζ_{xy}: disease state of an edge involving x and y.

Using this notation, the master equation for the dynamics of $[SI]$ can now be represented as the sum of all the events (listed above) as follows:

$$\frac{d[SI]}{dt} = \sum_{\zeta_{xy}=SS} \tau(n_{xy}(I))(+1) + \sum_{\zeta_{xy}=SI} \tau(n_{xy}(I))(-1) + \sum_{\zeta_{xy}=SS_p} \tau_p(n_{xy}(I))(+1) + \sum_{\zeta_x=S} \sigma(n_x(I))(-1) + \sum_{\zeta_{xy}=SI} \psi(n_{xy}(I))(-1) + \sum_{\zeta_{xy}=SI} \xi(n_{xy}(S_p))(-1) + \sum_{\zeta_{xy}=SI} \rho(n_{xy}(I))(-1) + \sum_{\zeta_x=I} \kappa(n_x(S_p))(+1).$$

The *positive (+)* and *negative (−)* signs in the master equation above indicate that the corresponding events *create* or *destroy* $S-I$ pairs, respectively.

Next we replace quantities such as $n_x(I)$ and $n_{xy}(I)$ by their population-averaged values (means) plus the stochastic deviations of those quantities from the means at nodes x and pairs xy. Let $n(i|j)$ be the population-averaged value of $n_x(i)$ when $\zeta_x = j$ and let $n(i|jk)$ be the population-averaged value of $n_{xy}(i)$ when $\zeta_{xy} = jk$. Then at each node we replace $n_{xy}(I)$ by $n(I|SI) + \theta_{xy}(I|SI)$ where $\theta_{xy}(I|SI)$ represents the stochastic fluctuation from the mean. The resulting expression is then simplified by taking out constants such as $n(I|SI)$ and the model parameters out of the sums and further noting that terms such as $\sum_{\zeta_x=S} \theta_x(I|S)$ that represent fluctuations are zero by definition. Furthermore the following identities (which apply to all network types):

$n(i|jk) = \frac{[ijk]}{[jk]}$; $n(i|ji) = 1 + \frac{[iji]}{[ji]}$; $n(i|j) = \frac{[ij]}{[j}$ and $n(i|i) = 1 + \frac{[ii]}{[i]}$,

enable us to write the equation of motion for $[SI]$ as

$$\frac{d[SI]}{dt} = \tau([ISS] - [ISI] - [SI]) + \tau_p[SS_pI] - \sigma[SI] - \xi[S_pSI] + \kappa[S_pI] - \rho([ISI] + [SI]).$$

We assume the disease spreads a regular network where neighbors of an individual are themselves conditionally independent, therefore, third order correlations take the form

$$n(i|jk) = \frac{(n-1)}{n} n(i|j) \text{ and } n(i|ji) = 1 + \frac{(n-1)}{n} n(i|j).$$

That is, to close the system (i.e. approximate higher-order moments by lower-order moments) of equations we use the binomial ordinary pair approximation (OPA):

$$[ijk] = \frac{(n-1)}{n} \frac{[ij][jk]}{[j]}. \tag{C.2}$$

The binomial OPA is based on the idea that the disease state of a node j is directly influenced by the states of two of its indirectly connected neighbors i and k. That is, there are *no triangles* in the network.

C.2 Derivation of the basic reproduction number

Here we derive the expressions for C_{SI}^{min} and $C_{S_pI}^{min}$, and present expressions of the basic reproduction number resulting from a number of disease scenarios.

$C_{SI} = \frac{N}{n} \frac{[SI]}{[S][I]}$, therefore the equation of motion for C_{SI} is given by

$$\frac{d}{dt} C_{SI} = \frac{N}{n} \left(\frac{1}{[S][I]} \frac{d}{dt}[SI] + \frac{[SI]}{[S][I]} \left(-\frac{1}{[I]} \frac{d}{dt}[I] - \frac{1}{[S]} \frac{d}{dt}[S] \right) \right).$$

We substitute the equations of motion for the number of susceptible-infectious pairs, $[SI]$, the number of infectious individuals, $[I]$, and the number of susceptible individuals, $[S]$ from Equation (4.1) into the equation above, and approximate triples by the OPA to show that

$$\frac{d}{dt}C_{SI} = \tau(n-1)\frac{[S]}{[N]}C_{SS}C_{SI} - \tau(n-1)\frac{[I]}{N}C_{SI}^2 - \tau C_{SI} + \tau_p(n-1)\frac{[S_p]}{N}C_{S_pS}C_{S_pI} - \sigma C_{SI} - \xi(n-1)\frac{[S_p]}{N}C_{S_pS}C_{SI} + \kappa\frac{[S_p]}{[S]}C_{S_pI} - \rho(n-1)\frac{[I]}{N}C_{SI}^2 - \rho C_{SI} - \tau n\frac{[S]}{N}C_{SI}^2 - \tau_p n\frac{[S_p]}{N}C_{S_pI}C_{SI} + \sigma C_{SI} + \tau n\frac{[I]}{N}C_{SI}^2 + \xi n\frac{[S_p]}{N}C_{S_pS}C_{SI} - \kappa\frac{[S_p]}{[S]}C_{SI} + \rho n\frac{[I]}{N}C_{SI}^2.$$

Similarly, the equation of motion for the correlation between susceptible individuals who protect and infectious individuals can be written as

$$\frac{d}{dt}C_{S_pI} = \tau(n-1)\frac{[S]}{[N]}C_{SS_p}C_{SI} + \tau_p(n-1)\frac{[S_p]}{N}C_{S_pS_p}C_{S_pI} - \tau_p(n-1)\frac{[I]}{N}C_{S_pI}^2 - \tau_p C_{S_pI} - \sigma C_{S_pI} + \xi(n-1)\frac{[S]}{N}C_{S_pS}C_{SI} - \kappa C_{S_pI} + \rho\frac{[S]}{[S_p]}C_{SI} - \tau_p n\frac{[S_p]}{N}C_{S_pI}^2 - \tau n\frac{[S]}{N}C_{S_pI}C_{SI} + \sigma C_{S_pI} + \tau_p n\frac{[I]}{N}C_{S_pI}^2 - \xi n\frac{[S]}{N}C_{S_pS}C_{S_pI} + \kappa C_{S_pI}.$$

We make biologically reasonable assumptions about the disease to simplify the equations above as follows. At the beginning of the epidemic there are very few infectious individuals (initial inoculation: $[I] = 1$) such that the entire population, N comprises almost only of susceptible individuals who protect, $[S_p]$ and those who do not protect, $[S]$ i.e. $[I] << N$ (where total population N is very large) and $[S_p] + [S] \approx N$. We remind the reader that our derivation of R_0 is based on the idea that both social and exposure learning take place only after the disease has been introduced. Therefore, we assume that at the initial stage of an outbreak the public has little information about the disease and only a small proportion of the population is aware and can decide to

practice NPIs. Thus, at the beginning of an outbreak $[S_p]/N = s_p$, $[S]/N = 1 - s_p$, where $0 < s_p << 1$. Therefore, we can simplify further the equations of motion for C_{SI} and C_{S_pI} above by equating to zero all terms in which the denominator is large and $[I]$ is the numerator.

Although it may be necessary to also derive the equations of motion for three other correlation functions (for C_{SS}, C_{S_pS} and $C_{S_pS_p}$) that appear in the equations of motion for C_{SI} and C_{S_pI} above, we estimate them from the network configuration of the disease at the beginning of an outbreak. This step will help explore the relationship between the initial network configuration of the population with respect to the disease, and the evolution of the epidemic outbreak. We assume that at the beginning of the outbreak susceptible neighboring individuals mix homogeneously. That is, $C_{SS} \approx 1$. This value remains constant throughout calculations of the basic reproduction number for the initial network configurations considered in this paper, but the same does not hold for C_{S_pS} and $C_{S_pS_p}$, since the latter take different values depending on various initial distributions of state S and state S_p individuals around the infection source. Since at the beginning of the outbreak s_p is very small, it is reasonable to assume that $[S] \approx N$. Therefore, at the initial stage of an infection $C_{S_pS} = \frac{N}{n}\frac{[S_pS]}{[S_p][S]} \approx \frac{1}{n}\frac{[S_pS]}{[S_p]}$ while $C_{S_pS_p} = \frac{N}{n}\frac{[S_pS_p]}{[S_p][S_p]}$. These values are calculated from actual initial network configurations as shown in Figure 4.1. We proceed with the derivation of C_{SI}^{min} and $C_{S_pI}^{min}$.

Note that now

$$\frac{d}{dt}C_{SI} = \tau(n-1)(1-s_p)C_{SI} - \tau C_{SI} + \tau_p(n-1)s_pC_{S_pS}C_{S_pI} + \xi s_pC_{S_pS}C_{SI} + \kappa s_pC_{S_pI} - \rho C_{SI} - \tau n(1-s_p)C_{SI}^2 - \tau_p n s_pC_{S_pI}C_{SI} - \kappa s_pC_{SI}$$

and

$\frac{d}{dt}C_{S_pI} = \tau(n-1)(1-s_p)C_{S_pS}C_{SI} + \tau_p(n-1)s_pC_{S_pS_p}C_{S_pI} - \tau_pC_{S_pI} + \xi(n-1)(1-s_p)C_{S_pS}C_{SI} + \rho\frac{1-s_p}{s_p}C_{SI} - \tau_pns_pC_{S_pI}^2 - \tau n(1-s_p)C_{S_pI}C_{SI} - \xi n(1-s_p)C_{S_pS}C_{S_pI}$.
Solving $\frac{d}{dt}C_{SI} = 0$ and $\frac{d}{dt}C_{S_pI} = 0$ yields:

$$C_{SI}^{min} = \frac{R - \tau_pns_pC_{S_pI}^{min} + \sqrt{(R-\tau_pns_pC_{S_pI}^{min})^2 + 4\tau ns_p(1-s_p)\Big(\tau_p(n-1)C_{S_pS} + \kappa\Big)C_{S_pI}^{min}}}{2\tau n(1-s_p)}, \tag{C.3}$$

$$C_{S_pI}^{min} = \frac{T - \tau n(1-s_p)C_{SI}^{min} + \sqrt{\Big(T-\tau n(1-s_p)C_{SI}^{min}\Big)^2 + 4\tau_pns_p(1-s_p)\Big((n-1)(\tau+\xi)C_{S_pS} + \rho/s_p\Big)C_{SI}^{min}}}{2\tau_pns_p}, \tag{C.4}$$

where

$R = \tau(n-1)(1-s_p) - \tau - \rho - \kappa s_p + \xi s_pC_{S_pS}$ and $T = \tau_p(n-1)s_pC_{S_pS_p} - \tau_p - \xi n(1-s_p)C_{S_pS}$.

Simplifying assumptions

Note that at the beginning of an outbreak the initial network configuration constitutes very few susceptible individuals who practice NPIs, so that while $s_p \approx O(1/N)$ (for a network where the infection source has at least 1 protective contact), C_{S_pI} is large (i.e. $C_{S_pI}^{min} = O(N)$). Therefore we can simplify Equation (C.3) by assuming that $s_pC_{S_pI}^{min} \approx 1$, so that

$$C_{SI}^{min} \approx \frac{R-\tau_pn+\sqrt{(R-\tau_pn)^2+4\tau n(1-s_p)\Big(\tau_p(n-1)C_{S_pS}+\kappa\Big)}}{2\tau n(1-s_p)} = \chi$$

is a constant determined by the initial proportion of susceptible individuals who protect, s_p, the model parameters $\tau, \tau_p, \sigma, \rho, \xi$ and κ, as well as the initial network configuration-specific values of correlation functions C_{S_pS} and $C_{S_pS_p}$. Substituting χ

and the resulting expression of $C_{S_pI}^{min}$ into Equation (4.10) yields

$$R_0 \approx \frac{T + n\tau(1-s_p)\chi + \sqrt{\Big(T - \tau n(1-s_p)\chi\Big)^2 + 4\tau_p n s_p(1-s_p)\Big((n-1)(\tau+\xi)C_{S_pS} + \rho/s_p\Big)\chi}}{2\sigma}, \tag{C.5}$$

where

$$T = \tau_p(n-1)s_pC_{S_pS_p} - \tau_p - \xi n(1-s_p)C_{S_pS},$$

$$\chi \approx \frac{R - \tau_p n + \sqrt{(R-\tau_p n)^2 + 4\tau n(1-s_p)\Big(\tau_p(n-1)C_{S_pS} + \kappa\Big)}}{2\tau n(1-s_p)}$$

and

$$R = \tau(n-1)(1-s_p) - \tau - \rho - \kappa s_p + \xi s_p C_{S_pS}.$$

Simulation results involving the basic reproduction number (in the Results section) are based on Equation (C.5).

Below we explore other scenarios of the disease to present simpler expressions of R_0. We consider cases where protective susceptible individuals are assumed to maintain the habit of practicing NPIs throughout the epidemic outbreak (i.e. $\kappa = 0$). Also let the initial network configuration constitute 1 infectious individual with 1 state S_p neighbor (who also has 1 state S_p contact) and let the rest of the population be state S individuals so that for a large population size, initially $[S] \approx N$. Thus, the properties of the network at the initial stage of an outbreak are $s_p = 2/N, C_{S_pS} = 5/2n, C_{S_pS_p} = N/4n$.

(a) Adoption of NPIs through social learning only

Here individuals are assumed to learn about the disease, and therefore adopt NPIs, from their contacts who already practice preventative behavior, and not from their infectious neighbors. That is we let $\xi > 0$, and $\rho = 0$.

If the population size, N is very large, and there are very few state S_p individuals at the beginning of the outbreak, so that $s_p = \frac{[S_p]}{N} \approx 0$, then we can simplify R by noting that $1 - s_p \approx 1$ and $\xi s_p C_{S_pS} \approx 0$ (since $0 \leq \xi \leq 1$ and $C_{S_pS} = O(1)$). Therefore $R \approx \tau(n-2)$.

Also, we simplify T by further noting that $s_p C_{S_pS_p} \approx O(1)$ and $nC_{S_pS} \approx O(1)$, so that

$T \approx \tau_p(n-2) - \xi$.

Thus, the expression of the basic reproduction number can be written as

$$R_0 \approx \frac{\tau_p(n-2) - \xi + \tau n\chi + \sqrt{\Big(\tau_p(n-2) - \xi - \tau n\chi\Big)^2 + 4\tau_p s_p(n-1)(\tau+\xi)\chi}}{2\sigma}, \tag{C.6}$$

where $\chi \approx \frac{\tau(n-2) - \tau_p n + \sqrt{\Big(\tau(n-2) - \tau_p n\Big)^2 + 4\tau\tau_p(n-1)}}{2\tau n}$.

High efficacy case

Here we estimate the expression of R_0 for a case where individuals acquire preventive behavior through interaction with contacts who practice NPIs only, and the adopted NPIs are highly effective (i.e. τ_p is small so that $\tau_p^2 \approx 0$). Therefore, $\Big(\tau_p(n-2) - \xi - \tau n\chi\Big)^2 = \tau^2 n^2\chi^2 - 2\tau_p(n-2)(\xi + \tau n\chi) + \xi(\xi + 2\tau n\chi) + \tau_p^2(n-2)^2 \approx \tau^2 n^2\chi^2 - 2\tau_p(n-2)(\xi + \tau n\chi) + \xi(\xi + 2\tau n\chi)$

and

$\Big(\tau(n-2) - \tau_p n\Big)^2 = \tau^2(n-2)^2 - 2\tau\tau_p n(n-2) + \tau_p^2 n^2 \approx \tau^2(n-2)^2 - 2\tau\tau_p n(n-2) = \tau(n-2)\Big(\tau(n-2) - 2\tau_p n\Big)$.

The resulting expression of the basic reproduction number is

$$R_0 \approx \frac{\tau_p(n-2) - \xi + \tau n\chi + \sqrt{\tau^2 n^2\chi^2 - 2\tau_p(n-2)(\xi + \tau n\chi) + \xi(\xi + 2\tau n\chi) + 4\tau_p s_p(n-1)(\tau+\xi)\chi}}{2\sigma} \tag{C.7}$$

where

$$\chi \approx \frac{\tau(n-2)-\tau_p n+\sqrt{\tau(n-2)\Big(\tau(n-2)-2\tau_p n\Big)+4\tau\tau_p(n-1)}}{2\tau n}.$$

Model parameter-based R_0 for high efficacy case

We simplify Equation (C.7) further by prescribing a reasonable model parameter regime. Let $N = 40000, s_p = 2/N, n = 4$, $\tau = 1\ day^{-1}$, $\tau_p = 0.0025\ day^{-1}$, $\sigma = 0.25\ day^{-1}$ and $\xi = 0.25\ day^{-1}$. Then the following features of Equation (C.7) become apparent:

$\tau(n-2) >> \tau_p n$;

$\tau(n-2) >> 2\tau_p n$;

$\xi >> \tau_p(n-2)$;

$\tau n\chi >> \tau_p(n-2)$;

$\tau^2 n^2\chi^2 >> 4\tau_p s_p(n-1)(\tau+\xi)\chi$;

$\tau^2 n^2\chi^2 >> 2\tau_p(n-2)(\xi+\tau n\chi)$;

$\xi(\xi+2\tau n\chi) >> 4\tau_p s_p(n-1)(\tau+\xi)\chi$;

$\xi(\xi+2\tau n\chi) >> 2\tau_p(n-2)(\xi+\tau n\chi)$.

We use these observations to cancel terms of Equation (C.7) that are insignificant (as per the prescribed parameter regime) to write the expression of the basic reproduction number as

$$R_0 \approx \frac{\tau n\chi - \xi + \sqrt{\tau^2 n^2\chi^2 + \xi(\xi+2\tau n\chi)}}{2\sigma}, \tag{C.8}$$

where $\chi \approx \frac{\tau(n-2)+\sqrt{\tau^2(n-2)^2+4\tau\tau_p(n-1)}}{2\tau n}$.

(b) Adoption of NPIs due to exposure learning only

Here we consider a scenario where individual members of the population gain awareness about the disease, and in turn adopt NPIs, due to being next to infectious contacts only. Thus, we assume $\rho > 0$ and $\xi = 0$.

Applying similar arguments as in part *(a)* above, we simplify the original values of

R, T and χ so that $R \approx \tau(n-2) - \rho$, $T \approx \tau_p(n-2)$ and

$$R_0 \approx \frac{\tau_p(n-2) + \tau n\chi + \sqrt{\Big(\tau_p(n-2) - \tau n\chi\Big)^2 + 4\tau_p n s_p\Big(\tau(n-1)C_{S_p S} + \rho/s_p\Big)\chi}}{2\sigma}, \tag{C.9}$$

where

$$\chi \approx \frac{\tau(n-2)-\rho-\tau_p n+\sqrt{\Big(\tau(n-2)-\rho-\tau_p n\Big)^2 +4\tau\tau_p(n-1)}}{2\tau n}.$$

High efficacy case

Applying the condition for a high efficacy case (i.e. $\tau_p << \tau$) and simplifying assumptions also applied in part *(a)* to a scenario where susceptible individuals adopt positive behavior through exposure learning only, transforms Equation (C.9) to

$$R_0 \approx \frac{\tau_p(n-2) + \tau n\chi + \sqrt{\Big[\tau^2 n^2\chi - 2\tau\tau_p n(n-2) + 4\tau\tau_p s_p(n-1) + 4\tau_p\rho n\Big]\chi}}{2\sigma}, \tag{C.10}$$

where

$$\chi \approx \frac{\tau(n-2) - \rho - \tau_p n + \sqrt{\tau^2(n-2)^2 - 2\tau(n-2)(\rho+\tau_p n) + \rho(\rho+2\tau_p n) + 4\tau\tau_p(n-1)}}{2\tau n}.$$

.

Model parameter-based R_0 for high efficacy case

We prescribe the same parameter regime used in part *(a)* above, but note that here $\xi = 0$. Thus, $N = 40000, s_p = 2/N, n = 4$, $\tau = 1\ day^{-1}$, $\tau_p = 0.0025\ day^{-1}$, $\sigma = 0.25\ day^{-1}$ and $\rho = 0.25\ day^{-1}$. We cancel out parts of Equation (C.10) that are numerically less significant so that the expression of the basic reproduction number becomes

$$R_0 \approx \frac{\tau n\chi + \sqrt{\Big(\tau^2 n^2\chi + 4\tau_p\rho n\Big)\chi}}{2\sigma}, \tag{C.11}$$

where

$$\chi \approx \frac{\tau(n-2) - \rho + \sqrt{\tau^2(n-2)^2 - 2\tau\rho(n-2) + \rho^2 + 4\tau\tau_p(n-1)}}{2\tau n}.$$

.

C.3 Supplementary Material

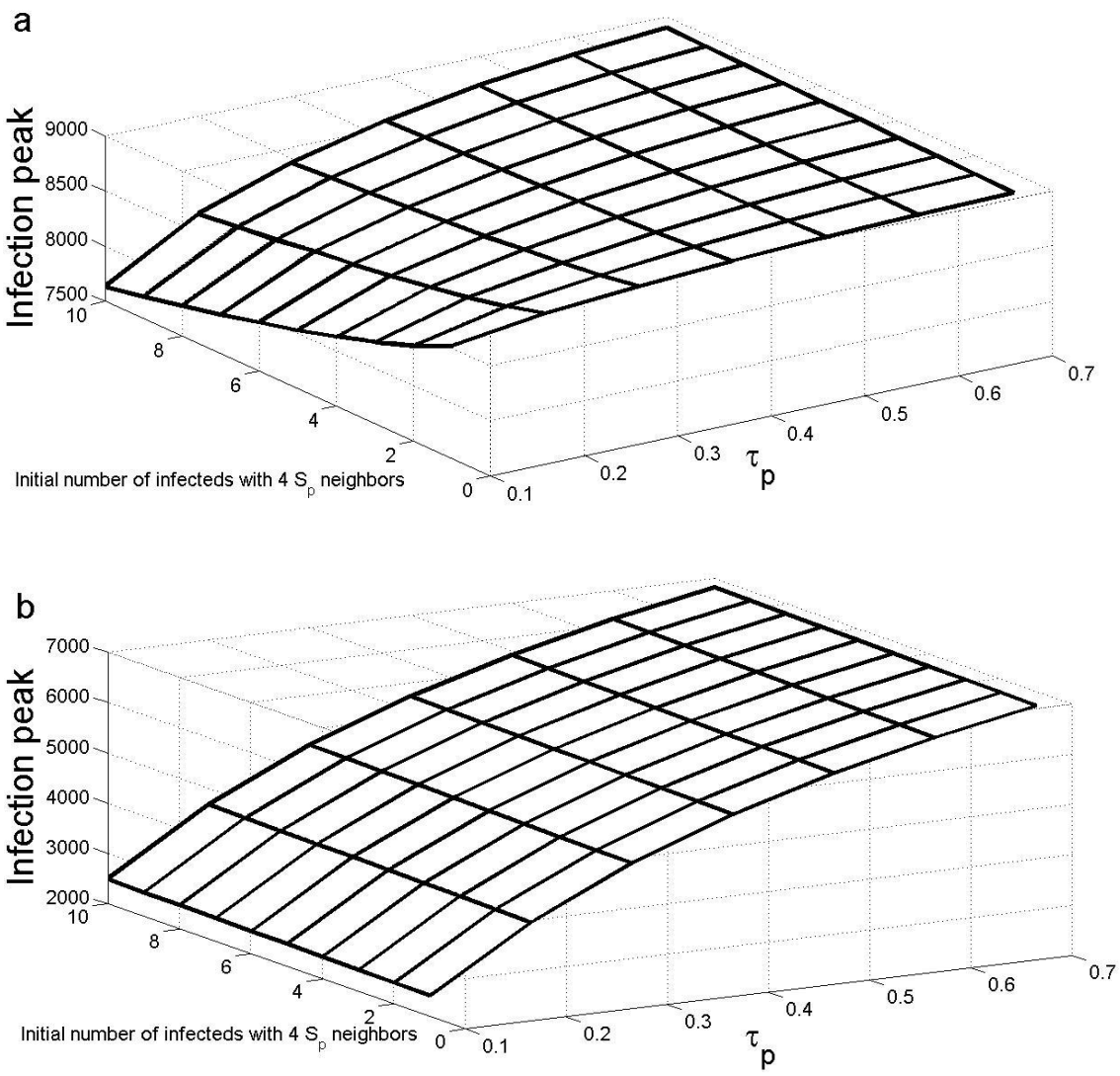

Figure C.1: Infection peak versus rate of disease transmission to protective individuals, τ_p, and the initial distribution of *single infected individuals with 4 state* S_p *neighbors* (and all other members of the host population are fully susceptible, S), where $\xi = 0.25\ day^{-1}$, $\rho = 0\ day^{-1}$ (a) and $\xi = 0\ day^{-1}$, $\rho = 0.25\ day^{-1}$ (b). Other model parameters are $\tau = 0.8\ day^{-1}$, $\sigma = 0.25\ day^{-1}$ and $\kappa = 0\ day^{-1}$.

Appendix D

MATLAB codes for simulation results

We provide prototypes of *MATLAB* codes that were developed to obtain simulation results presented in this thesis.

Plotting time series for the number of infectious individuals in Figure 1.2a. Other graphs in this figure are obtained from the same code by choosing desired time series or varying model parameters.

(i) Function m-file:

```
% This is a function file (named  Not_thesis) for a
% compartmental SIR model where time-dependent variables
% y(1), y(2) and y(3) represent the numbers of susceptible
% infectious and recovered individuals, respectively.
% Model parameters are beta and sigma and they are rates
% of transmission and recovery, respectively. For example,
% dy(1) represents the equation of motion for the number
% of susceptible individuals.

function dy = Not_thesis(t,y)
global beta  sigma  % declaration of model parameters
dy=zeros(3,1); % 3 by 1 variable-size matrix
dy(1)=-tau.*y(1).*y(2);
dy(2)=tau.*y(1).*y(2)-sigma.*y(2);
dy(3)=sigma.*y(2);
```

(ii) Script m-file:

```
% This script file inputs prescribed model parameters, beta
% and sigma and initial conditions S(0) = 99, I(0) = 1 and
% R(0) = 0, to solve the SIR model and output a graph for
% the time evolution of infectious individuals.


clc;clear all
global beta sigma
beta=0.01;
sigma=0.1;
YY = zeros(1,3);
T = zeros(1,1);
options=odeset('RelTol',1e-4,'AbsTol',[1e-4 1e-4 1e-4]);
for i = 0:60 % simulation period is from day 0 to day 60
      if i == 0
        [t,y]=ode45('Not_thesis',[i i+1],[99 1 0],options);
            else if i > 0
        [t,y]=ode45('Not_thesis',[i i+1],y(end, :)',options);
             end
      end
T = [T;t];
YY = [YY;y];
end
plot(T,YY(:,2),'k--','LineWidth',4); % plotting I(t)
xlabel('Time (days)');
ylabel('Infectious individuals');
```

Plotting time series for the number of infectious individuals in Figure 1.8 (when $n = 4$). The other graph in this figure (for a case where $n = 2$) is produced from the same code by changing the value of n as well as the initial conditions.

(i) Function m-file:

```
% This is a function file (named  Not_thesis_b) for a
% compartmental SIR pair approximation model where
% time-dependent variables y(1),...,y(9)
% represent the numbers of singletons and pairs of
% individuals as indicated below.
% Model constants tau, sigma and f are rates
% of transmission, recovery and (n-1)/n, where n
% is the neighborhood size, respectively.

function dy = Not_thesis_b(t,y)
global tau  sigma f  % declaration of model parameters
dy=zeros(9,1); % 9 by 1 variable-size matrix

dy(1)= -tau.*y(5);  % [S]
dy(2)= tau.*y(5)-sigma.*y(2); % [I]
dy(3)= sigma.*y(2); % [ R]
dy(4)= -2.*tau.*f.*y(4).*y(5)./y(1); % [SS]
dy(5)= f.*tau.*y(4).*y(5)./y(1)-f.*tau.*y(5).*y(5)./y(1)-
        tau.*y(5)-sigma.*y(5);% [SI]
dy(6)= -f.*tau.*y(5).*y(6)./y(1)+sigma.*y(5); % [SR]
dy(7)= 2.*tau.*f.*tau.*y(5).*y(5)./y(1)+2.*tau.*y(5)-
        2.*sigma.*y(7); % [II]
dy(8)= tau.*f.*tau.*y(5).*y(6)./y(1)+sigma.*y(7)-
        sigma.*y(8); % [IR]
dy(9)= 2.*sigma.*y(8);  % [RR]
```

(ii) Script m-file:

```
% This script file inputs prescribed model parameters, tau
% and sigma, and a constant f as well as the initial
% conditions (indicated below), to solve the SIR pair
```

```
% approximation model and output time series for
% infections individuals, when the neighborhood size
%  is n = 4.

clc;clear all
global tau sigma f
tau=0.9;
sigma=0.1;
f = 0.75;

YY = zeros(1,9);
T = zeros(1,1);
options=odeset('RelTol',1e-4,'AbsTol',[1e-4 1e-4 1e-4 1e-4
            1e-4 1e-4 1e-4 1e-4 1e-4]);
 for i = 0:60 % simulation time is 60 days
     if i == 0
       [t,y]=ode45('Not_thesis_b',[i i+1],[99 1 0 196 4 0 0 0
                0],options); % initial conditions
     else if i > 0
    [t,y]=ode45('Not_thesis_b',[i i+1],y(end, :)',options);
         end
     end
  T = [T;t];
  YY = [YY;y];
 end

plot(T,YY(:,2),'k--','LineWidth',4); % plotting time series
xlabel('Time (days)');
ylabel('Infectious individuals');
```

```
hold on
```

Plotting time series in Figure 2.1a. Other graphs in this figure were produced by varying model parameters of the same code. The number of outbreaks and average infection peaks were obtained through variation of model parameters in the same function file and script file presented below, to produce graphs in Figure 2.2. Similarly, graphs in Figures 2.3 and 2.6a were produced by the same code but varying model parameters in the script m-file presented here.

(i) Function m-file:

```
% This is a function file (named  Notice) for a
% 'susceptible-exposed-infectious-recovered-vaccinated'
% (SEIRV) pair approximation model where time-dependent
% variables y(1), y(2), y(3), y(4), y(5) and y(6), y(7), y(8),
% y(9), y(10), y(11), y(12), y(13), y(14), y(15), y(16),
% y(17), y(18), y(19), y(20) represent the numbers of
%  states S, E, I, R, V farms and S-S, S-E, S-I, S-R,
% S-V, E-E, E-I, E-R, E-V, I-I, I-R, I-V, R-R, R-V, V-V pairs
% of farms, respectively. Model parameters are tau, nu,
% sigma, psi_r, psi_p, omega and theta and they are rates
% of transmission, latency, recovery, ring vaccination,
% prophylactic vaccination, natural immunity waning, vaccine
% waning, respectively. For example, dy(6) represents the
% equation of motion for the number
% of 'susceptible-susceptible' pairs of farms.

function dy = Notice(t,y)
global tau  nu  sigma  mu_cp mu_ip psi_r  psi_p omega theta
dy=zeros(20,1);
dy(1)=-tau.*y(8)-psi_r.*y(8)-psi_p.*y(1)+omega.*y(4)+
```

```
        theta.*y(5)-mu_cp.*y(8);
dy(2)=tau.*y(8)-nu.*y(2)-psi_r.*y(12)-psi_p.*y(2)-
        mu_cp.*y(12);
dy(3)=nu.*y(2)-sigma.*y(3)-mu_ip.*y(3);
dy(4)=sigma.*y(3)-omega.*y(4);
dy(5)=psi_r.*y(8)+psi_r.*y(12)+psi_p.*y(1)+psi_p.*y(2)-
        theta.*y(5);
dy(6)=-2.*tau.*0.75.*y(6).*y(8)./y(1)-
        2.*psi_r.*0.75.*y(6).*y(8)./y(1)-2.*psi_p.*y(6)+
        2.*omega.*y(9)+2.*theta.*y(10)-
        2.*mu_cp.*0.75.*y(6).*y(8)./y(1);
dy(7)=-tau.*0.75.*(y(8).*y(7)./y(1)-y(6).*y(8)./y(1))-
        nu.*y(7)-  psi_r.*(0.75.*y(8).*y(7)./y(1)+
        0.75.*y(7).*y(12)./y(2))-1.*psi_p.*y(7)+
        omega.*y(13)+theta.*y(14)-
        mu_cp.*(0.75.*y(8).*y(7)./y(1)+
        0.75.*y(7).*y(12)./y(2));
dy(8)=-tau.*(0.75.*y(8).*y(8)./y(1)+y(8))+nu.*y(7)-
        sigma.*y(8)-psi_r.*(0.75.*y(8).*y(8)./y(1)+y(8))-
        psi_p.*y(8)+omega.*y(16)+theta.*y(17)-
        mu_cp.*(0.75.*y(8).*y(8)./y(1)+y(8))-mu_ip.*y(8);
dy(9)=-tau.*0.75.*y(8).*y(9)./y(1)+sigma.*y(8)-
        psi_r.*0.75.*y(8).*y(9)./y(1)-psi_p.*y(9)-
        omega.*y(9)+1.*omega.*y(18)+theta.*y(19)-
        mu_cp.*0.75.*y(8).*y(9)./y(1);
dy(10)=-tau.*0.75.*y(8).*y(10)./y(1)-
          psi_r.*0.75.*y(8).*y(10)./y(1)-
          psi_p.*y(10)+1.*psi_r.*0.75.*y(6).*y(8)./y(1)+
        psi_p.*y(6)+psi_p.*0.75.*y(7).*y(12)./y(2)+
        psi_p.*y(7)+omega.*y(19)+2.*theta.*y(20)-
```

```
            theta.*y(10)-mu_cp.*0.75.*y(8).*y(10)./y(1);
dy(11)=0.75.*2.*tau.*y(7).*y(8)./y(1)-2.*nu.*y(11)-
            2.*psi_r.*0.75.*y(11).*y(12)./y(2)-2.*psi_p.*y(11)-
            2*mu_cp.*0.75.*y(11).*y(12)./y(2);
dy(12)=tau.*(0.75.*y(8).*y(8)./y(1)+y(8))+nu.*(y(11)-
            y(12))-sigma.*y(12)-
            psi_r.*(0.75.*y(12).*y(12)./y(2)+y(12))-
            psi_p.*y(12)-
            mu_cp.*(0.75.*y(12).*y(12)./y(2)+y(12))-
            mu_ip.*y(12);
dy(13)=tau.*0.75.*y(8).*y(9)./y(1)nu.*y(13)+
            sigma.*y(12)-psi_r.*0.75.*y(12).*y(13)./y(2)-
            psi_p.*y(13)-omega.*y(13)-
            mu_cp.*0.75.*y(12).*y(13)./y(2);
dy(14)=tau.*0.75.*y(8).*y(10)./y(1)-nu.*y(14)-
            psi_r.*0.75.*y(12).*y(14)./y(2)-
            psi_p.*y(14)+psi_r.*0.75.*y(8).*y(7)./y(1)+
            psi_p.*y(7)+1.*psi_r.*0.75.*y(11).*y(12)./y(2)+
            psi_p.*y(11)-theta.*y(14)-
            mu_cp.*0.75.*y(12).*y(14)./y(2);
dy(15)=2.*nu.*y(12)-2.*sigma.*y(15)-2.*mu_ip.*y(15);
dy(16)=sigma.*(y(15)-y(16))+nu.*y(13)-omega.*y(16)-
            mu_ip.*y(16);
dy(17)=sigma.*y(17)+nu.*y(14)+
            psi_r.*(0.75.*y(8).*y(8)./y(1)+y(8))+
            psi_p.*y(8)+psi_r.*(0.75.*y(12).*y(12)./y(2)+y(12))+
           psi_p.*y(12)-theta.*y(17)-mu_ip.*y(17);
dy(18)=2*sigma.*y(16)-2.*omega.*y(18);
dy(19)=sigma.*y(17)-omega.*y(19)-
            theta.*y(19)+psi_r.*0.75.*y(8).*y(9)./y(1)+
```

```
        psi_p.*y(9)+psi_r.*0.75.*y(12).*y(13)./y(2)+
        psi_p.*y(13);
dy(20)=2.*psi_r.*0.75.*y(12).*y(14)./y(2)+
        2.*psi_p.*y(14)+2.*psi_r.*0.75.*y(8).*y(10)./y(1)+
        2.*psi_p.*y(10)-2.*theta.*y(20);
```

(ii) Script m-file:

```
% This script file inputs prescribed model parameters, tau,
% nu, sigma, psi_r, psi_p, omega, theta and the initial
% conditions to solve the SEIRV pair approximation model
% and output a graph for the time evolution of infectious
% farms.

clc;clear all
global tau nu  sigma  psi_r psi_p omega theta t_introduction
tau=0.6;
nu=1/4.0;
sigma=1/7;
psi_r=0;
psi_p=0;
omega = 0.0055;
theta = 1/180;
t_introduction = 800; % disease reintroduction 800 days
YY = zeros(1,20);
T = zeros(1,1);
options=odeset('RelTol',1e-4,'AbsTol',[1e-4 1e-4 1e-4
 1e-4 1e-4 1e-4 1e-4 1e-4 1e-4 1e-4 1e-4 1e-4 1e-4 1e-4
 1e-4 1e-4 1e-4 1e-4 1e-4 1e-4 ]);
for i = 0:7320 % simulation period is day 0 to day 20
        if i == 0
        [t,y]=ode45('notice',[i i+1],[39995 4 1 0 0 79984 12
```

```
    0 0 0 0 4 0 0 0 0 0 0 0 0],options); % initial conditions
        else if i > 0
        [t,y]=ode45('notice',[i i+1],y(end, :)',options);
        end
    end
    if mod(i,t_introduction)== 0 % disease is introduced by
% exposing the virus to 1 susceptible farm
        difference=y(end,1);
            if (difference > 1)
                y(end,1)= y(end,1)-1; % [S] decreases
                y(end,2)= y(end,2)+1; % [E] increases
                y(end,6)= y(end,6)-2 %  [SS] decreases
                y(end,8)= y(end,8)+2; % [SE] increases
          end
    end
    T = [T;t];
    YY = [YY;y];
end
plot(T,YY(:,3),'k','LineWidth',2.25);
xlabel('Time (years)');
ylabel('Infectious farms');
hold on
```

Constructing contour graph in Figure 3.1a. The same function m-file and variation of quantities V_i and Y_i and model parameters in the script m-file presented below, produced other graphs in this figure and mesh-plots in Figures 3.4, 3.6, B.1 and B.3. Time series in Figures 3.2, 3.3, 3.5 were also produced by altering only the script file so that rates take single values and not intervals

(i) Function m-file

```
% This is a function file (named  Notice_2) for a
```

```
% 'susceptible-exposed-infectious-recovered-vaccinated-
% culled' (SEIRVC) pair approximation model where time-
% dependent variables are as indicated below and model
% parameters are tau, nu, sigma, psi_r, psi_p, mu_ip,
% mu_cp, omega, theta and eta, and they are rates
% of transmission, latency, recovery, ring vaccination,
% prophylactic vaccination, IP culling, DC culling, natural
% immunity waning, vaccine waning and replacement of
% culled farms, respectively.

function dy = Notice_2(t,y)
global tau  nu  sigma  mu_cp mu_ip psi_r psi_p omega theta eta
dy=zeros(32,1);

dy(1)=-tau.*y(8)-psi_r.*y(8)-psi_p.*y(1)+omega.*y(4)+
        theta.*y(5)-mu_cp.*y(8)+eta.*y(26); % S
dy(2)=tau.*y(8)-nu.*y(2)-psi_r.*y(12)-psi_p.*y(2)-
        mu_cp.*y(12); % E
dy(3)=nu.*y(2)-sigma.*y(3)-mu_ip.*y(3); % I
dy(4)=sigma.*y(3)-omega.*y(4); % R
dy(5)=psi_r.*y(8)+psi_r.*y(12)+psi_p.*y(1)+psi_p.*y(2)-
         theta.*y(5); %V
dy(6)=-2.*tau.*y(6).*y(8)./y(1)-2.*psi_r.*y(6).*y(8)./y(1)-
        2.*psi_p.*y(6)+2.*omega.*y(9)+2.*theta.*y(10)-
        2.*mu_cp.*y(6).*y(8)./y(1)+2.*eta.*y(27); % SS
dy(7)=-tau.*(y(8).*y(7)./y(1)-y(6).*y(8)./y(1))-
          nu.*y(7)-psi_r.*(y(8).*y(7)./y(1)+y(7).*y(12)./y(2))-
          psi_p.*y(7)+omega.*y(13)+theta.*y(14)-
          mu_cp.*(y(8).*y(7)./y(1)+y(7).*y(12)./y(2))+
          eta.*y(28); % SE
```

```
dy(8)=-tau.*(y(8).*y(8)./y(1)+y(8))+nu.*y(7)-sigma.*y(8)-
        psi_r.*(y(8).*y(8)./y(1)+y(8))-
        psi_p.*y(8)+omega.*y(16)+theta.*y(17)-
        mu_cp.*(y(8).*y(8)./y(1)+y(8))-mu_ip.*y(8)+
        eta.*y(29); % SI
dy(9)=-tau.*y(8).*y(9)./y(1)+sigma.*y(8)-
         psi_r.*y(8).*y(9)./y(1)-psi_p.*y(9)-
         omega.*y(9)+1.*omega.*y(18)+theta.*y(19)-
         mu_cp.*y(8).*y(9)./y(1)+eta.*y(30); % SR
dy(10)=-tau.*y(8).*y(10)./y(1)-psi_r.*y(8).*y(10)./y(1)-
          psi_p.*y(10)+1.*psi_r.*y(6).*y(8)./y(1)+
          psi_p.*y(6)+psi_p.*y(7).*y(12)./y(2)+
          psi_p.*y(7)+omega.*y(19)+ theta.*y(20)-theta.*y(10)-
          mu_cp.*y(8).*y(10)./y(1)+eta.*y(31);% SV
dy(11)=2.*tau.*y(7).*y(8)./y(1)-2.*nu.*y(11)-
          2.*psi_r.*y(11).*y(12)./y(2)-2.*psi_p.*y(11)-
          2*mu_cp.*y(11).*y(12)./y(2); % EE
dy(12)=tau.*(y(8).*y(8)./y(1)+y(8))+nu.*(y(11)-y(12))-
         sigma.*y(12)-psi_r.*(y(12).*y(12)./y(2)+y(12))-
         psi_p.*y(12)-mu_cp.*(y(12).*y(12)./y(2)+y(12))-
         mu_ip.*y(12); % EI
dy(13)=tau.*y(8).*y(9)./y(1)-nu.*y(13)+sigma.*y(12)-
         psi_r.*y(12).*y(13)./y(2)-psi_p.*y(13)-omega.*y(13)-
         mu_cp.*y(12).*y(13)./y(2); % ER
dy(14)=tau.*y(8).*y(10)./y(1)-nu.*y(14)-
          psi_r.*y(12).*y(14)./y(2)-
          psi_p.*y(14)+psi_r.*y(8).*y(7)./y(1)+psi_p.*y(7)+
          psi_r.*y(11).*y(12)./y(2)+1.*psi_p.*y(11)-
          theta.*y(14)-mu_cp.*y(12).*y(14)./y(2); % EV
dy(15)=2.*nu.*y(12)-2.*sigma.*y(15)-2.*mu_ip.*y(15); %   II
```

```
dy(16)=sigma.*(y(15)-y(16))+nu.*y(13)-omega.*y(16)-
        mu_ip.*y(16); % IR
dy(17)=-sigma.*y(17)+nu.*y(14)+psi_r.*(y(8).*y(8)./y(1)+
        y(8))+psi_p.*y(8)+psi_r.*(y(12).*y(12)./y(2)+y(12))+
        psi_p.*y(12)-theta.*y(17)-mu_ip.*y(17); % IV
dy(18)=2*sigma.*y(16)-2.*omega.*y(18); % RR
dy(19)=sigma.*y(17)-omega.*y(19)-
        theta.*y(19)+psi_r.*y(8).*y(9)./y(1)+psi_p.*y(9)+
        psi_r.*y(12).*y(13)./y(2)+psi_p.*y(13); % RV
dy(20)=2.*psi_r.*y(12).*y(14)./y(2)+2.*psi_p.*y(14)+
        2.*psi_r.*y(8).*y(10)./y(1)+2.*psi_p.*y(10)-
        2.*theta.*y(20); % VV
dy(21)=mu_ip*y(3); % total cumulative IP culled
dy(22)=mu_cp*y(8)+mu_cp*y(12); % total cumulative CP culled
dy(23)=nu.*y(2); % cumulative infections
dy(24)=psi_p.*(y(1)+y(2)); % number of prophylactic vacc
dy(25)=psi_r.*(y(8)+y(12)); % number of ring vacc
dy(26)=mu_cp.*(y(8)+y(12))+mu_ip.*y(3)-eta.*y(26); % C
dy(27)=mu_cp.*(2.*y(6).*y(8)./y(1)+y(7).*y(12)./y(2)-
        y(8).*y(27)./y(1))+mu_ip.*y(8)-eta.*y(27)+
        eta.*y(32); % SC
dy(28)=mu_cp.*(2.*y(11).*y(12)./y(2)+y(8).*y(7)./y(1)-
        y(12).*y(28)./y(2))+mu_ip.*y(12)-eta.*y(28); %EC
dy(29)=mu_cp.*(y(8).*y(8)./y(1)+y(12).*y(12)./y(2)+y(8)+
        y(12))-mu_ip.*y(29)-eta.*y(29); %IC
dy(30)=mu_cp.*(y(8).*y(9)./y(1)+y(12).*y(13)./y(2))+
        mu_ip.*y(16)-eta.*y(30); % RC
dy(31)=mu_cp.*(y(8).*y(10)./y(1)+y(12).*y(14)./y(2))+
        mu_ip.*y(17)-eta.*y(31); % VC
dy(32)=2.*mu_cp.*(y(8).*y(27)./y(1)+y(12).*y(28)./y(2))+
```

```
2.*mu_ip.*(y(29)+y(15))-2.*eta.*y(32); % CC
```

(ii) Script m-file:

```
% This script file inputs prescribed model parameters, tau,
% nu, sigma, psi_r, psi_p, mu_ip, mu_cp, omega, theta and the
% initial conditions to solve a SEIRVC pair approximation
% model and output a column vector of cumulative infections
% in 20 years, i.e. y(end,23), which correspond to a plane
% containing vaccination rates. The resulting column vector
% was converted into a matrix whose axes are prophylactic
% vaccination and ring vaccination while its entries are
% corresponding cumulative infections. This matrix was
% then transformed into a contour graph. The matrix can
% also be used to produce mesh-plots.

clc;clear all
global tau nu sigma mu_cp mu_ip psi_r psi_p omega theta eta V
global psi_p_active psi_r_active mu_cp_active mu_ip_active
global tau_active t_introduction vac Cu out psi_p_low
global  psi_p_high psi_p_new psi_r_new psi_r_low psi_r_high

eta= 0; % rate of replacement of culled farms
Cu = 2000; % culling capacity, Y_i
mu_ip_active = 0;
mu_cp_active = 0;
V= 10000; % vaccine capacity, V_i
psi_p_active = 0.00;
psi_r_active = 0.00;
tau_active =0.6;
tau=tau_active;
nu=1/4.0;
```

```
sigma=1/7;
mu_cp=mu_cp_active;
mu_ip=mu_ip_active;
% rates of prophylactic and ring vaccination range from 0 to
% 0.006
psi_p_low = 0.00;
psi_p_high = 0.006;
psi_r_low = 0;
psi_r_high = 0.006;
omega = 1/(180); % vaccine waning
theta = 1/(180); % natural immunity waning
vac = 366; % vaccination restocked each year
cull = 366; % culling resources restocked each year
t_introduction = 800; % disease reintroduction every 800 days



YY = zeros(1,32);
T = zeros(1,1);
psi_p = zeros(1,12);
psi_r = zeros(1,12);
options=odeset('RelTol',1e-4,'AbsTol',[1e-4 1e-4 1e-4 1e-4
 1e-4 1e-4 1e-4 1e-4 1e-4 1e-4 1e-4 1e-4 1e-4 1e-4 1e-4
1e-4 1e-4 1e-4 1e-4 1e-4 1e-4 1e-4 1e-4 1e-4 1e-4 1e-4
1e-4 1e-4 1e-4 1e-4 1e-4 1e-4 ]);


tic
% creating a plane of vaccination rates
for k = 0:11
    for l = 0:11
      psi_p_new = psi_p_low + (k/11)*(psi_p_high - psi_p_low);
```

```
      psi_r_new = psi_r_low + (1/11)*(psi_r_high - psi_r_low);
      psi_p = psi_p_new;
      psi_r = psi_r_new;
for i = 0:(366*20)
    if i == 0
     [t,y]=ode45('notice_2',[i i+1],[39995 4 1 0 0 79984 12 0
     0 0 0 4 0 0 0 0 0 0 0 0 0 0 0 0 0 0 0 0 0 0 0 0 0
     0 0 0],options); % initial conditions
    else if i > 0
    [t,y]=ode45('notice_2',[i i+1],y(end, :)',options);
        end
    end
 if mod(i,7320) == 0 && i > 0
  str2 = y(end,23);
  disp(str2); % OUTPUT: column vector of cumulative infections
   end

   if mod(i,366)== 0
     y(end,24)= 0;
     y(end,25)= 0;
   end

    if mod(i,800)== 0  % disease reintroduction every 800 days
    difference=y(end,1);
    if (difference > 1)
    y(end,1)= y(end,1)-1; %[S] decreases by 1
    y(end,2)= y(end,2)+1; %[E] increases by 1
    y(end,6)= y(end,6)-2; %[SS] decreases by 2
    y(end,8)= y(end,8)+2; %[SE] decreases by 2
    end
```

```
   end
end
     end
end
toc
```